EXPERIMENTAL INVESTIGATION ON HIGH-PRESSURE, HIGH-TEMPERATURE VISCOSITY OF GAS MIXTURES

A Dissertation

by

EHSAN DAVANI

Submitted to the Office of Graduate Studies of
Texas A&M University
in partial fulfillment of the requirements for the degree of

DOCTOR OF PHILOSOPHY

December 2011

Major Subject: Petroleum Engineering

Experimental Investigation on High-pressure, High-temperature Viscosity of Gas Mixtures

EXPERIMENTAL INVESTIGATION ON HIGH-PRESSURE, HIGH-TEMPERATURE VISCOSITY OF GAS MIXTURES

A Dissertation

by

EHSAN DAVANI

Submitted to the Office of Graduate Studies of
Texas A&M University
in partial fulfillment of the requirements for the degree of

DOCTOR OF PHILOSOPHY

Approved by:

Co-Chairs of Committee,	Gioia Falcone
	Catalin Teodoriu
Committee Members,	William D. McCain, Jr.
	Yuefeng Sun
Head of Department,	Stephen A. Holditch

December 2011

Major Subject: Petroleum Engineering

ABSTRACT

Experimental Investigation on High-pressure, High-temperature Viscosity of Gas Mixtures. (December 2011)

Ehsan Davani, B.S., Petroleum University of Technology, Iran;

M.S., Sahand University of Technology, Iran

Co-Chairs of Advisory Committee: Dr. Gioia Falcone
Dr. Catalin Teodoriu

Modeling the performance of high-pressure, high-temperature (HPHT) natural gas reservoirs requires the understanding of gas behavior at such conditions. In particular, gas viscosity is an important fluid property that directly affects fluid flow through porous media and along production flowlines. Accurate measurements of gas viscosity at HPHT conditions are both extremely difficult and expensive. Unfortunately, the correlations available today do not have a sufficiently broad range of applicability in terms of pressure and temperature since no measured gas viscosities at HPHT are currently available. Thus the correlation accuracy may be doubtful for the prediction of gas viscosity at HPHT conditions.

An oscillating-piston viscometer was used to measure the viscosity of mixtures of nitrogen and methane, and mixtures of CO_2 and methane at a pressure range of 5,000 to 25,000 psi, and a temperature range of 100 to 360°F. The viscosity of mixtures of nitrogen and methane, and mixtures of CO_2 and methane measured to take into account of the fact that the concentration of non-hydrocarbons increase significantly in HPHT reservoir. The recorded measured data were then used to evaluate the reliability of the

most commonly used correlations in the petroleum industry. Measured gas viscosity data at HPHT conditions suggest that the most common gas viscosity correlations return up to 9% relative error in gas recovery factor, which translates into a significant error in estimating the ultimate recovery for large HPHT natural gas reservoirs. Thus, the current gas viscosity correlations need to be adjusted to estimate gas viscosity at HPHT conditions. New gas viscosity correlations constructed for HPHT conditions developed based upon our experiment data provide more confidence on gas viscosity.

A rolling ball viscometer was also used to assess its capability to measure gas viscosity. Using gas instead of liquid to calibrate a rolling ball viscometer over the entire pressure and temperature range of interest appears to be satisfactory. Optimizing tube inclination angle and ball/tube diameter ratio prevents turbulent flow effects around the ball, thus enhancing the accuracy of the measurement. The proposed calibration method was then verified with pure CO_2 at a pressure range of 4,000 to 8,000 psi, and a temperature range of 98 to 240°F. Consequently, rolling ball viscometer was introduced as a good candidate to measure the gas viscosity; however it has not been tested at HPHT conditions yet.

DEDICATION

Dedicated to my mom, dad, sisters and most importantly, my lovely wife, for their love and support.

ACKNOWLEDGEMENTS

I would like to express my deepest gratitude and appreciation to my advisor and committee chair, Dr. Gioia Falcone, for her continuous encouragement, guidance, and support. Also, I would like to give special thanks to my co-chair Dr. Catalin Teodoriu, for his support and motivation during the course of this research. I would also like to extend my appreciation to Dr. William D. McCain, Jr., for his advice, inspiration, and valuable comments.

Appreciation is extended to Dr. Yuefeng Sun for serving on my committee, and for his help and encouragement.

I would also like to express my sincere appreciation to Darla-Jean Weatherford for the help she provided with editing and formatting the technical papers published related to this research.

Furthermore, I would like to extend my appreciation to Mr. John Maldonado, Sr. for his help in coordinating the lab facilities.

Besides, I would like to thank Mr. Daniel Airy from Cambridge Viscosity Inc. for his valuable help, comments, and suggestions he provided throughout the experimental work.

I would also like to thank my dear friend, Ehsan Safari, for his support and help during all the different steps of this work.

Many thanks are due to all faculty and staff of the Department of Petroleum Engineering at Texas A&M University, and my colleagues, who helped me throughout the course of this research.

Finally, I would like to acknowledge financial support from the Crisman Petroleum Research Institute at Texas A&M University for providing funding for this project. The facilities and resources provided by the Harold Vance Department of Petroleum Engineering of Texas A&M University are gratefully acknowledged.

NOMENCLATURE

Symbol	Description
atm	atmosphere
A	area
A	a layer in fluid flow between two plates
bar	pressure unit, 1 bar = 0.987 atms
cm	centimeter
cp	centipoise
CO_2	carbon dioxide
^oC	Celsius temperature
d_b	ball diameter
d_t	tube diameter
D	tube diameter
ft	foot or feet
F	electromagnetic force
F	resistance factor
^oF	degree Fahrenheit
g	gravity acceleration factor
gr	gram
h	thickness
H_2S	hydrogen sulfide
HPHT	high pressure high temperature
in	inch

Symbol	Description
I	identity matrix
J	optimization matrix
J^T	transposed of optimization matrix
k	permeability
kg	kilogram
K	calibration coefficient of viscometer
K’	constant for viscosity correlation
K_1	constant for viscosity correlation
K_2	constant for viscosity correlation
Kpa	thousand Pascal
^oK	Kelvin temperature
l	length, distance
L	length, distance
m	meter
M	molecular weight
N	Newton, force unit
N_2	nitrogen
N_{Re}	Reynolds number
p	pressure
Δp	pressure change
p_{pc}	pseudocritical pressure
psi	gauge pressure
psia	absolute pressure
psig	gauge pressure

Symbol	Description
P	poise
Pa	Pascal
p_c	critical pressure
p_{pr}	pseudoreduced pressure
p_r	reduced pressure
p_r	reservoir pressure
q	gas flow rate
Q	volumetric flow rate of fluid
r	distance from center of circle, tube, or pipe
r_e	drainage radius
r_c	sensor chamber radius
r_p	sensor piston radius
r_w	wellbore radius
R	universal gas constant
s	second
s	skin
sec	second
S	sum of square of derivation
t	time
t_d	time that the piston moves from right end to left end of the chamber
t_u	time that the piston moves from left end to right end of the chamber
T	temperature
T_c	critical temperature
T_{pc}	pseudocritical temperature

Symbol	Description
T_{pr}	pseudoreduced temperature
V	velocity
v	velocity
X	constant for viscosity correlation
y_{CO_2}	mole fraction of CO_2 in vapor
y_{H_2S}	mole fraction of hydrogen sulfide in vapor
y_{N_2}	mole fraction of nitrogen in vapor
$y_{N_2,\ CO_2,\ H_2S}$	mole fraction of the non-hydrocarbon component
Y	constant for viscosity correlation
z	z-factor

Greek

Symbol	Description
β	optimization parameter
δ	optimization parameter
γ_w	shear rate at wall of piston
γ_g	gas specific gravity
θ	inclination angle of tube to the horizontal
μ	viscosity
μ_m	measured viscosity
μ_c	corrected viscosity
μ_{1atm}	gas viscosity at 1 atmosphere
μ_g	gas viscosity
μ_{gSC}	gas viscosity at standard condition
μ^*	gas viscosity at low pressures

Symbol	Description
ξ	constant for viscosity correlation
π	a mathematical constant whose value is the ratio of any circle's circumference to its diameter
ρ	density
ρ_b	ball density
ρ_f	fluid density
ρ_g	gas density
ρ_g	sphere density
ρ_r	reduced density
τ_w	shear stress at piston wall
τ_{rz}	shear stress in direction of z
ψ_r	average reservoir real-gas pseudo-pressure
ψ_{wf}	average wellflow real-gas pseudo-pressure
Δ	indicates difference

Subscripts

Symbol	Description
1atm	1 atmosphere
Avg	average
CO_2	carbon dioxide
g	gas
H_2S	hydrogen sulfide
i	initial
N_2	nitrogen

TABLE OF CONTENTS

CHAPTER Page

CHAPTER Page

LIST OF FIGURES

Page

Page

Page

Page

Page

Page

LIST OF TABLES

Page

CHAPTER I

INTRODUCTION

1.1 Introduction

Natural gas is a global energy resource that plays a key role in meeting the world 's energy demand because it is clean and plentiful. Thus, gas production worldwide has been steadily increasing over the past 15 years but the world's natural gas reserves-to-production ratio declined to 60.3 years in 2007, even though reserves increased by more than 1 trillion m^3 (BP, 2008). To meet the increasing energy demand, exploration and production has increased around the world. Consequently, unconventional gas resources have become one of the best options for the petroleum industry because of their great potential and abundance. Targeting unconventional gas resources increased the world's natural gas reserves-to-production ratio to 62.8 years in 2009, and reserves also increased by more than 2.21 trillion m^3 (**Fig. 1.1)(** BP, 2010).

This growing demand for natural gas is driving the Exploration and Production (E&P) industry to look for new resources in previously unexplored and deeper areas, where HPHT reservoirs may be encountered.

1.2 HPHT reservoirs

According to the SPE E&P glossary (2010), "high temperature" is used when the

---

This dissertation follows the style and format of *SPE Reserv. Eval. Eng. J.*

undisturbed bottomhole temperature (at prospective reservoir depth or total depth) is over 300°F or 150°C. The definition for "high pressure" is met when the maximum anticipated pore pressure of the porous formation to be drilled goes beyond a hydrostatic gradient of 0.8 psi/ft, or the well requiring pressure control equipment has a rated working pressure greater than 10,000 psi or 69 MPa. **Table 1.1** shows a definition of HPHT wells provided by Halliburton (2010).

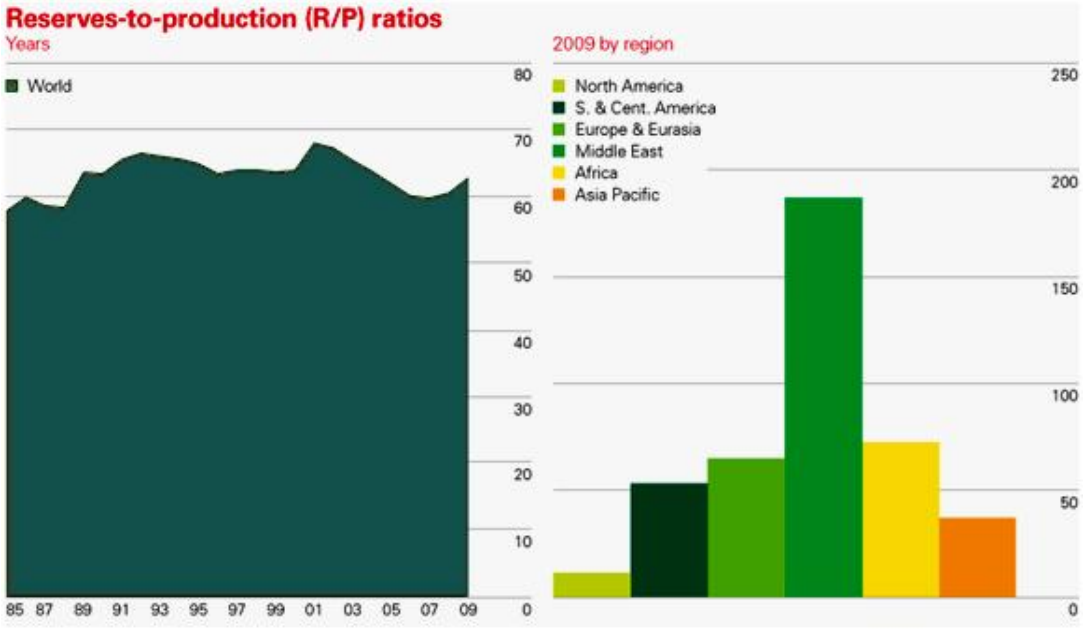

Fig. 1.1—World natural gas reserves-to-production ratio increased to 62.8 years in 2009 and reserves also increased by more than 2.21 trillion m^3 (BP, 2010).

Fig. 1.2 shows a map of HPHT plays across the world. Evaluating and modeling the performance of these unconventional reservoirs requires the understanding of gas behavior at HPHT conditions. One of the most important gas properties is viscosity,

which dictates the fluid mobility in the reservoir and subsequently has a significant impact on cumulative production forecasting during field development planning.

Table 1.1—HPHT definition (Halliburton, 2010)

	Borehole Temperature	Borehole Pressure
HPHT	>300°F - 350°F	>10,000 psi -15,000 psi
Extreme HPHT	>350°F - 400°F	>15,000 psi -20,000 psi
Ultra HPHT	>400°F and above	>20,000 psi and above

Fig. 1.2—HPHT plays distribution across the world (Halliburton, 2010).

At HPHT conditions, the reservoir fluids will be very lean gases, typically methane with small concentrations of inerts such as nitrogen, CO_2 and occasionally H_2S; therefore, the gas properties of HPHT gas reservoirs may be significantly different from those of at lower pressures and temperatures. Accurate measurements of gas viscosity at HPHT conditions are both extremely difficult and expensive. Therefore, gas viscosity is usually predicted from published correlations that are based upon laboratory data at low and moderate pressures and temperatures.

Davani *et al*. (2009) first indicated the sensitivity of IPR curves to gas viscosity uncertainty, which results in unrealistic well-flow models and misleads the well-performance investigation.

Later, Davani *et al*. (2009) reviewed a large database of published viscosity data for pure methane and mixed hydrocarbons and showed that they are limited in terms of both experimental conditions and quantity, and in some cases their accuracy is unknown. Davani *et al*. (2009) also performed a review of available gas viscosity correlations and indicated that they were developed from experimental data taken at low to moderate pressures and temperatures, and their applicability at HPHT conditions is therefore doubtful.

1.3 Laboratory measurement of gas viscosity

Many techniques are available to measure gas viscosity. However just a few of them are applicable at HPHT conditions. The following viscometers have been used to measure gas viscosity:

- Vibrating wire viscometer
- Capillary tube viscometer
- Falling (or rolling) ball viscometer
- Oscillating-piston viscometer

All of them are also used to measure liquid viscosity, but because of the low density and very low viscosity of gases, they need to be modified to be applicable to gas.

Rich natural gases usually contain some heavier components, making the viscosity measurement of these gases relatively easier than for lean gases, due to the lubricant effect of those heavy components. At HPHT conditions, most gas reservoirs contain lean gases, essentially methane, and the dry nature of lean gas creates erratic friction through the measurement process that obstructs the experiment. Low viscosity makes the effect of friction significant, and most of the basic formulations for each instrument should be modified to account for this complication.

1.3.1 Vibrating wire viscometer

The vibrating wire viscometer works based upon damping of transverse vibrations of a rigid wire in the fluid in order to reduce the effect of a hydrodynamic correction term. The vibrations' decay time relates to the viscosity of the fluid.

The motion of an oscillating wire in a dense fluid was first used by Bessel (1828) when he indicated the need for an added mass adjustment to the motion of pendulum in air. Later, Du Buat (1786) described this added mass effect. Stokes (1901) developed the added mass dependency on the surrounding fluid viscosity. Tough *et al*. (1964) used

vibrating wire to measure the viscosity of fluid for the first time. Since then, vibrating wire viscometers were developed widely with different wire materials, diameters, lengths, clamping devices, and with forced or transient modes of oscillation.

The vibrating wires have been made from tungsten, stainless steel, chrome, and NbZr alloy. Tungsten is the ideal material because of its high Young's modulus and density compared to those of other materials providing a stable resonance and sensitivity to the surrounding fluid. **Fig. 1.3** shows a typical vibrating wire viscometer.

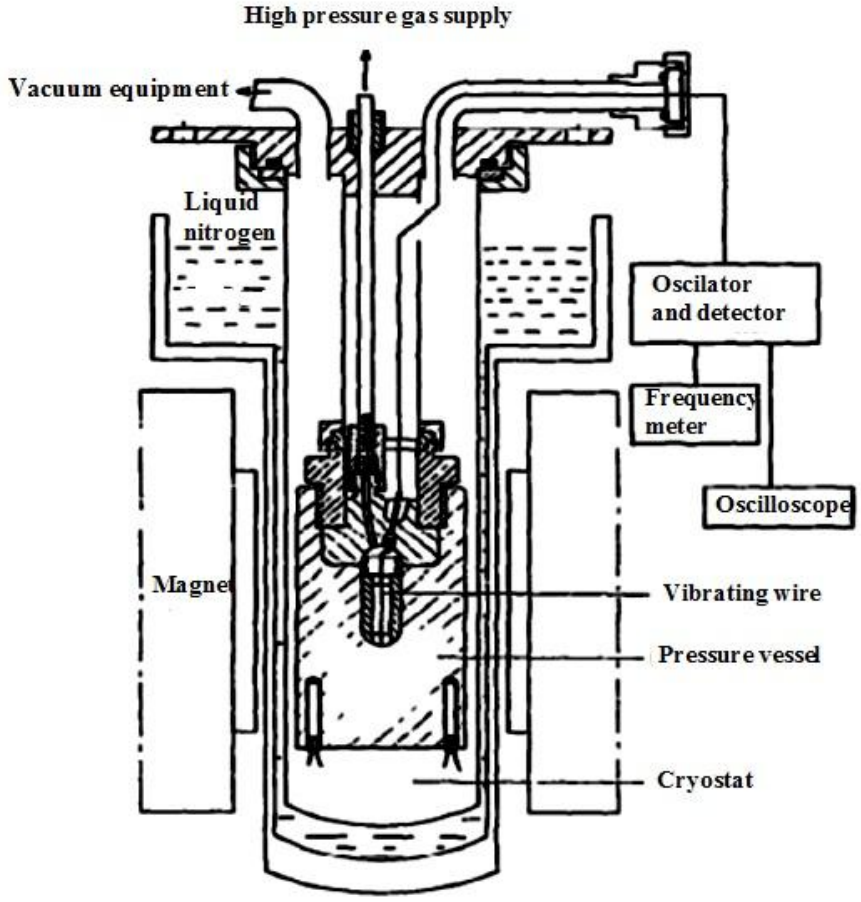

Fig. 1.3—Vibrating wire viscometer, after Trappeniers *et al.* (1980).

Different wire diameters have been used based on the fluid viscosity range. Smaller diameters are usually used for gases and low viscosity liquids and larger diameters are used for more viscous fluids.

Because of ease of operation, continuous readings, wide range and optional internal reference, the vibrating wire viscometer has been used widely to measure different type of fluids.

Tough *et al*. (1964) measured the viscosity of liquid helium at very low temperatures using the vibrating wire viscometer. Wilhelm *et al*. (1998) used a modified vibrating wire viscometer to measure the viscosity of dilute and dense gases for pressures up to 5,800 psi and temperatures as high as 480°F. Bruschi and Santini (1975) measured the viscosity of argon from atmospheric pressure to 440 psi and temperature of 70°F using the vibrating wire viscometer.

1.3.2 Capillary viscometer

The main feature of all capillary viscometers is a long straight tube of small diameter. By measuring the volumetric flow rate and pressure drop through the capillary tube, the viscosity of a fluid flowing within the tube can be calculated. However, the initial viscosity should be corrected to account for end effect (Van Wazer *et al*., 1963; Walters *et al*., 1975). Operation of the capillary viscometer consists of pumping the test fluid through a tube with a known length and diameter, and measuring the pressure drop at a known flow rate, the fluid viscosity is then calculated from Hagen-Poiseuille equation which is,

$$\mu = \frac{\pi \Delta p d_t^{\,4}}{128 L Q} \quad \text{.....(1.1)}$$

where μ is the viscosity of the fluid, Δp is the pressure drop through the tube, d_t is the diameter of the tube, L is the length of tube and Q is the volumetric flow rate of fluid through the tube. The classic capillary viscometer as used by Rankine (1910) to measure the viscosities of neon, xenon, and krypton is illustrated as **Fig. 1.4**. It is one of the oldest capillary viscometers (Coming *et al*, 1944).

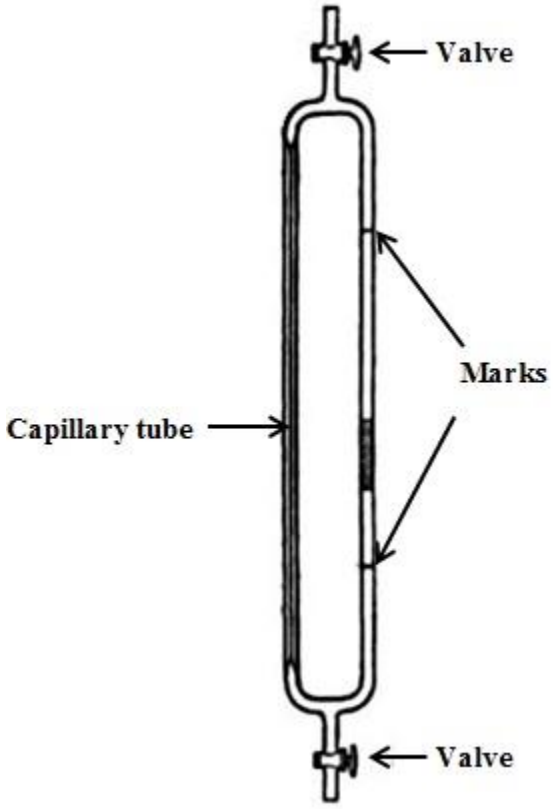

Fig. 1.4—A classic capillary viscometer, after Rankine (1910).

The measurements are easily and directly obtained, but the main difficulty is the precise determination of the small pressure drop needed to maintain laminar flow, different methods and techniques with a different materials have been developed to ensure laminar flow through the capillary tube. **Fig. 1.5** shows a typical glass capillary viscometer.

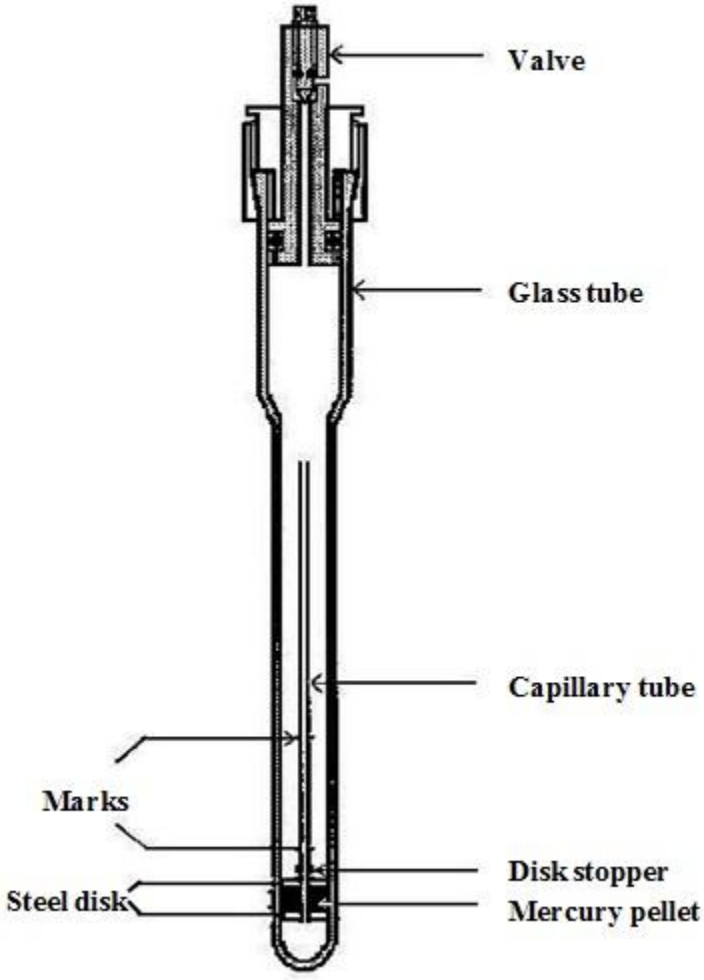

Fig. 1.5—Glass capillary viscometer enclosed in pressure vessel, after Kumagai *et al.* (1998).

Carr (1952) used two capillary tube viscometers to measure the viscosities of methane and three pipeline gas mixtures. These measurements were made to pressures as high as 10,000 psi over a temperature range of 70°F to 250°F.

The principle of the capillary viscometer is simple, but performing a precise measurement is not always easy. The inside of the capillary viscometer should be always clean and before running any test a full thorough drying should be ran inside the capillary. Temperature control is a key parameter since the capillary tube is subject to thermal expansion or contraction as a result of temperature change, particularly in lower viscosity ranges. These thermal influences might introduce errors to the results. Furthermore, capillary tube is hard to resist high pressures. A constant tube diameter and regular geometric shape at HPHT are essential to get an accurate result also it is difficult to associate a single pressure with the measured viscosity because the pressure changes along the capillary. Therefore capillary viscometer is appropriate for measurement at low-moderate pressure and temperature and probably not for HPHT.

1.3.3 Falling (or rolling) ball viscometer

The viscosity is obtained by calculating an initial value from a force balance around the falling object. The initial viscosity should be corrected to account for wall and end effects as well as for deviation from Stokes law (1901). The governing equation simplifies to

$$\mu = K\left(\rho_b - \rho\right)t \quad \text{.....} \quad (1.2)$$

where K is a viscometer geometry coefficient, t is the time of fall between two marks in the viscometer tube, ρ_b is falling object density and ρ is fluid density. **Fig. 1.6** illustrates a typical falling body viscometer.

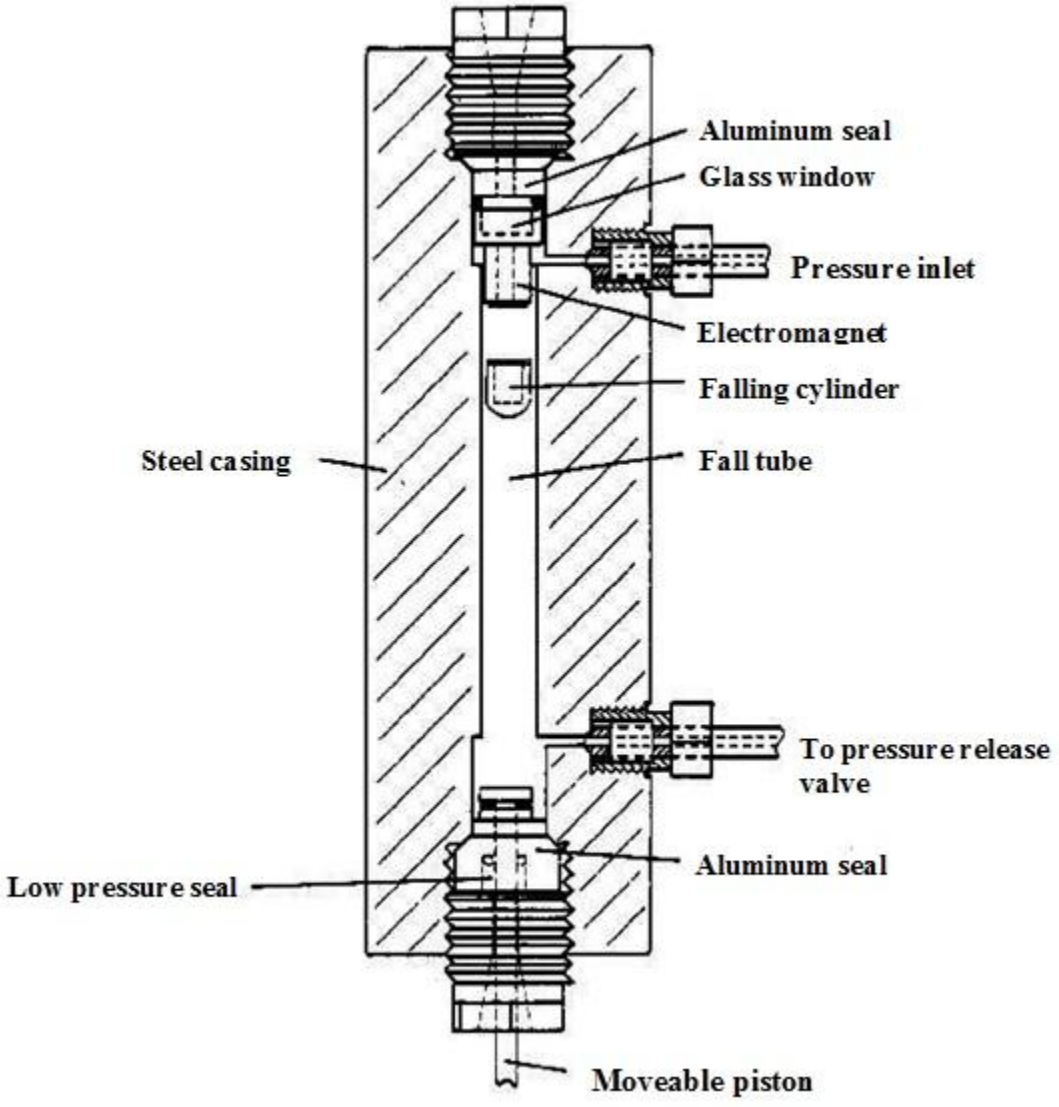

Fig. 1.6—Falling body viscometer, after Chan and Jackson (1985).

It is assumed that the fluid flow around the falling object is laminar. The major drawback of this technique is that in order to obtain accurate viscosity measurement, an accurate density is required as an input.

The applicability of rolling ball viscometers to measure the viscosity of gas was assessed under this study. More details on strengths and weaknesses of the rolling ball viscometer when used to measure gas viscosity can be found in Chapter II. A typical rolling ball viscometer is shown in **Fig. 1.7**.

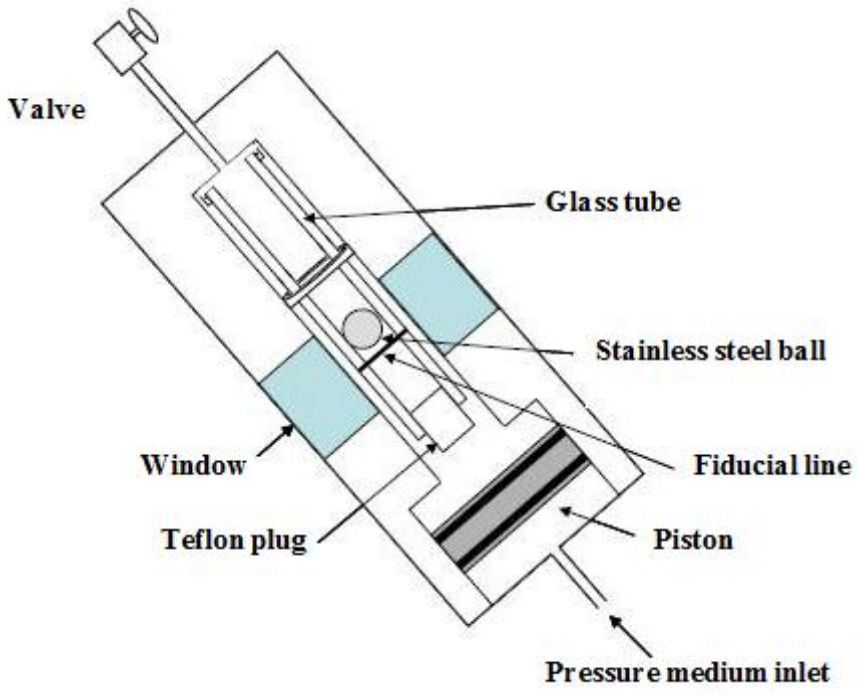

Fig. 1.7—Rolling Ball viscometer, after Tomida *et al*. (2005).

1.3.4 Oscillating-piston viscometer

The oscillating-piston viscometer consists of a piston that is driven electromagnetically at a constant force inside a chamber which contains a desired fluid.

The viscosity is related to the travel time of the piston inside the chamber. The main advantage of the oscillating-piston viscometer relative to the falling/rolling ball viscometer is that it is not required to know the density to obtain the viscosity. The oscillating-piston viscometer was used in this study and more details on the experimental procedure and the theory behind the viscosity measurement will be described in Chapter II. An oscillating-piston viscometer is shown in **Fig. 1.8**.

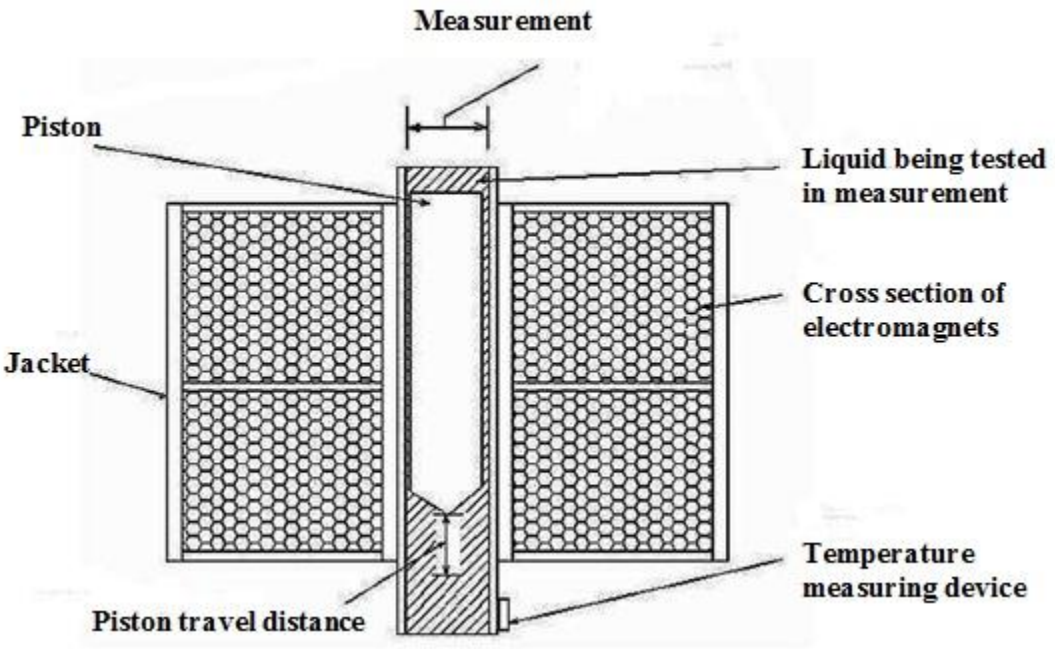

Fig. 1.8—Oscillating-piston viscometer, after Wikipedia (2011).

1.4 Natural gas viscosity data available

The first step in ensuring the validity of any gas viscosity correlation at HPHT conditions is to evaluate the measured data upon which the correlation is based. Most of the available databases of laboratory measurements are limited in terms of pressure and temperature ranges. Below is a review of the databases that are commonly used in the petroleum industry to develop gas viscosity correlations.

Carr (1953) used two Pyrex viscometers of the Rankine type to measure the viscosity of methane and three natural gas mixtures at pressures up to 10,000 psi and temperatures from 70 to 250ºF. Carr compared his measured data with accurate published data and he concluded that the maximum error is within one percent in most cases, and within two percent for the reminder.

Golubev (1959) used the capillary tube method to measure gas viscosity, using fluid samples that included pure light hydrocarbons (methane to propane), nitrogen, CO_2 and some mixtures, measured in a temperature range of –58.12 to 1292ºF, and a pressure range of 14.7 to 14,700 psia. This database is the only available database that covers HPHT conditions. However, **Fig. 1.9** shows that the data by Golubev are significantly different from the other available databases, possibly because of impurities in the gases samples, or because of a systematic error during the experiments. Thus, the accuracy of Golubev's data is uncertain and it is not recommended to use this database for the development and validation of gas viscosity correlations at HPHT conditions.

Lee (1965) collected the viscosity data of pure hydrocarbon gas, such as methane, ethane, propane and *n*-butane, and provided an organized database. Lee also used a

capillary tube viscometer and measured the viscosity of hydrocarbon gas mixtures (methane/propane, methane/butane, and methane/decane). The temperature range of Lee's database is 100 to 460ºF and the pressure range is 14.7 to 10,000 psia.

This database is one of the most comprehensive databases as it includes viscosity data for all pure hydrocarbon gases and simulated viscosity values for natural gas mixtures. However, it cannot be used for HPHT conditions because of its limited pressure range.

Gonzales *et al*. (1966) used a capillary tube viscometer to measure eight samples of natural gas, with a temperature range of 100 to 340ºF and a pressure range of 14.7 to 8,000 psia. The main difference between this database and Lee's original database is the direct measurement of natural gas viscosity, as opposed to simulated values. This database cannot be used to develop and validate HPHT gas viscosity correlations because its range of pressure and temperature conditions is not sufficiently wide.

Diehl *et al*. (1970) used a Geopal viscometer to determine the viscosity of pure hydrocarbon gas and nitrogen at a temperature between 32 and 302ºF and a pressure between 14.7 and 7,350 psia. Clearly, this database does not cover the conditions necessary for HPHT purposes.

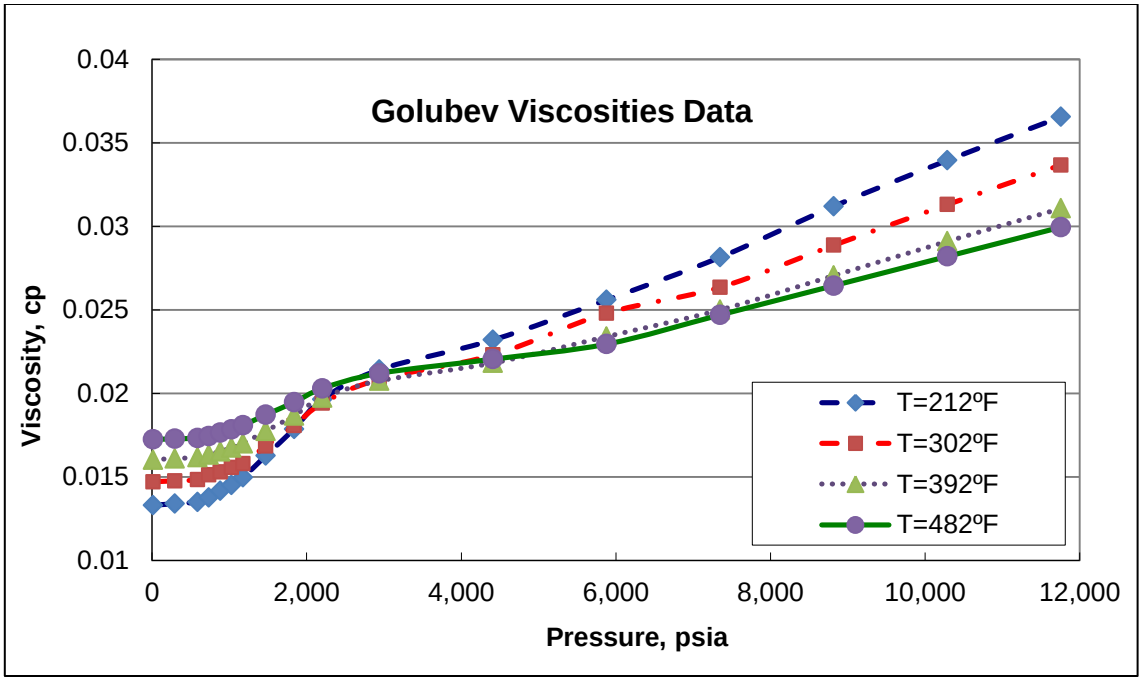

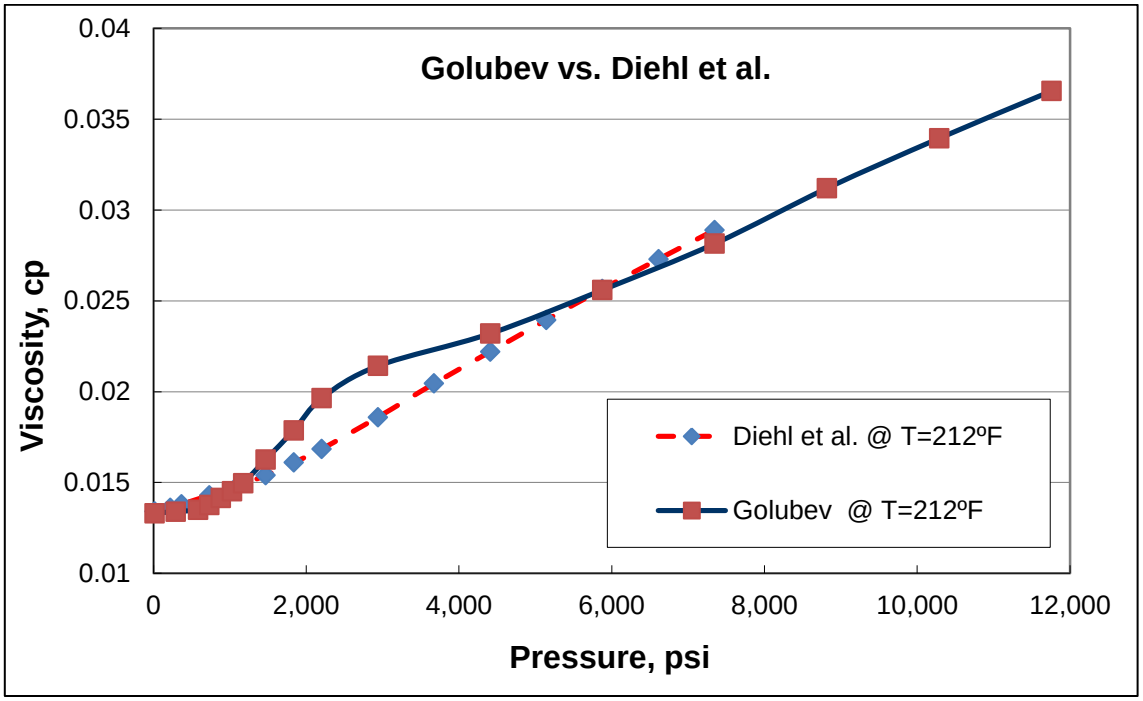

Fig. 1.9—The data by Golubev (1959) are not consistent with and show a significant difference from other available databases.

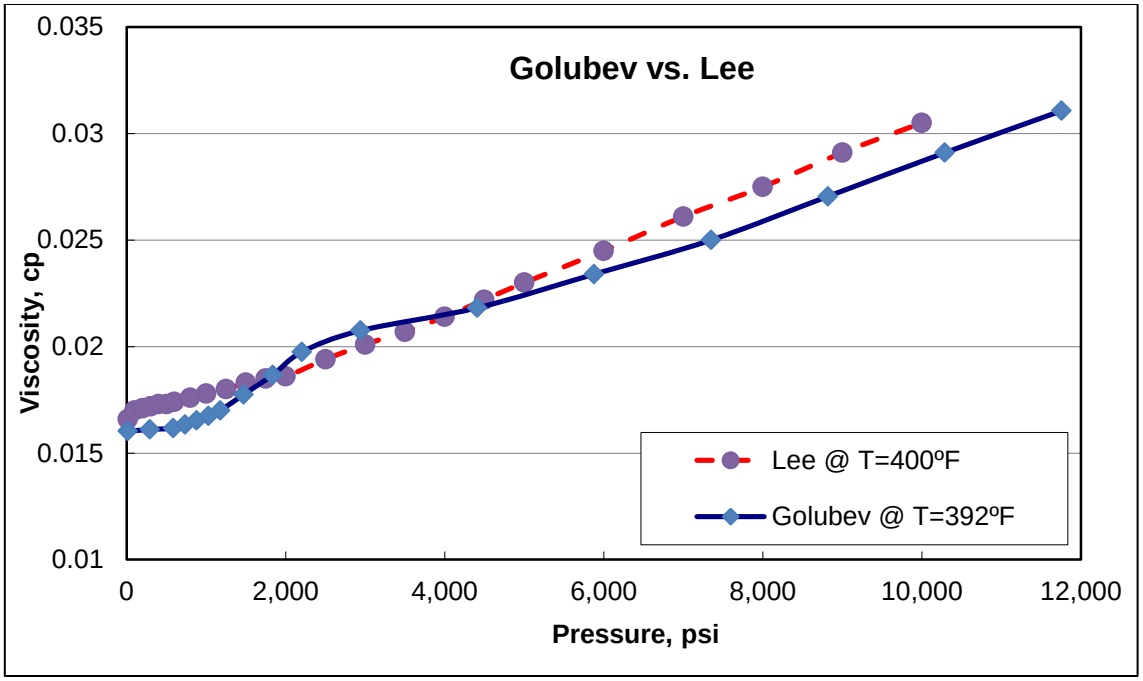
Golubev vs. Lee
Viscosity, cp
Pressure, psi
0.035
0.03
0.025
0.02
0.015
0.01
0
2,000
4,000
6,000
8,000
10,000
12,000
Lee @ T=400ºF
Golubev @ T=392ºF

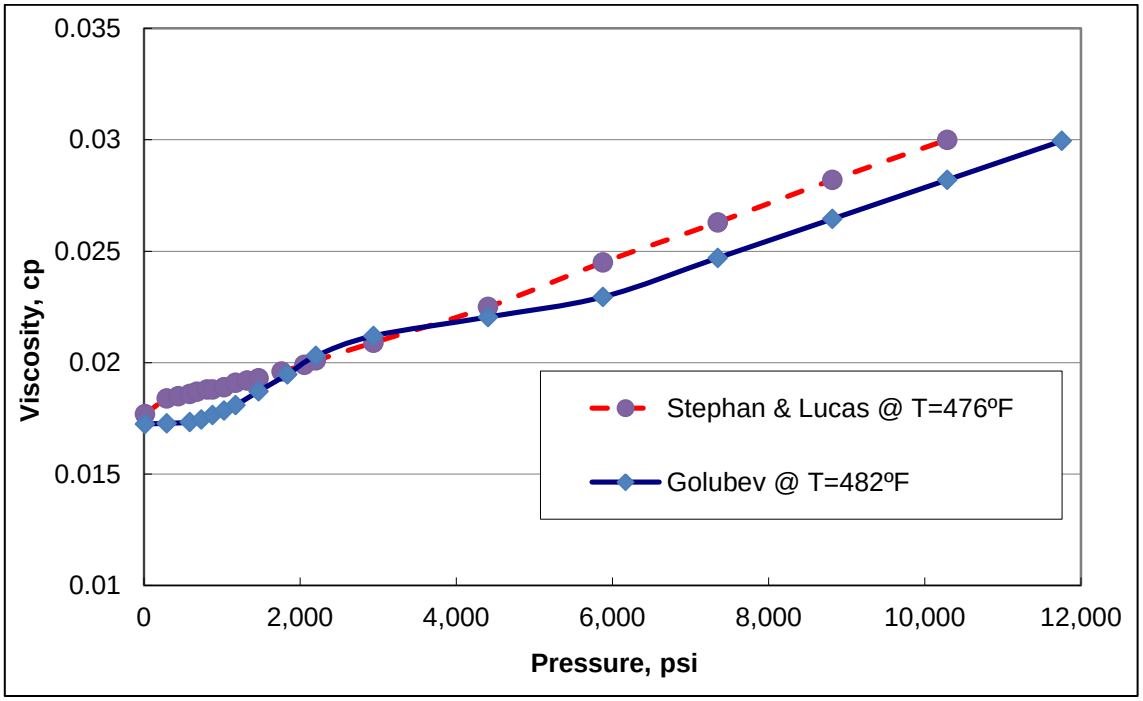
Viscosity, cp
Pressure, psi
0.035
0.03
0.025
0.02
0.015
0.01
0
2,000
4,000
6,000
8,000
10,000
12,000
Stephan & Lucas @ T=476ºF
Golubev @ T=482ºF

Fig. 1.9—Cont.

Stephan and Lucas (1979) collected a large database of gas viscosities measurements obtained by several investigators with different techniques. The viscometers used include torsional crystal, oscillating disk, rolling ball, rotating cylinder, capillary tube, and falling ball. The tested gases included pure hydrocarbons (methane to *n*-decane), nitrogen, and CO_2. The range of temperature and pressure varies from one component to another. Overall, the temperature range is 212 to 1,832ºF and the pressures range is 14.7 to 10,290 psia, making this database not fully representative of HPHT conditions in terms of pressure.

Knapstad *et al*. (1990) measured the viscosity of a mixture of *n*-decane and methane with an absolute oscillation vessel viscometer for a temperature range of 68 to 302ºF and a pressure range of 14.7 to 5,801 psia. These conditions do not reflect those of HPHT occurrences.

Canet *et al*. (2002) provided a set of viscosity data for mixtures of *n*-decane and methane. A falling body viscometer was used with mixtures containing 31.24, 48.67, 60, 75.66 and 97.75 mole % of methane. The temperature range for this database is 67.91to 212ºF and the pressure range is 14.7 to 20,305 psia, making this one of the few references that includes data at high pressure conditions, though the temperature is lower than the generally accepted value for the HPHT definition. Thus, this is a database that could be adopted to develop and validate gas viscosity correlations for HPHT gas condensates with significant amounts of heptanes-plus, but keeping in mind its temperature limitations.

Audonnet and Pádua (2003) also obtained gas viscosity for mixtures of *n*-decane and methane. Their experimental range covered temperatures from 86 to 245ºF and pressures from 14.5 to 10,877 psia. Five compositions were measured simultaneously using a vibrating-wire sensor. The reported uncertainty for the data is ±3%. Although this database could be used to evaluate the applicability of gas viscosity correlations for gas condensate with significant amounts of heptanes-plus, its range of temperature and pressure conditions does not apply to HPHT investigations.

Table 1.2 summarizes the above-mentioned databases. Note that as some information is missing from the original sources, the table cannot be exhaustive.

If the data by Golubev are excluded because of their significant drift from other available databases, it can be concluded that no database exists which fully covers HPHT conditions and reflects the typical composition of natural HPHT gas occurrences.

1.4.1 Viscosity of mixtures of methane and nitrogen

Diller (1982) measured the viscosity of mixtures of nitrogen and methane at temperatures between -279.67 and 80.33°F and at pressures to about 4,350 psia with a piezoelectric quartz crystal viscometer. The accuracy of the measurements varies from about 0.5% at high densities to about 1% at low densities. The average error ranges from about 2% at high densities to about 4% at low densities. Diller used two different mixtures of 50.115% nitrogen and 49.885% methane and also 68.341% nitrogen and 31.659% methane.

Table 1.2—Summary of available gas viscosity data

Investigator	Pure hydrocarbon gas data	Mixed hydrocarbon gases data	Temperature and Pressure range
Carr (1953)	methane	natural gas	70 to 250ºF 14.7 to 10,000 psia
Golubev (1959)	methane to *n*-butane, nitrogen, and CO_2	methane/ethane, methane/ propane, ethane/propane, CO_2/propane and natural gas	–58.12 to 1,292ºF 14.7 to 14,700 psia
Lee (1965)	methane to *n*-butane	methane/propane, methane/butane, and methane/decane	100 to 460ºF 14.7 to 10,000 psia
Gonzales *et al*. (1966)	*iso*-butane	natural gas	100 to 340ºF 14.7 to 8,000 psia
Diehl *et al*. (1970)	methane to *n*-butane, nitrogen, and CO_2	—	32 to 302ºF 14.7 to 7,350 psia
Stephan & Lucas (1979)	methane to *n*-butane, nitrogen, and CO_2	—	212 to 1,832ºF 14.7 to 10,290 psia
Knapstad *et al*. (1990)	—	*n*-decane and methane mixture	68 to 302ºF 14.5 to 5,801 psia
Canet *et al*. (2002)	—	*n*-decane and methane mixture	67.91to 212ºF 14.5 to 20,305 psia
Audonnet and Pádua (2003)	—	*n*-decane and methane mixture	86 to 245ºF 14.5 to 10,877 psia

1.4.2 Viscosity of mixtures of methane and CO_2

Jackson (1956) used a capillary tube viscometer to measure the binary gas mixtures of methane and CO_2 at temperature of 77°F and atmospheric pressure. Jackson used different proportion of methane and CO_2 in mixtures for which the composition ranged from 0 to 100 mole % of each component. In particular, Jackson measured the viscosity of mixtures which a molar% of methane of 0, 2.2, 10.3, 18.3, 29.7, 42.1, 53.7, 65.1, 73, 78.9, 85, 90.5, 93.3 and 100%. Jackson found a maximum error of ±0.2% in his measurementa.

DeWitt and Thodos (1966) used an unsteady-state capillary viscometer to measure the viscosity of three binary mixtures of methane and CO_2 at temperatures of 122, 212, 302, 392°F and pressures of 500 to 1,000 psi. The compositions of these mixtures were 24.3, 46.4 and 75.5 mole % of methane.

1.5 Well-known gas viscosity correlations

Several well-known correlations are used in the petroleum industry to estimate gas viscosity. The Lee, Gonzalez, and Eakin (LGE) correlation (1966) is one the most famous models to predict the viscosity and still the most useful and applicable correlation. The Sutton correlation (2007) is a newer model that modified the original LGE correlation. The National Institute of Standards and Technology (NIST, 2010) provides gas viscosity values based on its confidential model. Below is a review of key correlations implemented in the petroleum industry.

1.5.1 Carr, Kobayashi, and Burrrow correlation

The Carr, Kobayashi and Burrrow (1954) correlation includes two steps to estimate natural gas viscosity. First, a value of gas viscosity at atmospheric pressure is determined and the some corrections are applied to account for the effect of impurities such as N_2, CO_2 and H_2S on natural gas viscosity (**Fig. 1.10).** Dempsey (1965) developed **Eqs.1.3** through **1.7**, which are used in this calculation procedure. The value of viscosity at atmospheric conditions is adjusted to reservoir conditions by corrections based on the charts presented in **Figs. 1.11** and **1.12**. A value of gas viscosity ratio (μ_g/μ_{1atm}) is estimated from either of these figures and used to adjust the value of gas viscosity at atmospheric pressure to reservoir conditions.

$$\mu_{1atm} = (\mu_{1atm}\ \text{uncorrected}) + (N_2\ \text{correction}) + (CO_2\ \text{correction}) + (H_2S\ \text{correction}) \quad \text{..... (1.3)}$$

$$\mu_{1atm}\ \text{uncorrected} = (1.709\times10^{-5} - 2.062\times10^{-6}\gamma_g)T + 8.188\times10^{-3} - 6.15\times10^{-3}\log\gamma_g \quad \text{..... (1.4)}$$

$$N_2\ \text{correction} = y_{N_2}\left[(8.48\times10^{-3})\log\gamma_g + 9.59\times10^{-3}\right] \quad \text{..... (1.5)}$$

$$CO_2\ \text{correction} = y_{CO_2}\left[(9.08\times10^{-3})\log\gamma_g + 6.24\times10^{-3}\right] \quad \text{..... (1.6)}$$

$$H_2S\ \text{correction} = y_{H_2S}\left[(8.49\times10^{-3})\log\gamma_g + 3.73\times10^{-3}\right] \quad \text{..... (1.7)}$$

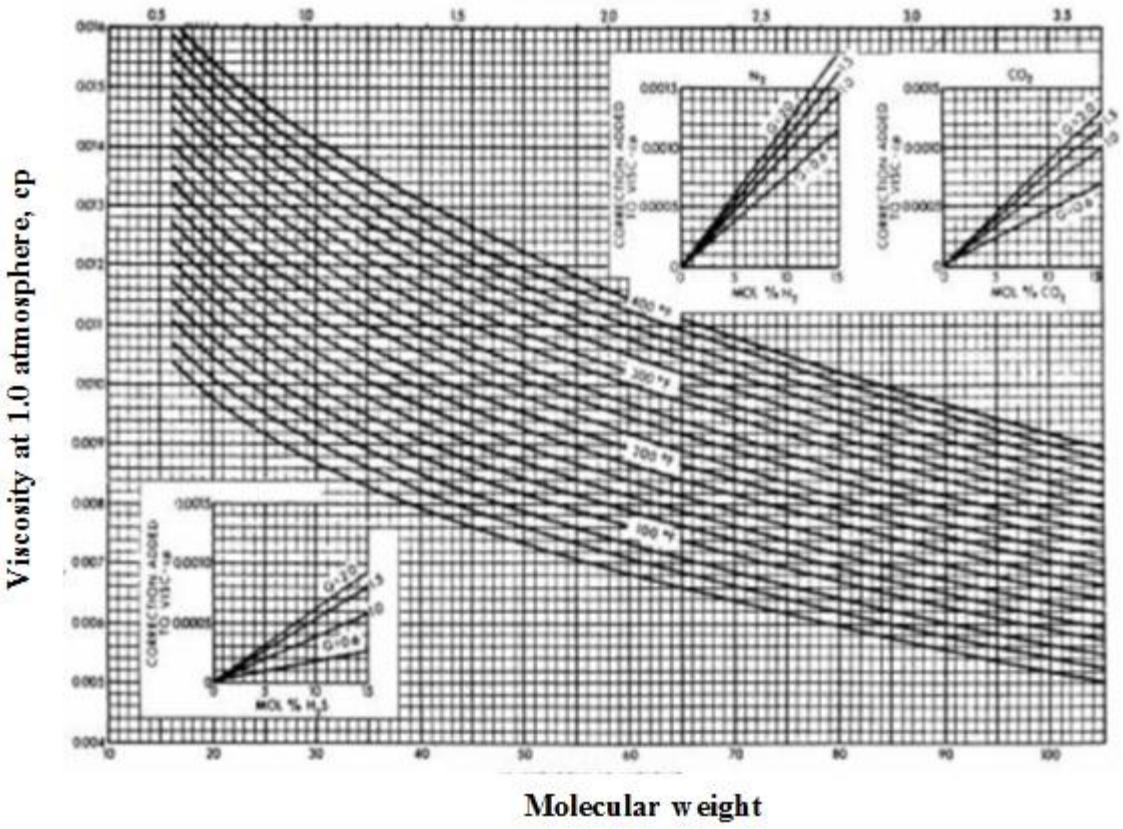

Fig. 1.10—Viscosity of hydrocarbon gas mixture at atmospheric pressure and correction for nitrogen, CO_2 and H_2S, from Carr *et al.* (1954).

The advantage of the Carr *et al*. correlation is that it can correct for the effect of non-hydrocarbons that significantly affect the gas viscosity. According to Carr *et al*., this correlation leads to a 1.5% absolute error in estimating gas viscosity.

One limitation of the Carr *et al*. correlation is that it is based on a limited (30) number of data points. These data points are related to measurements of viscosities of pure gases, such as nitrogen, CO_2, methane, ethane, ethylene, propane, and a few mixture samples. Thus, the universal accuracy of this correlation for real hydrocarbon reservoirs

still needs to be proved. Carr *et al*. claimed that their correlation is appropriate for gas specific gravities from 0.55 to 1.55 and temperatures from 100 to 300°F, but gave no information about the corresponding pressure range.

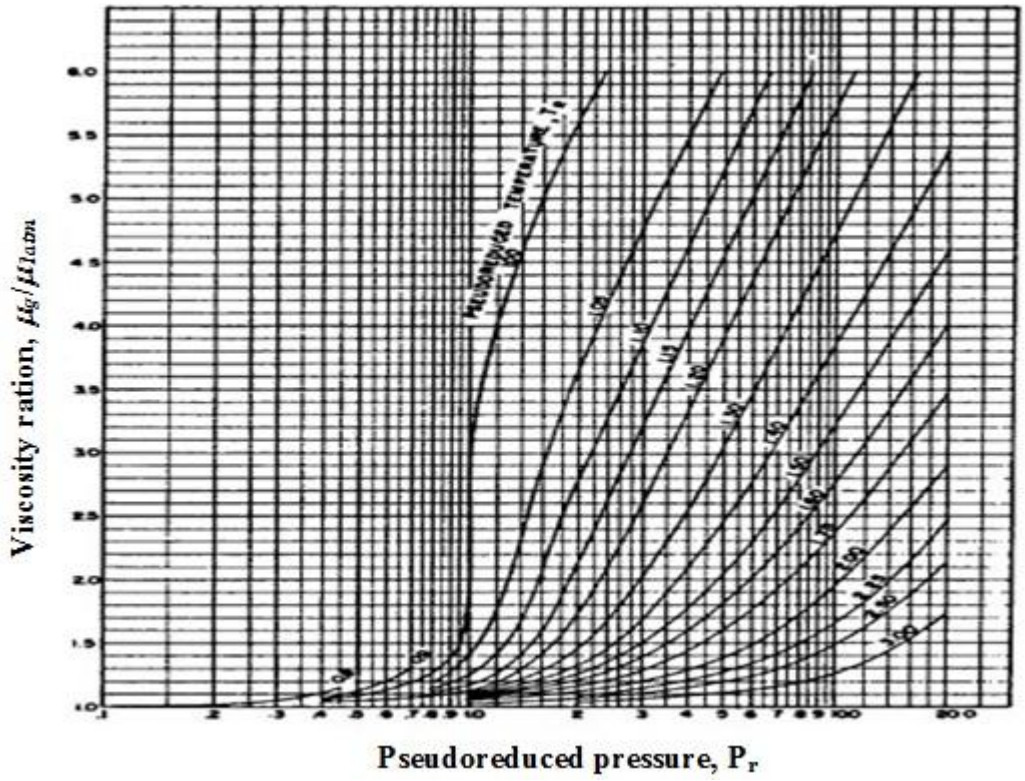

Fig. 1.11—Viscosity ratio vs. pseudo-reduced pressure for hydrocarbon gases, from Carr *et al*. (1954).

Another inconvenience of the Carr *et al*. correlation comes from the use of charts to get gas viscosity at the conditions of interest. To date, there is no satisfactory curve fit for Figs. 1.11 and 1.12, which have not been digitized for use in computers over theirs entire range.

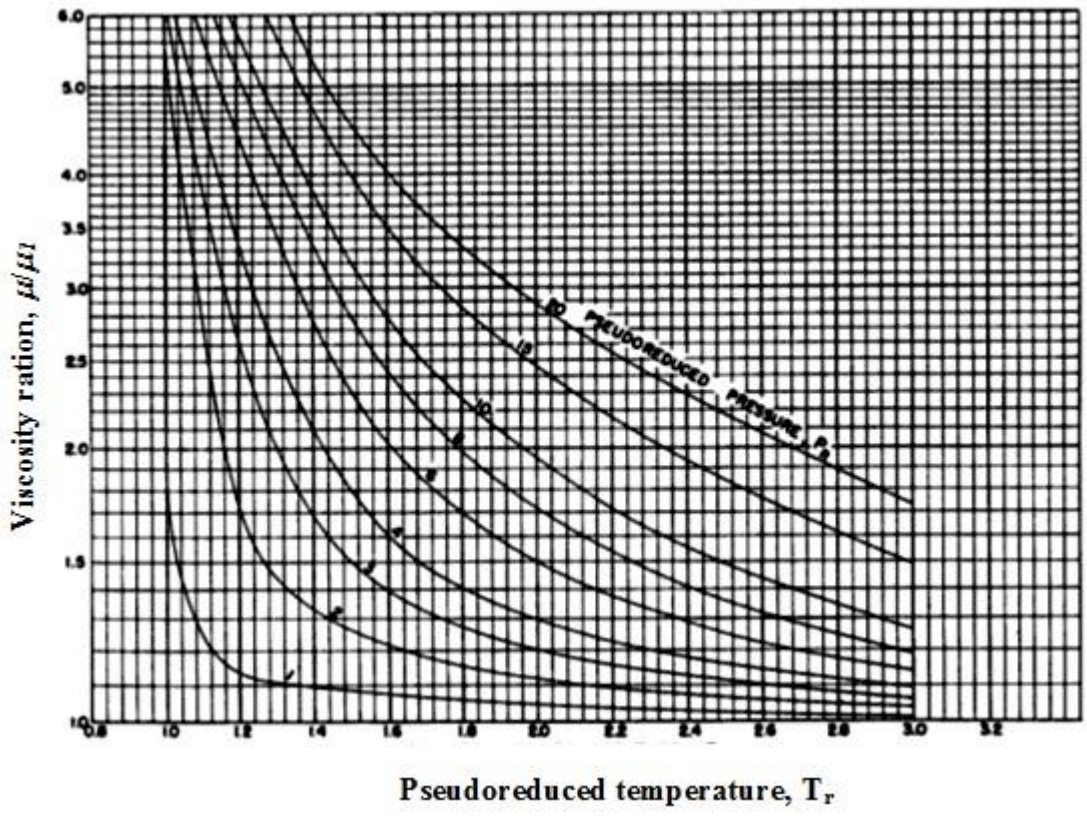

Fig. 1.12—Viscosity ratio vs. pseudo-reduced temperature for hydrocarbon gases, from Carr *et al.* (1954).

1.5.2 Jossi, Stiel, and Thodos Correlation (JST) correlation

Jossi, Stiel, and Thodos (1962) proposed a new correlation for gas mixture viscosity. They included pure components such as argon, nitrogen, oxygen, CO_2, sulfur dioxide, methane, ethane, propane, butane, and pentane in their correlation. Their database included methane viscosity data from Comings and Egly (1940), Comings *et al*. (1944), Baron *et al*. (1959), Swift *et al*. (1959), and Kuss (1952), The correlation required

reduced density at a specific temperature and pressure, critical properties of the gas as well as the molecular weight to predict gas viscosity.

The JST correlation for gas viscosity is given as:

$$\left[(\mu_g - \mu^*)\xi + 10^{-4}\right]^{\frac{1}{4}} = f(\rho_r) \quad \text{.....(1.8)}$$

where:

$$f(\rho_r) = \ 0.1023 + 0.023364\rho_r + 0.058533\rho_r{}^2 - 0.0400758\rho_r{}^3 + 0.0093324\rho_r{}^4 \quad \text{.....(1.9)}$$

$$\xi = \frac{T_c^{\frac{1}{6}}}{M^{\frac{1}{2}} p_c^{\frac{2}{3}}} \quad \text{.....(1.10)}$$

Jossi, Stiel, and Thodos (1962) reported an average absolute error(AAE) of 4% for their correlation comparing to the measured data.

1.5.3 Lee, Gonzalez, and Eakin (LGE) correlation

Lee *et al*. (1966) derived correlations by modifying that of Starling and Ellington (1964) to predict gas viscosity at reservoir conditions. The LGE correlation is based upon measured data of pure component gases and eight natural gas mixtures with specific gravities of less than 0.77. **Eqs. 1.8** through **1.11** can be used to estimate the gas viscosity, provided that the molecular weight and density at the relevant conditions are known.

$$\mu_g = 10^{-4} K \exp(X \rho_g{}^Y) \quad \text{.....(1.11)}$$

$$K = \frac{(9.379 + 0.01607M)T^{1.5}}{209.2 + 19.26M + T} \quad \text{.....(1.12)}$$

where

$$X = 3.448 + \left[\frac{986.4}{T}\right] + 0.01009M \quad \text{.....(1.13)}$$

$$Y = 2.447 - 0.2224X \quad \text{.....(1.14)}$$

The LGE correlation fitted 234 data points to within a 2% average absolute error at low pressure and 4% at high pressure, providing better results for gas specific gravity less than 1. It can be used to predict gas viscosities at temperatures from 100 to 340^{o}F and pressures from 100 to 8,000 psia.

Although this correlation does not take into account natural gases that contain high quantities of non-hydrocarbon components, it is considered to be reliable to predict the viscosity of natural gases below HPHT conditions.

Jeje and Mattar (2004) compared the LGE correlation to the Carr *et al*. correlation for both sweet and sour gases. They found that, for sweet gases, both give almost identical results. However, for sour gases, the differences between the LGE correlation and Carr *et al*. correlation can be significant and the former, which was derived for sweet gases only, should not be applied to sour gases.

1.5.4 Londono correlation

Londono (2001) optimized the JST and LGE correlation by using a total of 13656 data points from former investigators and proposed two different models based upon the

JST and LGE formulation to predict the gas viscosity. Londono found an AAE of 5.26% for the JST correlation, and 3.34% for the LGE correlation. Londono then refitted these models with his optimized correlations and obtained an AAE of 4.43 for the optimized JST correlation and 2.29% for the optimized Lee correlation. The optimized JST correlation is given as:

$$\left[\left(\mu_g - \mu^*\right)\xi + 10^{-4}\right]^{\frac{1}{4}} = 0.170018 + 0.990675\rho_r - 0.407490\rho_r^2 - 0.066959\rho_r^3 + 0.007359\rho_r^4 \quad (1.15)$$

$$\rho_r = \frac{\rho_g}{\rho_c} \quad (1.16)$$

$$\xi = \frac{T_c^{4.76271}}{M^{3.83480} p_c^{2.72582}} \quad (1.17)$$

The optimized LGE correlation is

$$\mu_g = 10^{-4} K \exp\left(X \rho_g{}^{Y}\right) \quad (1.18)$$

$$K = \frac{(19.9216 + 0.0326212M)T^{1.38392}}{210.076 + 18.5762M + T} \quad (1.19)$$

$$X = 3.84699 + \left[\frac{991.303}{T}\right] + 0.00924455M \quad (1.20)$$

$$Y = 2.11068 - 0.136279X \quad (1.21)$$

1.5.5 Sutton correlation

Sutton (2005) developed a correlation for associated gas and gas condensate viscosity, based on a large database from previous investigators that included viscosity data for methane, propane, methane/propane, methane/butane, methane/*n*-decane, and natural gases, plus gas condensate viscosities measured in the laboratory. Sutton also used methane/decane binary mixtures to estimate the behavior of gas condensates with significant amounts of heptanes-plus. The database does not include pure methane viscosities data above 10,000 psia; therefore, the correlation is not proved to be suitable for HPHT gas reservoirs.

$$\mu_{gsc}\xi = 10^{-4}[0.807T_{pr}^{0.618} - 0.357\exp(-0.449T_{pr}) + 0.340\exp(-4.058T_{pr}) + 0.018] \quad (1.22)$$

$$\mu_g = \mu_{gsc}\exp\left(X\rho_g^{\,Y}\right) \quad (1.23)$$

where

$$\xi = 0.949\left(\frac{T_{pc}}{M^3 p_{pc}^4}\right)^{\frac{1}{6}} \quad (1.24)$$

$$X = 3.47 + \left[\frac{1.588}{T}\right] + 0.0009M \quad (1.25)$$

$$Y = 1.66378 - 0.04679X \quad (1.26)$$

1.5.6 National Institute of Standards and Technology model

NIST (2010) developed a computer program to predict thermodynamic and transport properties of hydrocarbon fluids. The program, called SUPERTRAP, uses the principle of "extended corresponding states" and was developed from pure components and mixture data. The maximum pressure and temperature that can be used in the program are 44,100 psia and 1,340°F, respectively. However, its applicability to HPHT conditions has not been validated against experimental data.

1.5.7 Viswanathan correlation

Viswanathan (2007) used NIST values at temperatures of 100, 150, 200, 250, 300, 350, and 400^{o}F and pressures of 5000 to 30000 psia to modify the LGE correlation and improve it for HPHT condition. Since Viswanathan did not use any measured data for his correlation, the latter has not been validated against any measured data.

The Viswanathan correlation is as follow:

$$\mu_g = K \exp\left(X \rho_g{}^{Y} \right) \quad (1.27)$$

$$K = \frac{0.0001*(5.0512 - 0.2888 M_w) T^{1.832}}{-443.8 + 12.9 M_w + T} \quad (1.28)$$

where

$$X = -6.1166 + \left[\frac{3084.9437}{T} \right] + 0.3938 M_w \quad (1.29)$$

$$Y = 0.5893 - 0.1563 X \quad (1.30)$$

1.6 Research objective

The main objective of this research is to design and conduct appropriate experimental work to measure the gas viscosity of mixtures of methane and non-hydrocarbon gases (CO_2 and nitrogen) at HPHT conditions to develop a gas viscosity correlation that covers the HPHT range and can be readily used by the industry.

Chapter II describes in detail the experimental design, the procedure, the planning and the theory behind all the measurements. The main source of error and difficulties encountered during the experimental campaign are also described. The applicability of the rolling ball viscometer to the measurement of gas viscosity is discussed in Chapter II and a new calibration equation is proposed to improve the performance of the viscometer. To validate the new proposed equation, CO_2 viscosity was measured at different pressures and temperatures.

The viscosity measurements of gas mixtures and their accuracy are presented in Chapter III.

The ultimate target of this research is to develop a HPHT gas viscosity correlation based upon the measured gas viscosity data. Chapter IV explains the approach to develop a correlation.

Another objective of this research is to determine the effect of inaccurate gas viscosity estimation on production forecasting. Chapter V summarizes the sensitivity analysis on gas viscosity uncertainty to forecast the ultimate production for a synthetic field case. The accuracy of the current gas viscosity models to estimate the gas viscosity is also evaluated.

Chapter VI summarizes the conclusions drawn from this systematic experimental study on gas viscosity and also the recommendations for future work.

CHAPTER II

EXPERIMENTAL STUDY

2.1 Experimental facility

The facility used for this work consists of a gas source, a gas booster system, a viscometer, and a data acquisition system. **Fig. 2.1** shows the schematic diagram of the entire viscosity measuring system.

Mixtures of nitrogen and methane and also CO_2 and methane (obtained with accurate mixing procedure) were used in this work. A cylinder of mixed gas at 2,000 psig is connected to the inlet of the gas booster system to provide the desired fluid for testing.

2.1.1 Gas booster system

The gas booster system consists of a hydraulic pump coupled with a booster cylinder to compress the inlet gas from 2,000 psig and up to 25,000 psig. The system is rated for use up to 30,000 psig.

2.1.2 Oscillating-piston viscometer

Oscillating-piston viscometer which includes the Cambridge SPL440 High Pressure Research Viscosity sensor was used to measure the viscosity of the gas at HPHT conditions, with a manufacture reported accuracy of 1% of the full scale in the manual of the sensor. The system was integrated with RS-232 serial communication support, allowing synchronization of the measurements with a desktop computer.

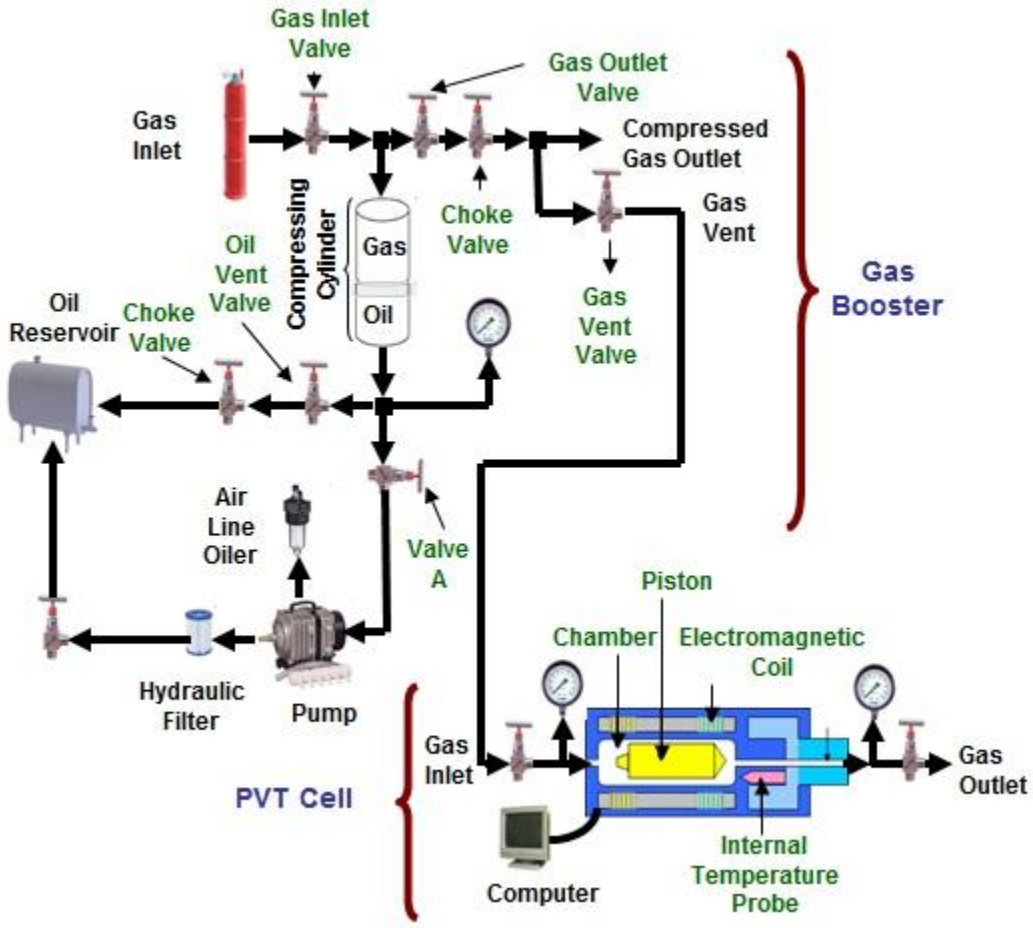

Fig. 2.1—Schematic diagram of the viscosity measurement system including gas booster and viscometer.

2.2 Theory

The oscillating-piston viscometer includes a piston placed inside a chamber. Fluid is contained in the annular gap between the piston, with radius r_p and length L, and a chamber, with inner radius r_c. The piston is driven axially by a magnetic force, F,

provided by two coils located at two ends of the chamber. The travel time of the piston to move from one end to the other end and come back to its initial position is accurately measured. This travel time is correlated through **Eq. 2.6** to the viscosity of the contained fluid. **Fig. 2.2** shows the geometry of the piston and chamber. For simplicity, the following assumptions are made in the calculations:

1. There is no acceleration during the piston movement. This is a reasonable assumption since the acceleration time is very short compared to the total travel time of the piston.
2. The test fluid is Newtonian which is the case in these experiments.
3. The electromagnetic force is constant and uniform throughout the experiment.
4. Gas viscosity is constant inside the chamber. Since the measured pressure drop between the two ends of the chamber is less than 10 psi and the temperature distribution is uniform, this is reasonable assumption.
5. Chamber and piston are made of the same material and have the same roughness.
6. The piston does not touch the wall of the chamber.
7. There is no gas slip on the surface of piston or chamber.
8. Flow around the piston is always laminar.

Dealy (1982) described the relationship between viscosity and travel time of the piston as follows:

The shear stress at the wall of the sliding piston related to the magnetic force, F, is given by **Eq. 2.1**.

$$\tau_w = -\tau_{rz}(r_i) = \frac{F}{2\pi r_c L} \quad \text{..... (2.1)}$$

Eq. 2.2 describes the velocity profile for a Newtonian fluid.

$$v(r) = V\left(\frac{\ln r / r_p}{\ln r_c / r_p}\right) \quad \text{..... (2.2)}$$

The shear rate at the wall of the sliding piston is given by **Eq. 2.3**.

$$\gamma_w = -\left(\frac{\partial v}{\partial r}\right)_{r_i} = \frac{V}{r_c \ln(r_p / r_c)} \quad \text{..... (2.3)}$$

The viscosity of a Newtonian fluid can then be calculated as follows:

$$\mu = \frac{\tau_w}{\gamma_w} = \frac{F \ln(r_c / r_p)}{2\pi L V} \quad \text{..... (2.4)}$$

The velocity of the piston can be obtained using **Eq. 2.5** where t_{up} is the time that the piston moves from the left end to the right end of the chamber and t_{down} is the time that the piston moves from right to left.

$$V = \frac{2L}{t_{up} + t_{down}} \quad \text{..... (2.5)}$$

replacing Eq. 2.5 in Eq. 2.4 gives:

$$\mu = \frac{F \ln(r_c / r_p)\left(t_{up} + t_{down}\right)}{4\pi L^2} \quad \text{..... (2.6)}$$

This equation should be calibrated with a known viscosity fluid and the effect of the pressure and temperature should also be taken into account to get more accurate result.

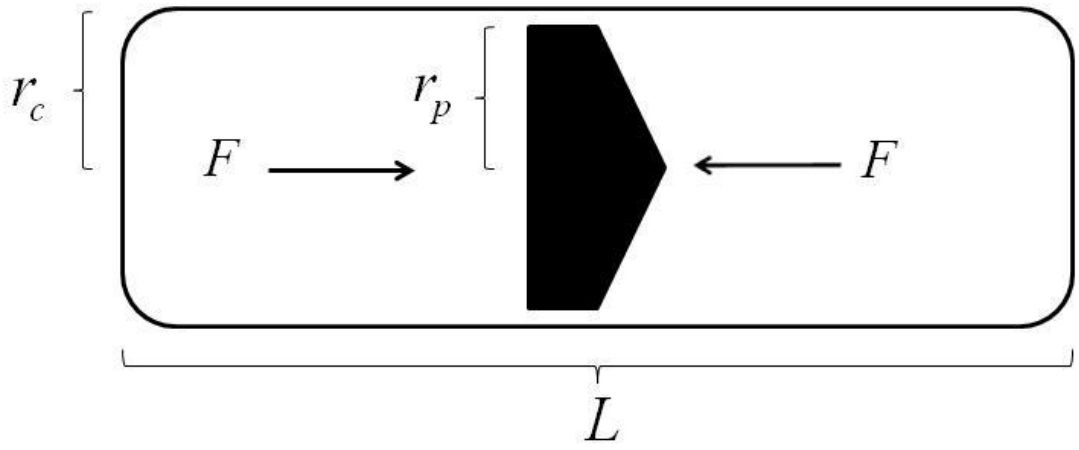

Fig. 2.2—Piston moves back and forth inside the chamber driven by magnetic force, the travel time of the piston relates to the viscosity of the contained fluid.

2.2.1 Viscosity equation calibration

Eq. 2.6 should be calibrated with a fluid of known viscosity; two calibration coefficients, K and K_2, can be added to **Eq. 2.6** as shown in **Eq. 2.7**.

$$\mu = K\left[\frac{F\ln(r_c / r_p)\left(t_{up} + t_{down}\right)}{4\pi L^2}\right] + K_2 \quad \text{..... (2.7)}$$

Table 2.1 provides the geometric description of the viscometer. **Eq. 2.8** defines the parameter of K', which includes the piston and chamber geometry and the electromagnetic force applied to the piston.

$$K' = \frac{F\ln(r_c / r_p)}{4\pi L^2} \quad \text{..... (2.8)}$$

Table 2.1—Dimensions of chamber and piston (Ling, 2010)

Overall length of piston (Include the cone)	0.9412	in
Length of piston flank(rectangle part, exclude height of cone)	0.87658	in
Outer diameter of piston	0.312	in
Base angle of the cone (θ)	22.5	degree
Height of the cone	0.06462	in
Surface area of the cone(exclude base area)	0.07808	in^2
Surface area of the piston flank (exclude the base and cone)	5.50773	in^2
Weight of piston	4.807	gr
Inner diameter of chamber	0.314	in
Length of chamber	1.4	in

Since we assumed that the piston and chamber geometry and also the electromagnetic force remain constant during the experiment, Eq. 2.7 can be simplified as **Eq. 2.9**.

$$\mu = K_1\left[\left(t_{up} + t_{down}\right)\right] + K_2 \quad \text{..... (2.9)}$$

where K_1 is

$$K_1 = K' \times K \quad \text{..... (2.10)}$$

The Cambridge SPL440 High Pressure Research Viscosity sensor only returns a value of "measured viscosity", without providing any information about the calibration coefficients K_1 and K_2. **Fig. 2.3** shows the viscosity data returned by the Cambridge SPL440 High Pressure Research Viscosity sensor against loop time. The viscosity was measured for mixture of 95% methane and 5% nitrogen for different temperatures up to

300°F and pressure up to 20,000 psi. A linear model was fitted to the data; as shown in the graph, the R^2 is pretty close to unity and it confirms the goodness of the fit. The calibration coefficients K_1 and K_2 can be determined from the fitted model equation. **Eq. 2.11** represents the calibrated equation for the oscillating-piston viscometer.

$$\mu_m = 0.006326\left(t_{up} + t_{down}\right) - 0.005234 \quad \text{..... (2.11)}$$

Eq. 2.11 does not account for the pressure and temperature effect. Based on the material properties of the sensor, the manufacturer provided **Eq. 2.12** to compensate for the effect of pressure on the measured data.

$$\mu_C = \mu_m * ((A + 0.0000461 * p) / A)^{2.875} \quad \text{..... (2.12)}$$

where

p = pressure, psia

μ_m = measured viscosity, cp

μ_c = pressure-corrected viscosity, cp

A = annulus (measurement chamber diameter-piston diameter) in thousandths of an inch.

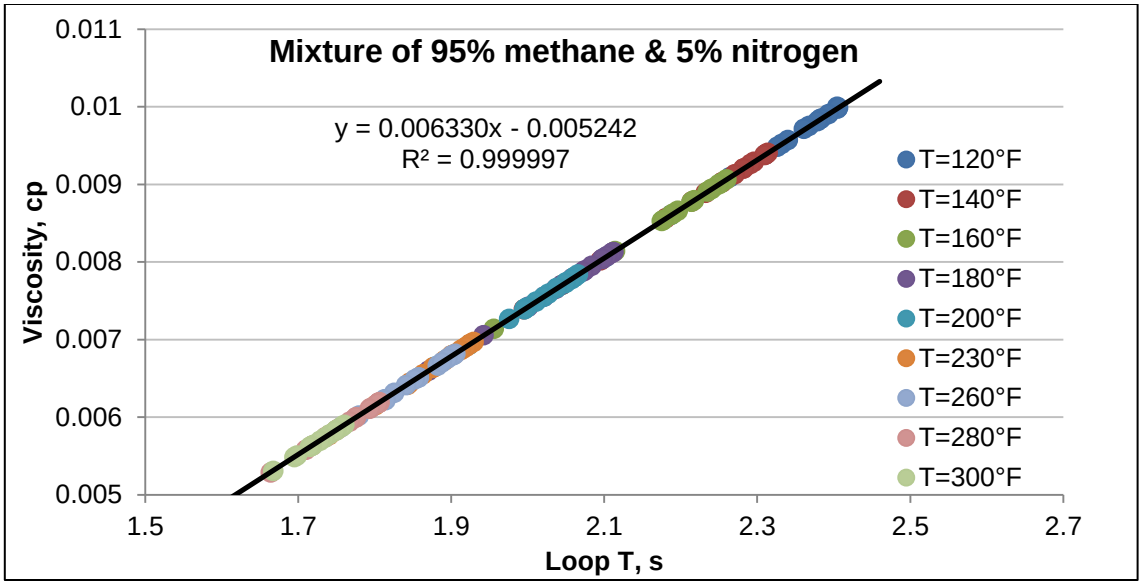

Fig. 2.3—Calibration coefficients K_1 and K_2 can be obtained by plotting viscosity data provided by Cambridge SPL440 High Pressure Research Viscosity sensor against loop time.

Fig. 2.4 shows that the Eq. 2.12 does not properly compensate for pressure, and it also neglects the effect of temperature on the material properties of the sensor.

To determine the influence of pressure and temperature, we used a computer-based statistical algorithm created by Xue *et al*. (1997) to perform an optimal non-parametric regression of the data. This algorithm yields an optimal regression of data, but does not provide a functional form for the correlation. To develop a correlation that includes the effect of pressure and temperature into the viscometer equation, a non-linear regression technique was used and **Eq. 2.13** was developed. To honor the gas viscosity at low-moderate pressures provided by former investigators, the LGE correlation was used as the calibration goal. The data were calibrated to the LGE correlation estimates at a

pressure range of 5,000 to 8,000 psig using pressure and temperature as variables in the calibrating equation.

$$\mu = \frac{0.000642P - 0.00617T + 4.324428}{204.8737} - \frac{70.5925\left[\left(0.006326\left(t_{up} + t_{down}\right) - 0.005234\right)\left((A + 0.0000461 * P)/A\right)^{2.875}\right]}{204.8737} \quad (2.13)$$

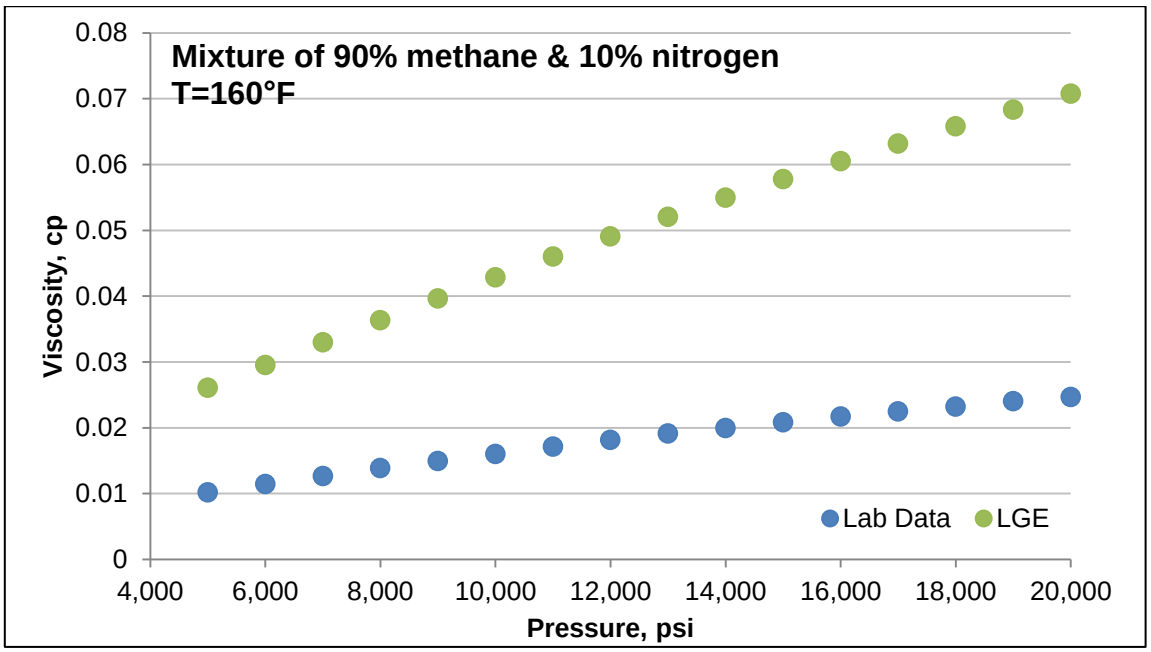

Fig. 2.4—Lab data do not match with the LGE model at low and moderate pressures after applying the manufacturer provided compensation equation, because the compensation equation neglects the effect of temperature, and underestimates the effect of pressure on Cambridge SPL440 High Pressure Research Viscosity sensor.

Fig. 2.5 shows that after correcting the measured data to include pressure and temperature effects, a good match between corrected lab data and the LGE model can be achieved at low and moderate pressures.

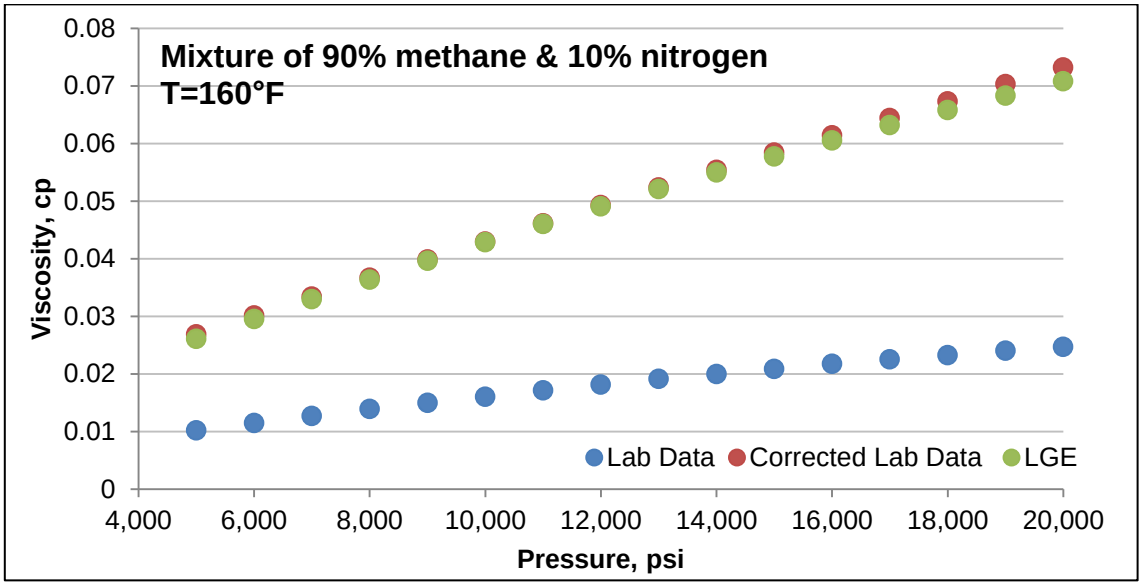

Fig. 2.5—Corrected lab viscosity data matches with the LGE model at low and moderate pressures.

2.3 Measurement procedure

The measurement procedure of gas viscosity involves boosting up the gas pressure and then measuring the travel time of the piston inside the chamber at a certain temperature, and finally analyzing the data and using the viscosity equation to correlate the gas viscosity to the travel time of the piston.

2.3.1 Gas pressurizing procedure

The following steps are followed to pressurize the desired gas up to the certain pressure; the following steps should be taken to boost up gas pressure:

1. Close all the valves except the outlet valve of the gas bottle and the inlet valve of the gas booster and let the gas booster cylinder be filled with the gas by pushing the piston down.
2. Open the oil vent valves and let the remaining hydraulic oil in the gas booster cylinder move into the oil reservoir. This lets the piston fully come down, so that more gas can be accommodated in the gas booster cylinder. When the pressure inside the gas booster cylinder and the gas bottle equalize, close all the valves, including outlet valve of the gas bottle and inlet valve of the gas booster, and also oil vent valves.
3. Open valve A, which controls the air supply for the hydraulic pump. Then use the regulator and slowly close it to operate the pump and boost up the gas pressure to the desired pressure.
4. Close valve A and release the regulator to avoid pressurizing the gas accidently and make sure that all valves are closed.
5. Open the gas outlet and let the gas enter the viscometer slowly.
6. After finishing the experiment, open the oil vent valve to decrease the gas pressure to atmospheric, and open the gas vent valve to vent the inside gas out of the gas booster system.

Note that, the gas booster cylinder pressure is always monitored viatwo different pressure gauges to make sure that it is not going beyond the capacity of the gas booster and -more importantly- the capacity of the viscometer. Any small leakage can be detected by a leak detector placed behind the gas booster and also by monitoring the gas booster cylinder pressure.

Pressurizing the gas is a critical step which should be done slowly in order to minimize the safety hazard and the risk of damage to the equipment. The viscometer system used in this research is illustrated in **Fig. 2.6**.

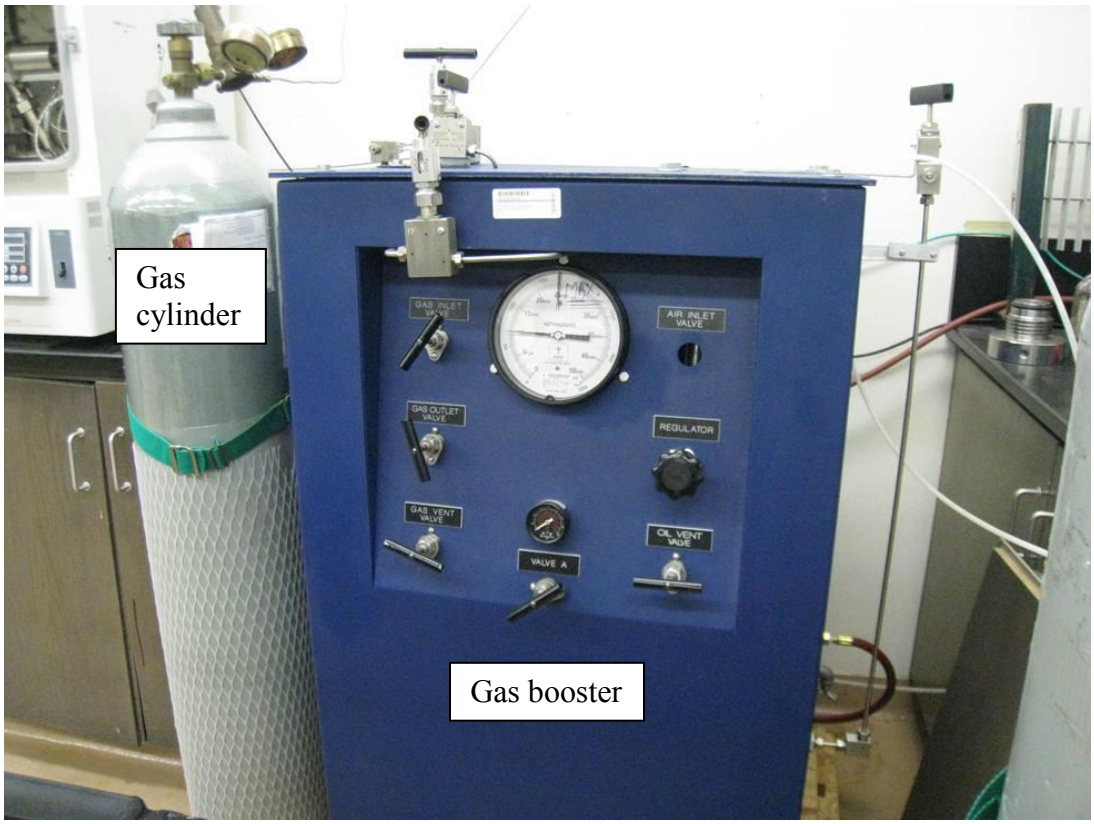

Fig. 2.6—Pressure boosting system includes a hydraulic pump and a gas cylinder.

Valves and O-rings are very sensitive and can be easily damaged by pressurizing the gas quickly and improperly. It is recommended to always run several experiments at low pressure and check all the valves and pipeline to make sure that everything is set properly, and follow the facility's operating instructions during each step of the experiment.

2.3.2 Gas viscosity measurement

After pressurizing the gas to the desired pressure, the viscometer chamber should be filled with the gas by opening the viscometer gas inlet valve. The viscometer used for this research was placed inside an oven manufactured by Yamato Scientific America Inc. The operation temperature of the oven varies from 0 to 608^{o}F. The overheat protection function keeps the viscometer in an appropriate temperature range and prevents system damage. The viscometer system used in work is shown in **Fig. 2.7**.

Temperature has the biggest impact on gas viscosity variation, therefore it is important to ensure that the temperature is stabilized before running any experiment. **Fig. 2.8** shows that in these experiments the temperature had to be let stabilize for least 10 hrs before running any experiment; otherwise the accuracy of the data would be doubtful.

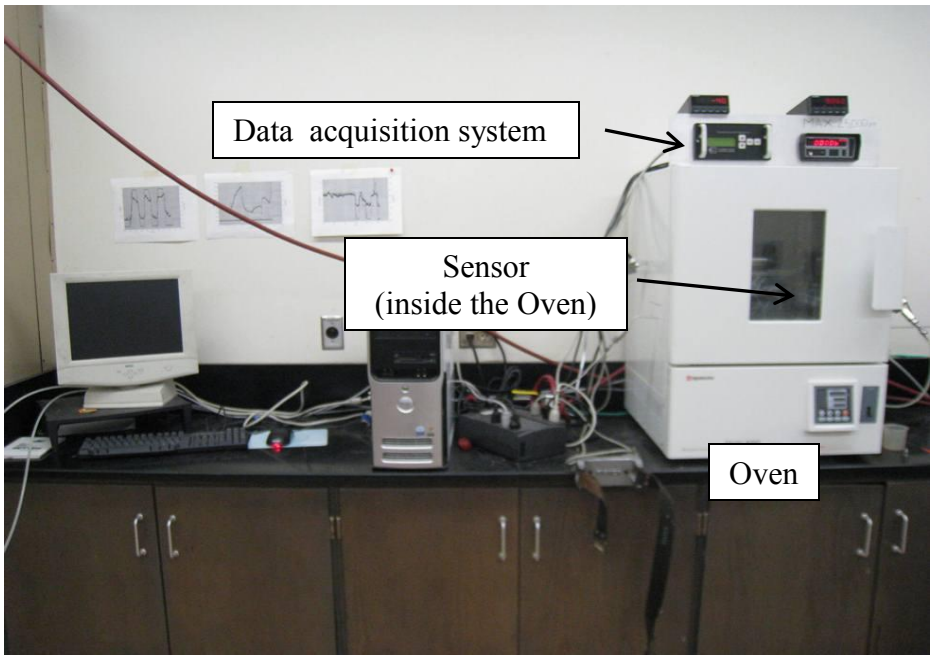

Fig. 2.7—Viscometer system includes an oven, a sensor and a data acquisition system.

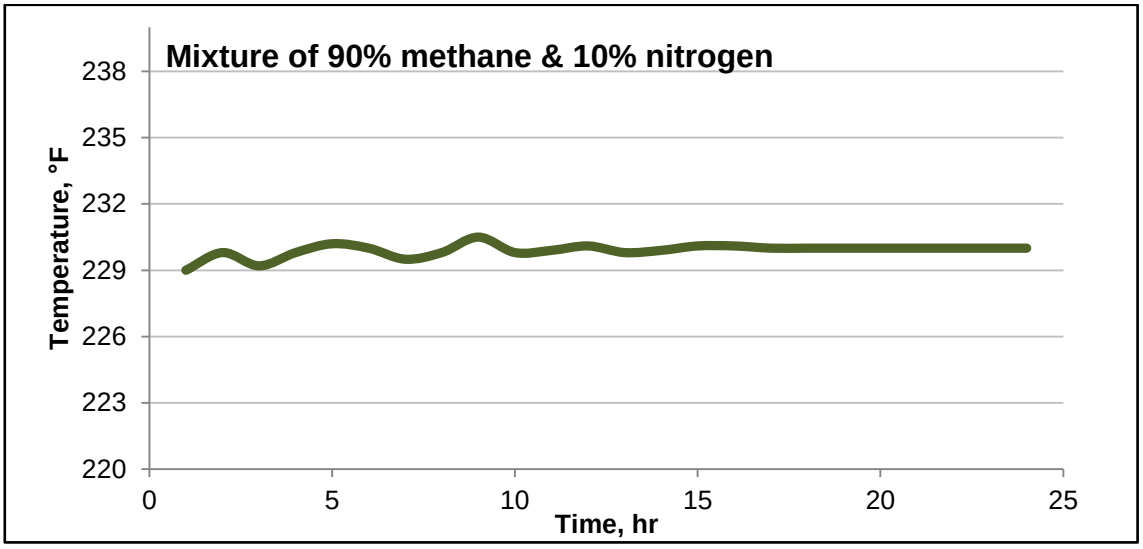

Fig. 2.8—Temperature needs to be stabilized at least for 10 hrs before running any experiment.

The Cambridge SPL440 High Pressure Research Viscosity sensor is used to measure the travel time of the piston. The sensor's measurable range for gas viscosity is 0.02 to 0.2 cp and the accuracy reported by the manufacturer is around 1% of the full scale. The maximum temperature that the sensor can stand is 380°F and the maximum pressure is 25,000 psi. **Fig. 2.9** shows the Cambridge SPL440 High Pressure Research Viscosity sensor used for this research.

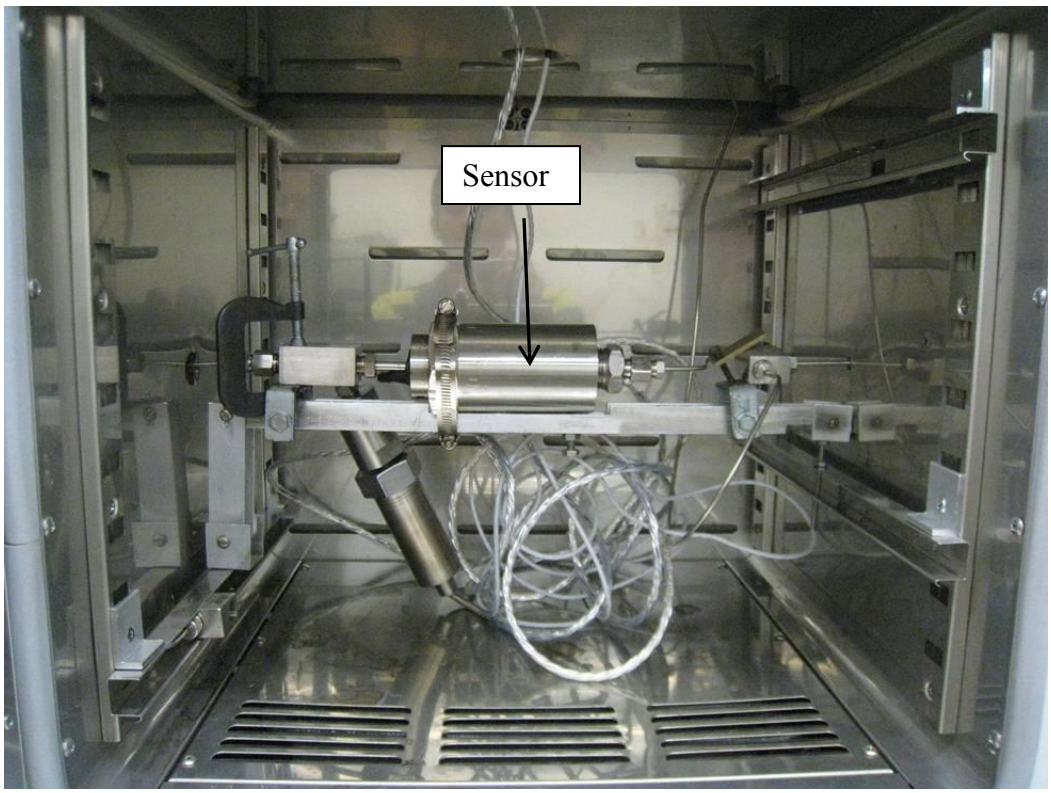

Fig. 2.9—Cambridge Viscosity SPL440 sensor is placed inside the oven.

The data acquisition system connected to the sensor transfers all the measurements to a desktop computer. DasyLab software is used to manipulate the measured data and

control the measuring system. The pressure and temperature inside the viscometer, the traveling time of the piston and the uncorrected viscosity are recorded during the experiment. **Fig. 2.10** illustrates a snapshot of the data monitoring system.

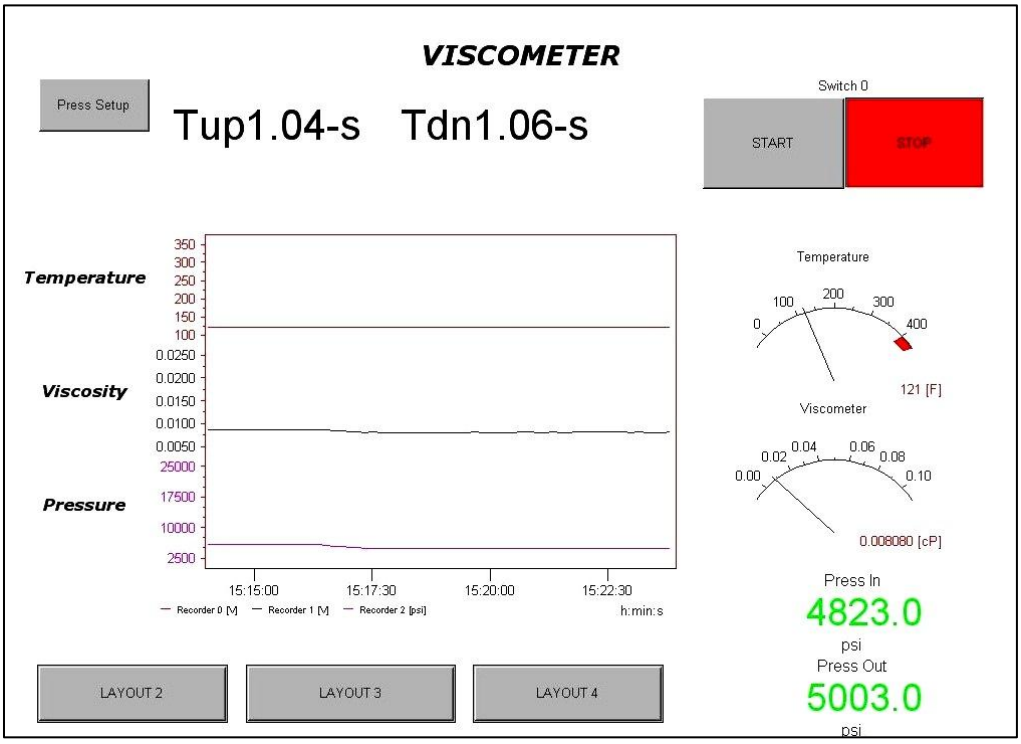

Fig. 2.10—A snapshot of the data monitoring system.

The following steps should be taken to measure the gas viscosity:

1. Clean chamber and piston properly and make sure that no contaminant remains inside the chamber.
2. Set the desired temperature and wait for at least 10 hrs to make sure that the temperature is stabilized inside the chamber.

3. Set the pressure inside the chamber manually by opening and closing the inlet and outlet valve of the viscometer and wait for 30 minutes.
4. Start measuring the traveling time of the piston, recording the data for 15-30 minutes.
5. Increase the pressure slowly and repeat step 3 and 4 for each desired pressure until the maximum pressure is reached. Then stop increasing the pressure and decrease it to the minimum value of interest.
6. Change the temperature and wait for another 10 hrs to make sure that the temperature is stabilized inside the chamber and then repeat step 3 to 5 to measure the traveling time of the piston for a different temperature.
7. Finish the experiment by depleting the gas from the chamber (opening the outlet valve of the viscometer and venting out the gas).

2.3.3 Repeatability of the data

Fig. 2.11 shows the results of four different runs to measure the viscosity of a mixture of 90% methane and 10% nitrogen. The results verified the repeatability of the measurments.

To measure each data point, the temperature was let to stabilize for 15 hrs and the pressure stabilized for half an hour. To obtain a single data point of viscosity for a certain pressure and temperature, measurements were repeated every 10 second for more than 1,000 times.

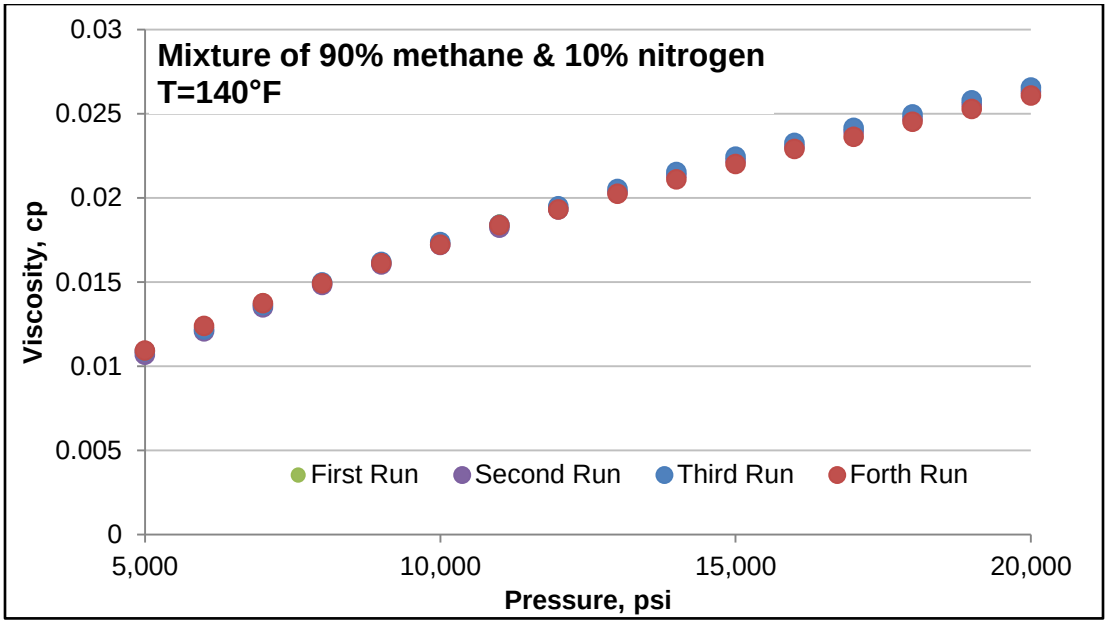

Fig. 2.11—Four different runs to measure the viscosity of a mixture of 90% methane & 10% nitrogen, showing the repeatability of the measurements.

Fig. 2.12 shows the measured traveling time data for a mixture sample of 90% methane and 10% nitrogen for about 18 minutes at a temperature of 140°F. After taking the measurements for a certain pressure and temperature, the data are analyzed and the noise is filtered out. Finally, statistical analysis is used to come up with one single value out of over 1,000 measured data for a certain pressure and temperature.

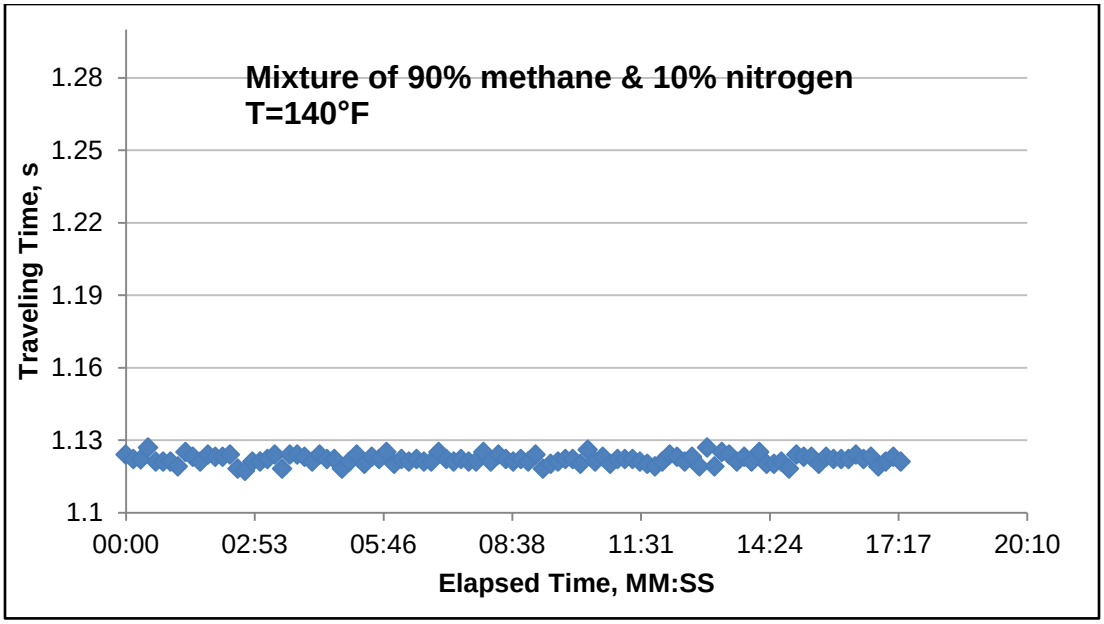

Fig. 2.12—To obtain a single data point of viscosity for a certain pressure and temperature, measurement were repeated every 10 second for over 1,000 times.

2.3.4 Contaminant inside the chamber

Contaminants can significantly influence the accuracy of the data. Before starting measuring with any new gas sample, the desired gas mixture should be circulated for several times to ensure that there is no contaminant left inside the chamber. **Fig. 2.13** shows how the presence of a the contaminant can influence the measurements.

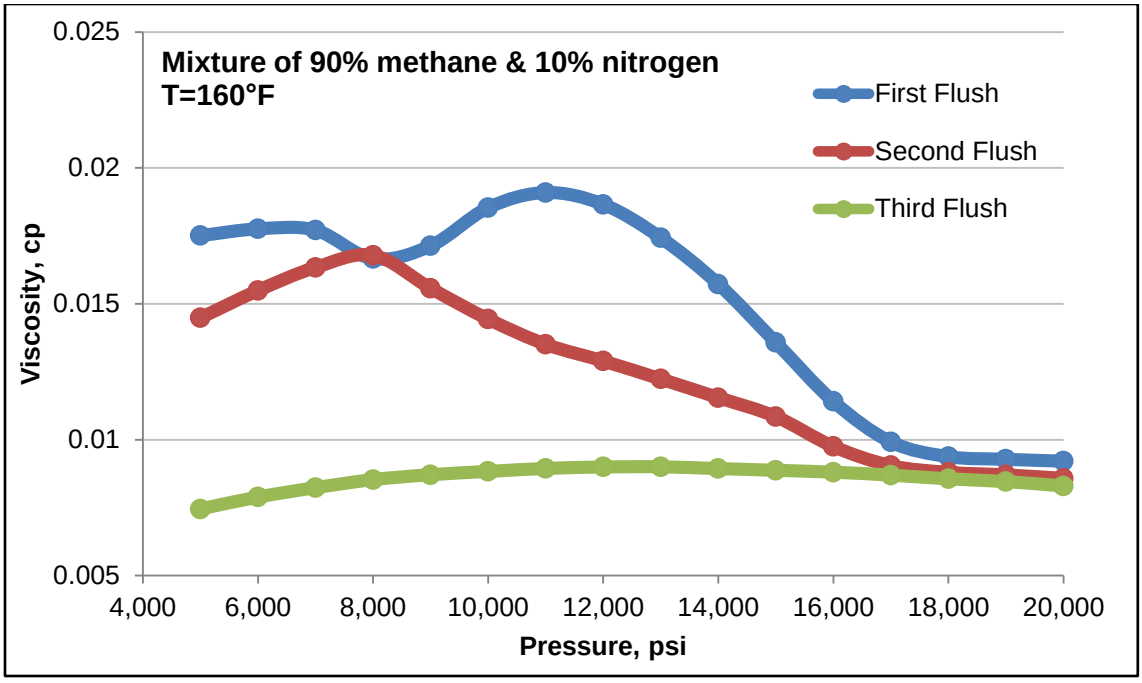

Fig. 2.13—Before starting measuring a new gas sample, the desired gas mixture should be circulated for several times to ensure that there is no contaminant left inside the chamber.

Chapter III presents the viscosity measurements of gas mixtures and their accuracy using oscillation-piston viscometer.

This study also introduces the rolling ball viscometer as an alternative method to measure the gas viscosity. Its potential and limitation were reviewed as follow.

2.4 Study of rolling ball viscometer

The viscometer made of an inclined tube and rolling ball was invented by Flowers (1914). A ball rolls by gravitational force in an inclined tube; as long as the flow regime

passing around the ball is laminar, the rolling time of the ball linearly relates to the absolute viscosity of the fluid. The theory of motion assumes that the ball rolls without sliding throughout the tube and only relative measurement can be made; thus, it should be first calibrated with a known viscosity fluid (**Fig. 2.14**).

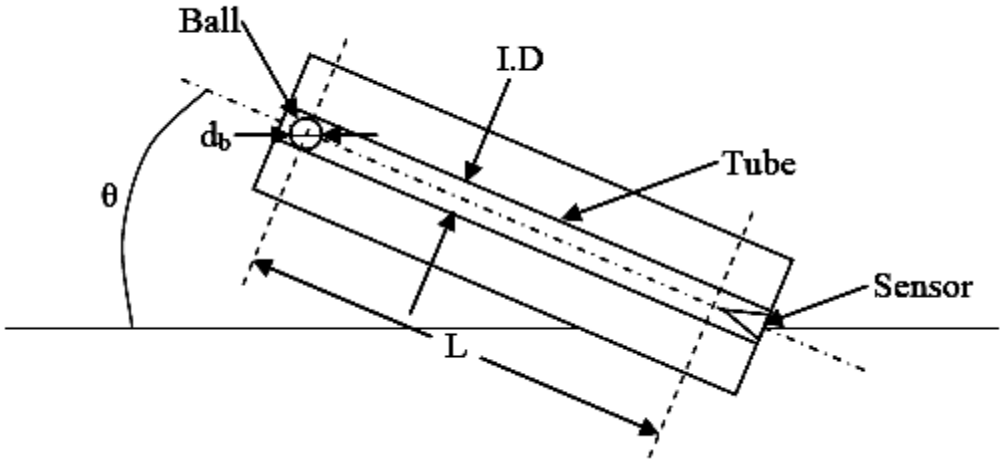

Fig. 2.14—A ball is positioned in the upper end of the tube slightly larger than the ball. As the ball rolls down through the tube at a constant angle, the displaced fluid must flow past it through the space between the ball and tube. As long as the flow passing around the ball is strictly laminar flow, the rolling time of the ball multiplied by the difference between the ball and fluid density (buoyancy factor) is a linear function of absolute viscosity of fluid (from Viswanathan, 2007).

Hersey and Wash (1916) developed a correlation based on a dimensional analysis of the variables involved. Hubbard and Brown (1943) complemented the work by Hersey

and Wash and developed a systematic dimensional analysis of the rolling ball viscometer, determining a dimensionless calibration curve used to design a viscometer to measure a wide range of viscosities. Block (1940) develpoed a method to determine whether the ball is moving by pure rolling or by a combination of rolling and sliding.

Hersey and Shore (1928) used the calibration for the first time to test lubricants up to pressures of 57,000 psia and temperature up to 284ºF. Sage and Lacey (1938a) described the use of the rolling ball viscometer to measure the viscosity of hydrocarbon solutions. Later Sage and Lacey (1938b) used it with a tight-fitting ball size to measure gas viscosity. They calibrated the viscometer with both gas and liquid at atmospheric pressure to measure the viscosity of methane and two natural gases at higher pressure. Comings *et al*. (1944) showed that the data of Sage and Lacey show a much greater increase with pressure than data obtained from the other investigators and this mismatch was probably because of the increase of turbulent effects at higher pressures.

Lewis (1953) proposed an equation to calculate the calibration coefficient based on the geometry of the viscometer. This equation is not accurate enough to replace with the calibration procedure using a standard fluid; however, it could be used to evaluate the accuracy of the calibration results.

Carmichael and Sage (1963) showed that the earlier *n*-butane gas data (Sage *et al*. 1939) were poor except for those measured at atmospheric pressure. This error was probably because Sage *et al*. (1939) extended their calibration result at atmospheric pressure to higher pressures.

Viswanathan (2007) calibrated the viscometer with a standard fluid at constant pressure and different temperatures and measured the viscosity of nitrogen and methane at higher pressures. He found more than 10% error in his results compared with previous published data.

The density of gases increases much more rapidly with pressure than does the viscosity. The Reynolds number thus increases rapidly with increasing pressure, and it is impossible to avoid turbulent conditions over portions of the pressure range covered, if the rolling ball viscometer is calibrated only at atmospheric pressure. Using the gas instead of liquid and calibrating the viscometer over the whole pressure and temperature range of interest provides reliable results. The tube inclination angle and the ball/tube diameter ratio are two important factors that control the flow regime around the ball. An optimal combination of these two factors guarantees laminar flow around the ball at different pressure and temperature conditions.

2.4.1 Method

The general equation for laminar flow in a rolling ball viscometer (Hubbard and Brown, 1943) is:

$$\mu = K_1\left(\rho_b - \rho\right)t. \quad \text{.....} \quad (2.14)$$

Hubbard and Brown (1943) proposed a correlation for the calibration coefficient, K_1:

$$K_1 = \frac{5\pi}{42l} Kg \sin\theta d(D+d). \quad \text{.....} \quad (2.15)$$

Lewis (1953) has shown an approximate treatment of the problem in terms of the hydrodynamic of viscous fluids that K is given by

$$K_1 = 0.891[1-\frac{d}{D}]^{5/2}. \quad \text{.....(2.16)}$$

Generally, the value of K_1 should be determined experimentally with fluids of known viscosity and density; however, the value of K_1 obtained through the **Eq. 2.16** serves as a check on the experimental values.

The rolling ball viscometer used in this research includes a diaphragm pump and a rolling ball viscometer shown in **Fig. 2.15**.

Based on the above considerations, the procedure to calibrate a rolling ball viscometer can be summarized as follows:

1. Clean the ball and tube completely.
2. Check the diameter and the density of the ball. These are the critical parameters towards accurate measurement of viscosity using this type of viscometer.
3. Place the ball into the tube and fill the tube with the known calibration fluid.
4. Open the outlet valve of the gas bottle and the inlet valve of the pump, and fill the pump with the desired fluid; turn the pump on to increase the gas pressure to the pressure-value of interest.
5. Open the outlet valve of the pump and the inlet valve of the rolling ball viscometer and fill the viscometer with gas; set the gas to the desired pressure and wait for half an hour.

6. Set the temperature and let it stabilize for an hour.

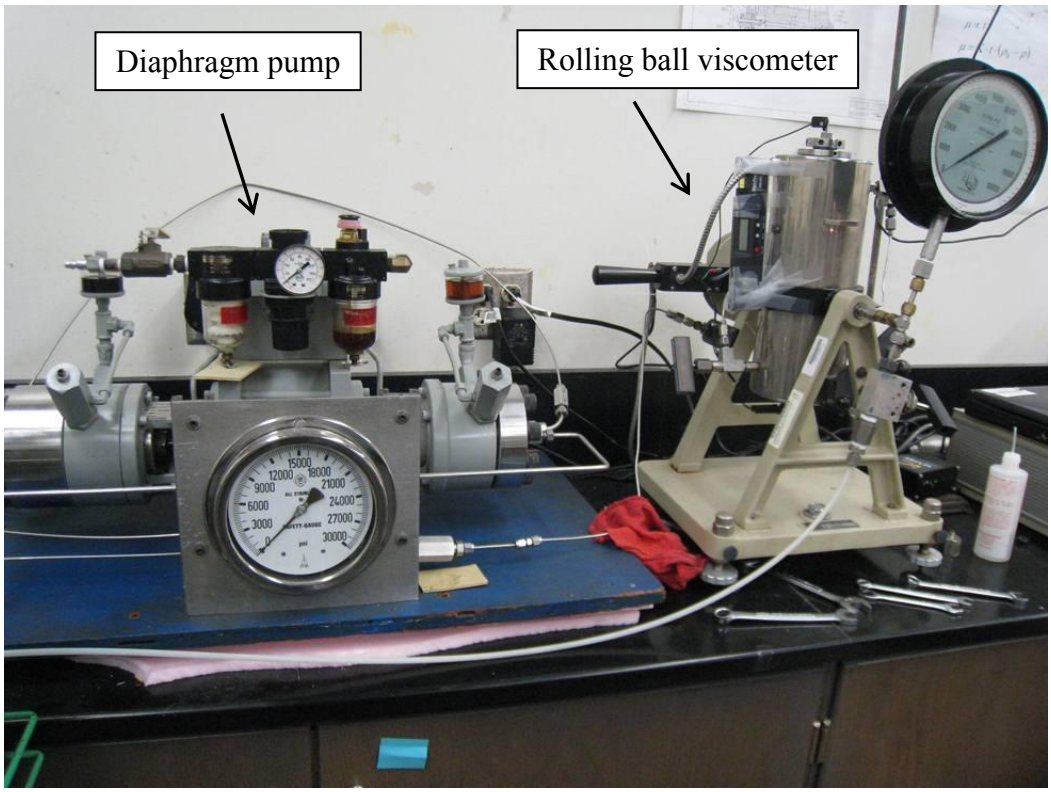

Fig. 2.15—Rolling ball viscometer system includes a used in this research diaphragm pump and a rolling ball viscometer.

7. Run the test at a fixed *d/D* ratio (the ratio of the ball diameter to the inner diameter of the tube), inclination angle, temperature and different pressures.
8. Measure the roll-time enough times to obtain statistically consistent values.
9. Multiply the average roll-time by the density difference of the ball and the fluid.
10. Plot the product of roll-time and density difference against the viscosity on a linear scale for each temperature.

11. Use the slope and the y-intercept of the plot to establish the equation for viscosity.
12. Change the temperature and repeat steps 7 to 11.

2.4.2 Calibration procedure

The calibration procedure mainly gives an estimate of the calibration coefficient (K_1). This type of viscometer normally calibrated with liquid, but in this case, nitrogen was used as the calibration fluid. The main distinction of this calibration procedure from other published procedures is that the viscometer was calibrated over the entire range of interest; all of the previously published procedures (Sage and Lacey, 1938a; Hubbard and Brown, 1943) only calibrated the viscometer at atmospheric pressure with a limited number of temperatures. The technique proposed here minimizes the turbulence effects were always the weakness of the rolling ball viscometer.

Laminar flow around the ball is the criterion for the calibration procedure. The (d/D) ratio and the tube inclination angle from the horizontal plane are the two main factors impacting on the fluid flow around the ball.

In this research six balls and two tubes with different diameters were used to calibrate the viscometer (**Table 2.2). Fig. 2.16** shows the rolling ball viscometer used in this research.

Table 2.2—Tubes and balls diameters, in.

Tube 1	Tube 2	Ball 1	Ball 2	Ball 3	Ball 4	Ball 5	Ball 6
0.2598	0.2610	0.2520	0.2480	0.2580	0.2587	0.2590	0.2600

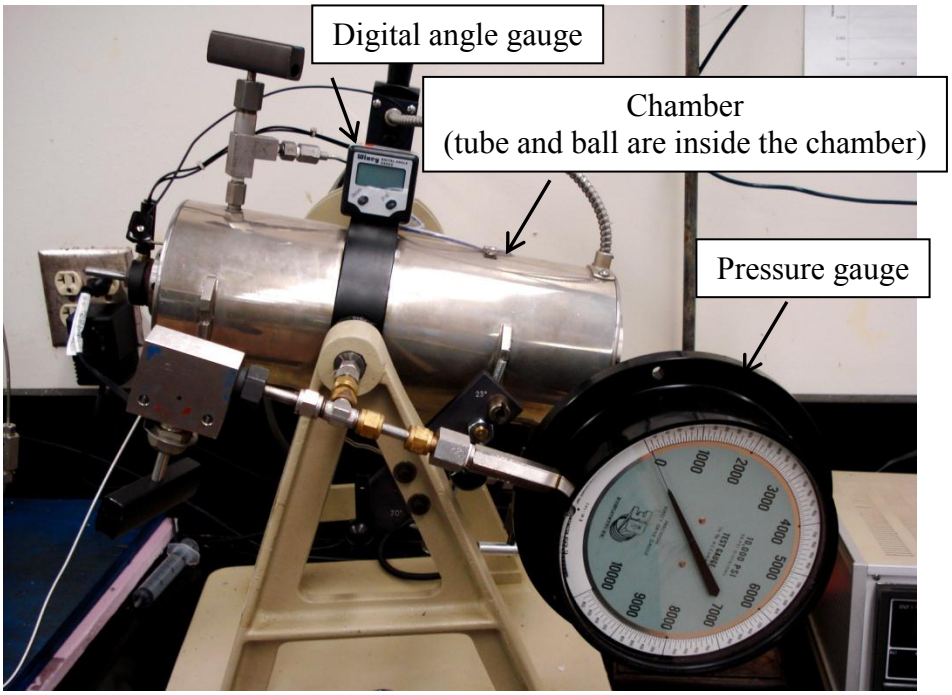

Fig. 2.16—Ruska rolling ball viscometer used in this research.

Previous investigators (Sage and Lacey, 1938a; Hubbard and Brown, 1943) found that the ratio of *d/D* should be over 0.9 for laminar flow to be achieved around the ball. In this study, different combinations of balls and tubes were used, and it was found that this ratio could be over 0.9 for some points, but in order to achieve the laminar flow over the entire pressure and temperature range of interest, it had to be kept above 0.99.

After performing over 100 tests, laminar flow was obtained using tube 1 and ball 4. **Fig. 2.17** shows the results at 170°F and at five different pressures (4,000, 5,000, 6,000, 7,000 and 8,000 ps)i. The straight line indicates laminar flow around the ball.

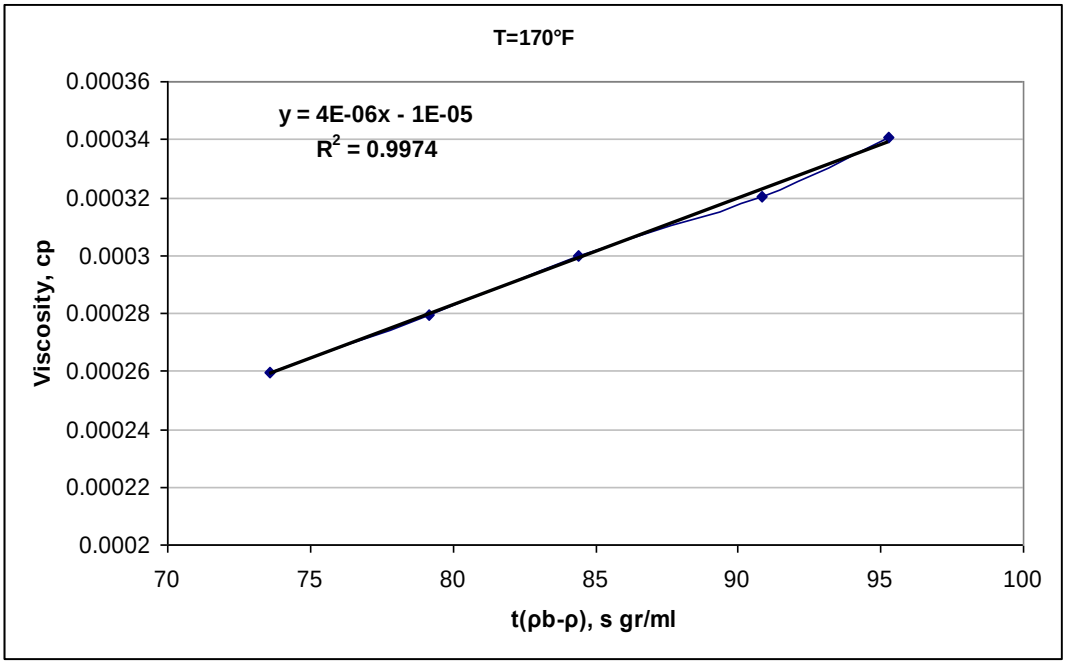

Fig. 2.17—The straight line indicates laminar flow around the ball.

Different inclination angles were used to achieve laminar flow around the balls. As the inclination angle decreases, the chance to get laminar flow increases, but at very low angles the ball does not fall down, because the gravity force can not overcome the high static friction between ball and tube surface; thus, finding the minimum angle that the ball can fall down is as important as the *d/D* ratio.

After finding the best ball and tube size, ten different angles (from 6 to 15°) were used to find the optimal value, and for each angle the roll-time was measured for the pressure and temperature range of interest. Then, the resistance factor and Reynolds number were calculated for all of the cases. The resistance factor and Reynolds number are defined as:

$$f = \frac{5\pi g}{42}\frac{(D+d)^2}{L^2 d}\frac{\rho_S - \rho}{\rho}t^2 \sin\theta, \quad \text{.....(2.17)}$$

$$N_{\mathrm{Re}} = \frac{Ld^2}{D+d}\frac{\rho}{\mu t}. \quad \text{.....(2.18)}$$

When plotting the resistance factor vs. the Reynolds number for all the angles, a straight line is obtained for laminar flow conditions. **Fig. 2.18** clearly indicates that for an inclination angle between 6 and 11°, the flow around the ball is laminar, but above 11°, the data deviate from the straight line, hence suggesting turbulent flow. As temperature increases, the angle that can provide laminar flow decreases. At the highest temperature, 260°F, this angle becomes 10°; however, as pressure increases, the angle that can provide laminar flow increases. At the highest pressure, 8,000 psi, this angle becomes 13°. Based on these observation, an angle of 8° was selected to ensure laminar flow over the entire pressure and temperature range of interest.

To simplify the calibration procedure, the calibration coefficient is assumed to be a constant value for all the viscosity measurements. In reality, this is a drastic assumption that adds error to the measurements. In fact, the calibration coefficient varies with temperature, and should therefore be more correctly defined as a function of

temperature. Also, the y-intercept in Fig. 2.17 is always ignored in the calibration procedure. Including the y-intercept as a function of temperature in the viscometer equation would considerably improve the accuracy of the results; thus, in this study, the main equation for the rolling ball viscometer was changed to:

$$\mu = K_1\left(\rho_b - \rho\right)t + K_2 . \quad \text{.....} \quad (2.19)$$

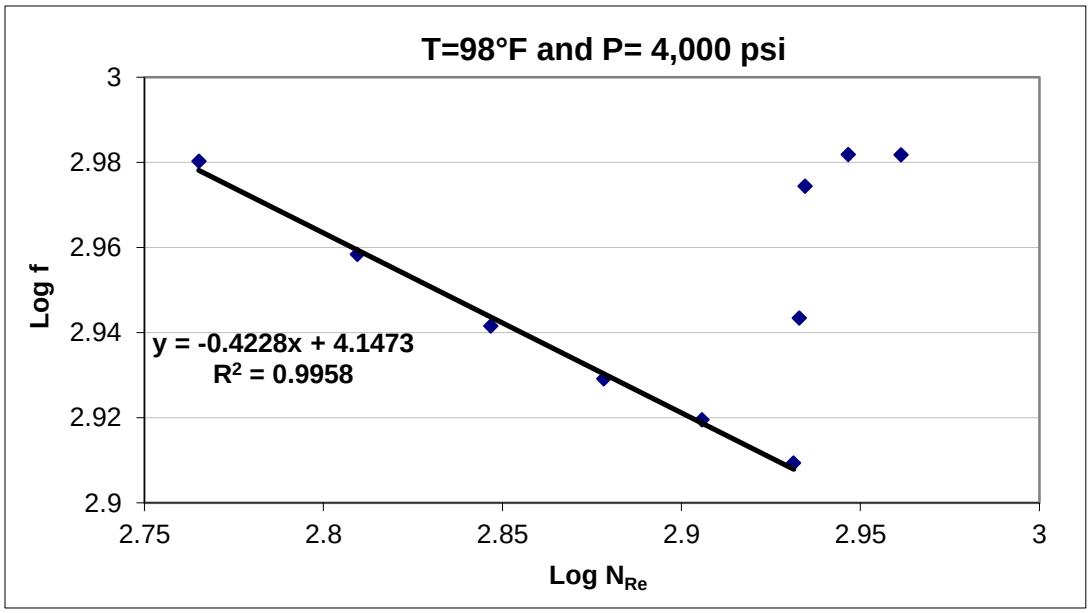

Fig. 2.18—For an inclination angle between 6 and 11°, the flow around the ball is laminar, but above 11°, the data deviate from the straight line, indicating turbulent flow.

The smart design of the Ruska rolling ball viscometer minimizes the tube expansion by balancing the inside and outside tube pressure. This allows to exclude the pressure

effect on the calibration coefficients and to consider temperature as the dominant when defining an equation for the calibration coefficients.

All the measured data were plotted (**Fig. 2.19**), and a regression performed to find the slope (K_1) and the y-intercept (K_2) separately, and to define them as a function of temperature (**Fig. 2.20**, **Fig. 2.21).**

By defining K_1 and K_2, the equation to measure gas viscosity with the rolling ball viscometer is:

$$\mu = \left(0.0000143324\mathrm{T}^{-0.2601953328}\right)\left(\rho_b - \rho\right)t - 0.0000000023\mathrm{T}^2 + 0.0000015333\mathrm{T} - 0.0002130017 . \quad (2.20)$$

Noted that K_1 and K_2 are viscometer characteristics and they must be redefined if the geometry of the viscometer changes.

The nitrogen viscosity data were re-interpreted with the new equation to check the quality and accuracy of the viscometer equation. **Fig. 2.22** shows the average relative error distribution.

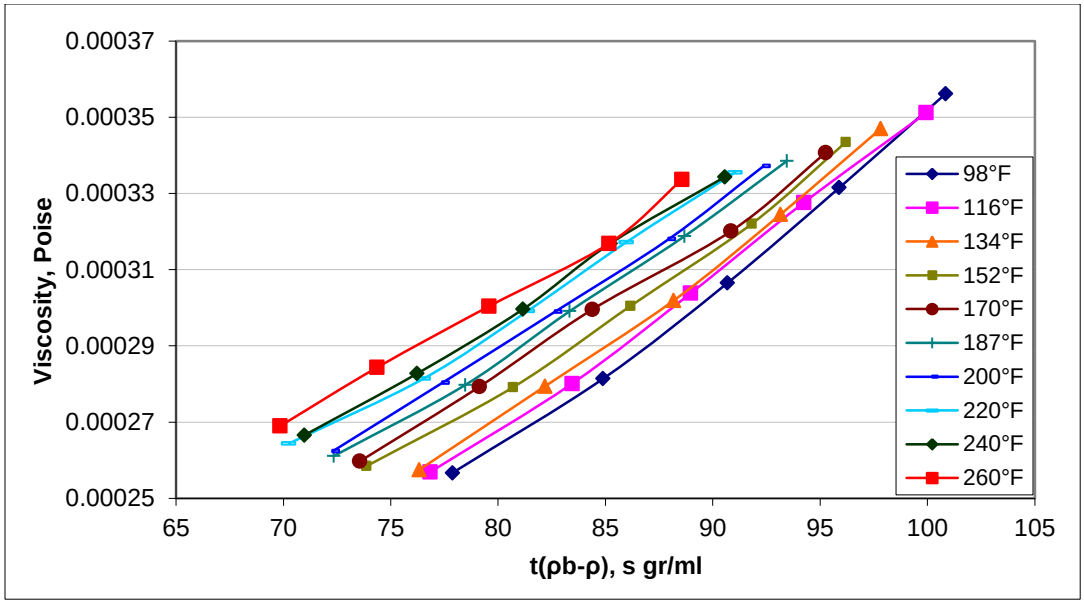

Fig. 2.19—All the measurements are taken in the laminar flow zone.

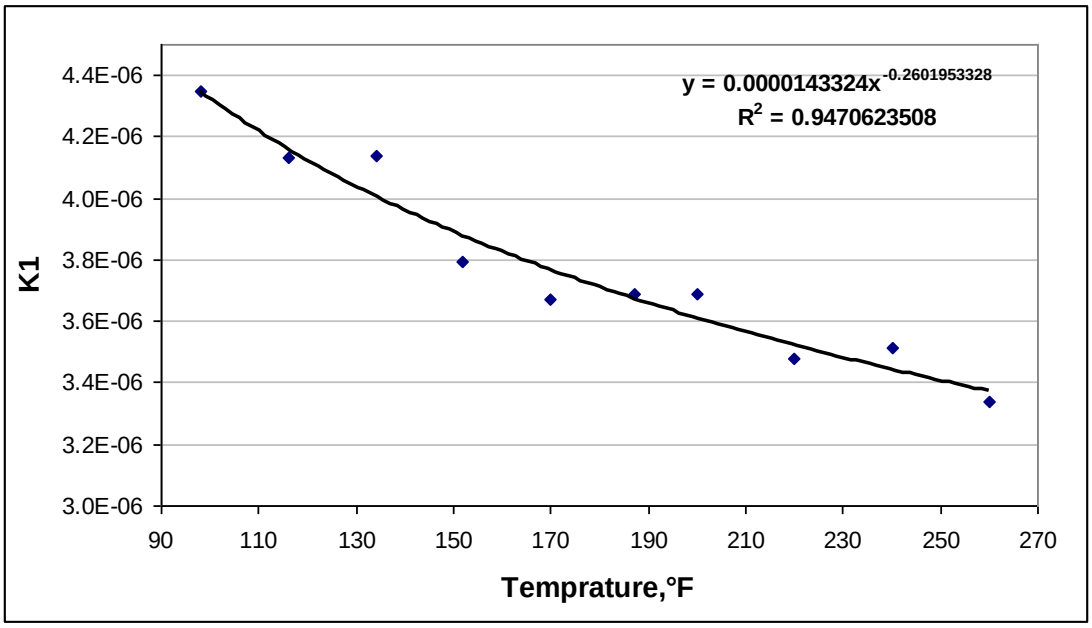

Fig. 2.20—K_1 should be a function of temperature and not to be assumed constant.

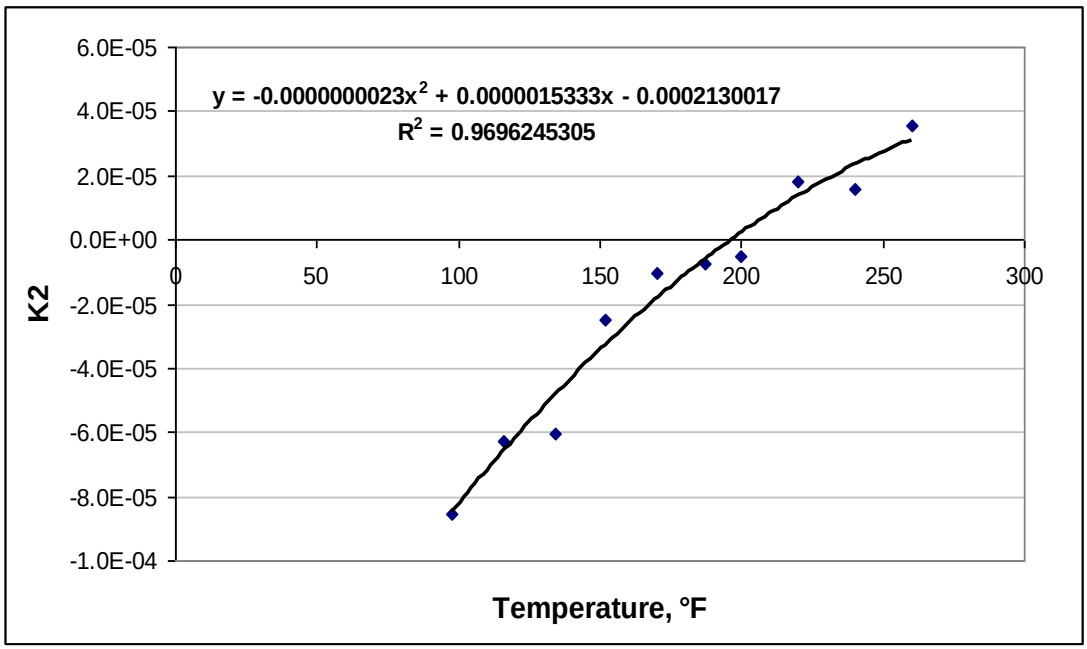

Fig. 2.21—K_2 is a function of temperature and should be included in the viscosity measurement.

The reasonable error in reproducing the viscosity values for nitrogen shows that the calibration procedure was successfully performed and the viscometer was ready to measure the viscosity of gases at pressures up to 8,000 psi and temperatures up to 260°F.

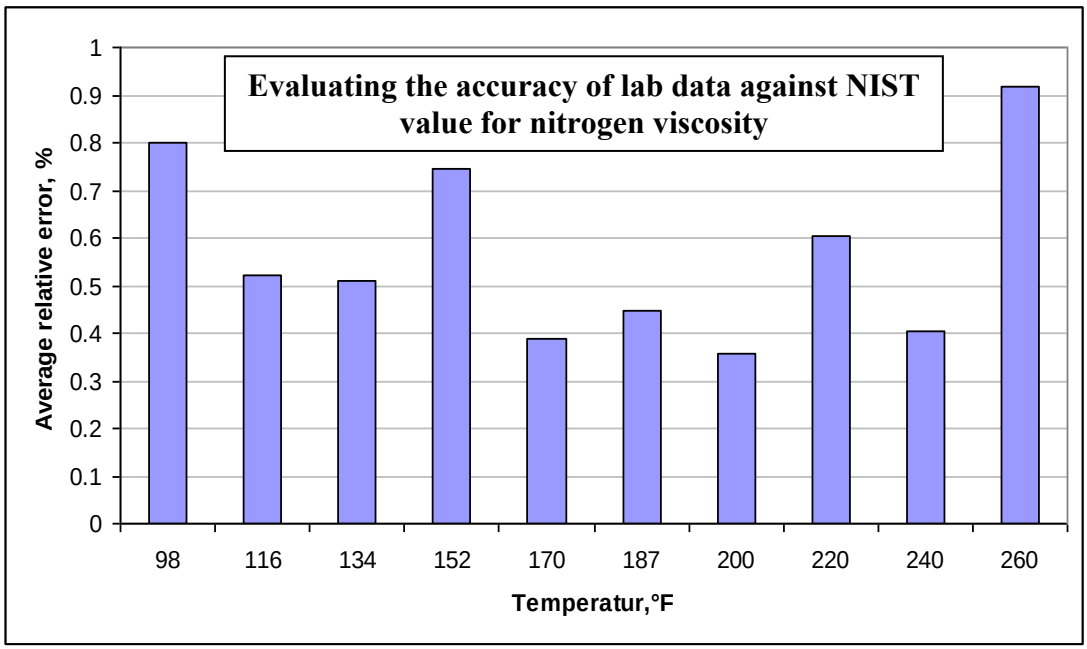

Fig. 2.22—The average relative error for all the temperatures are less than 1%. This shows that the accuracy of the results is acceptable. Also the results indicate no direct relationship between error and temperature.

2.4.3 CO_2 viscosity measurement

Ultra-high pure CO_2 gas was used to verify the new viscometer calibration function. Ultra-high pure CO_2 gas was prepared by Matheson Tri-Gas Company with primary standard purity. Initial pressure in the gas tank was 2,000 psig. 21 tests were performed on the CO_2 gas to cover a wide range of pressures and temperatures. Viscosity measurements were taken at pressures between 4,000 and 8,000 psi, and temperatures of 98, 116, 134, 152, 170, 187, 200, 220 and, 240°F.

Table 2.3 lists the measured viscosity of ultra-high pure CO_2 at different temperatures and pressures.

Table 2.3—CO_2 viscosity data

Pressures, psi	Temperature, °F				
	98	116	134	152	170
4,000	0.09579	0.08178	0.07470	0.06930	0.06070
5,000	0.10043	0.09088	0.08637	0.07561	0.07305
6,000	0.10807	0.09913	0.09084	0.08400	0.08160
7,000	0.12341	0.10779	0.10284	0.09006	0.08473
8,000	0.12514	0.11493	0.10720	0.10184	0.09103

Pressure, psi	Temperature, °F			
	187	200	220	240
4,000	0.05815	0.05188	0.04813	0.04450
5,000	0.06827	0.06153	0.05713	0.05503
6,000	0.07164	0.07184	0.06661	0.06265
7,000	0.08259	0.07945	0.07461	0.06607
8,000	0.08573	0.08289	0.07900	0.07501

Fig. 2.23 shows that the comparison between lab data with NIST values suggests that the calibration function worked well at 98°F and 240°F. Similar results can be observed for temperature of 116, 134, 152, 170, 187, 200, and 220°F.

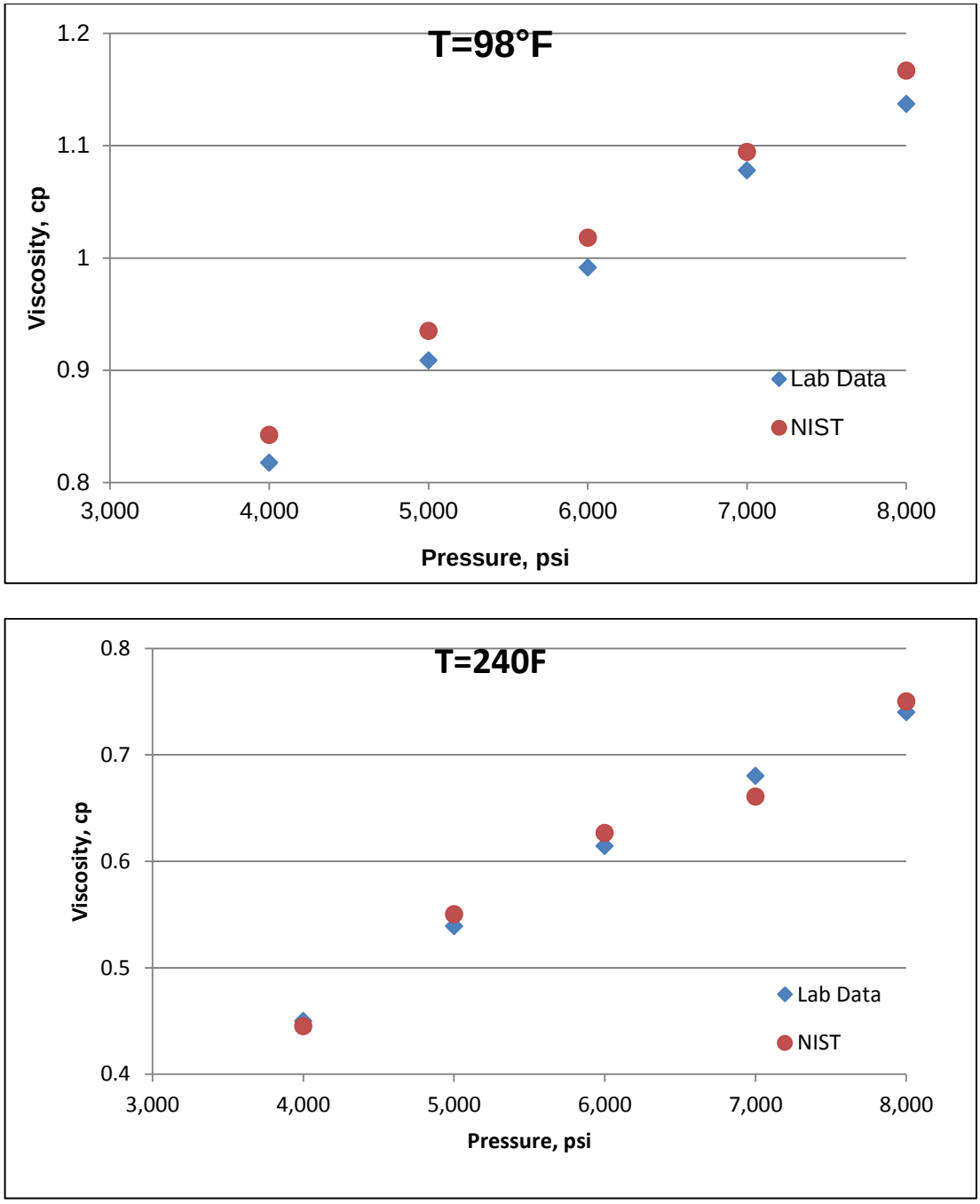

Fig. 2.23—The measured CO_2 data are relatively close to the NIST value.

Fig. 2.24 shows the average relative error distribution is less than 3% which is reasonable. The main source of error in these experiments was the temperature control system, which did not work properly, leading to a ±2 degree temperature variation that decreased the accuracy of the results.

Another source of error was introduced by the sensor reporting the roll time of the ball; this sensor proved to be extremely sensitive to temperature and it failed frequently at temperatures above 200°F. Using a better sensor would improve the accuracy of the system.

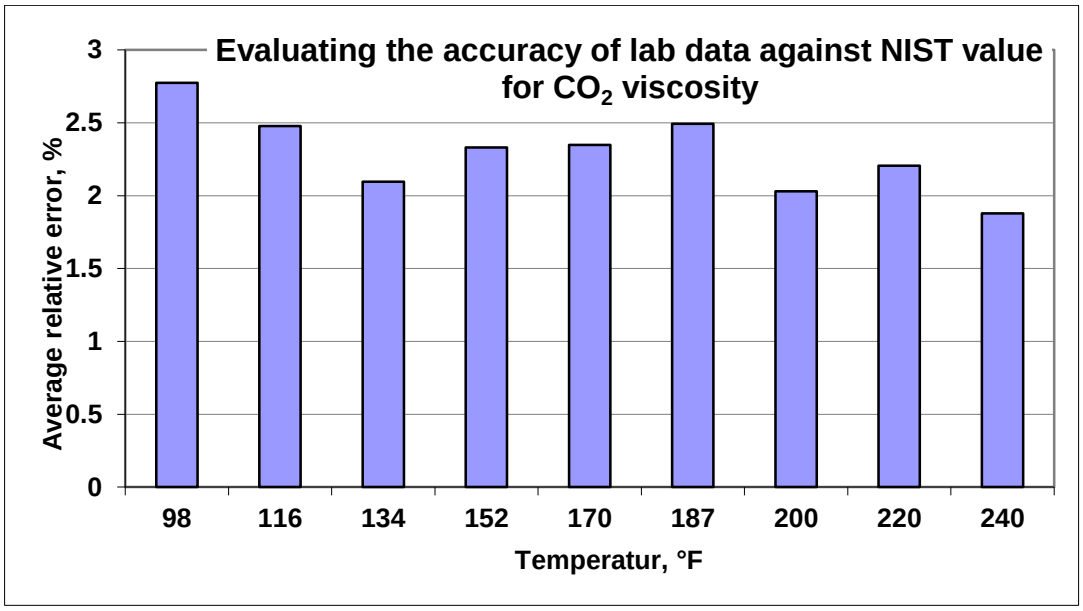

Fig. 2.24—The average relative error for all the temperatures are less than 3%. This shows that the accuracy of the results is acceptable. Also the results indicate no direct relationship between error and temperature.

In conclusion, the rolling ball viscometer can be used as an alternative method to measure gas viscosity at HPHT. However, because of its limitations, no measurements above 8,000 psi could be taken as part of this study, although a new technique was proposed to guarantee the laminar flow around the ball by calibrating the viscometer for the entire range of desired pressures and temperatures.

Fig. 2.25 shows the accuracy of the measured data compare to the NIST value for ultra-pure CO_2. The R^2 is close to unity, confirming that the measured data are acceptable and the proposed technique worked well.

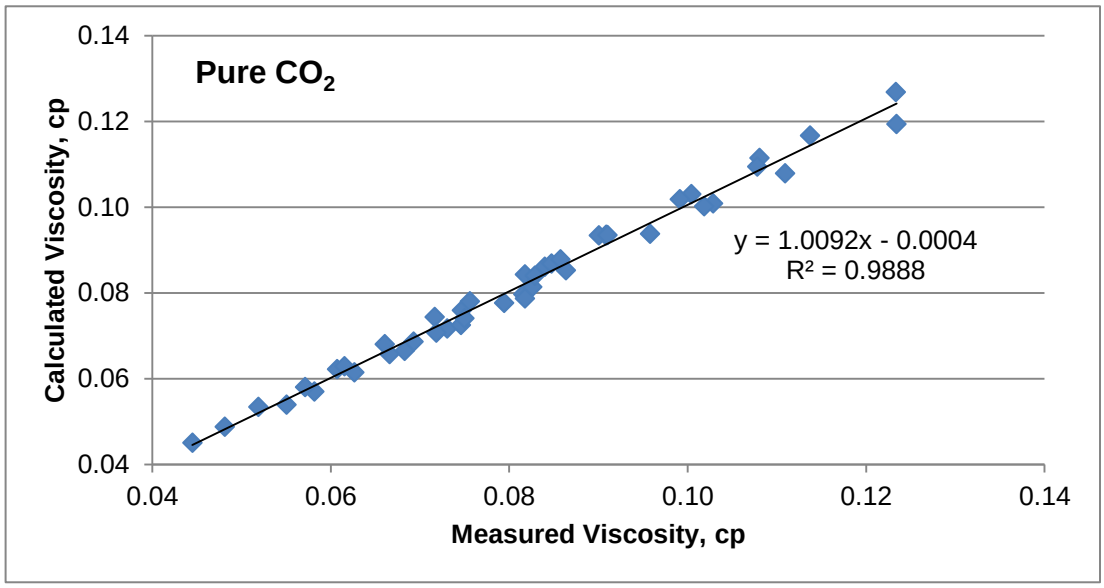

Fig. 2.25—Comparison of the measured data of ultra-pure CO_2 with NIST value confirmed the accuracy of the proposed technique to calibrate the rolling ball viscometer.

CHAPTER III

EXPERIMENTAL RESULTS AND DISCUSSIONS

3.1 Nitrogen and methane viscosity measurements

The oscillating-piston viscometer was already calibrated with nitrogen and N4 standard fluid, to ensure that it did not need a recalibration, several tests were performed with nitrogen and methane to check the repeatability of the measurements against those previously taken by Ling (2010). The comparison confirmed that the system was working properly and did not require recalibration.

An ultra-high purity nitrogen prepared by Acetylene Oxygen company was used and ten different tests were performed to measure the viscosity at pressures between 5,000 and 20,000 psi and temperatures of 152 and 200°F. **Fig. 3.1** shows that the nitrogen viscosity data measured by Ling (2010) could be accurately repeated.

An ultra-high purity methane prepared by Matheson Tri-Gas Company was used and 13 different tests performed to measure the viscosity at pressures between 5,000 and 20,000 psi and temperatures of 120 and 160°F. **Fig. 3.2** shows that the methane viscosity data measured by Ling (2010) were also accurately repeated

.

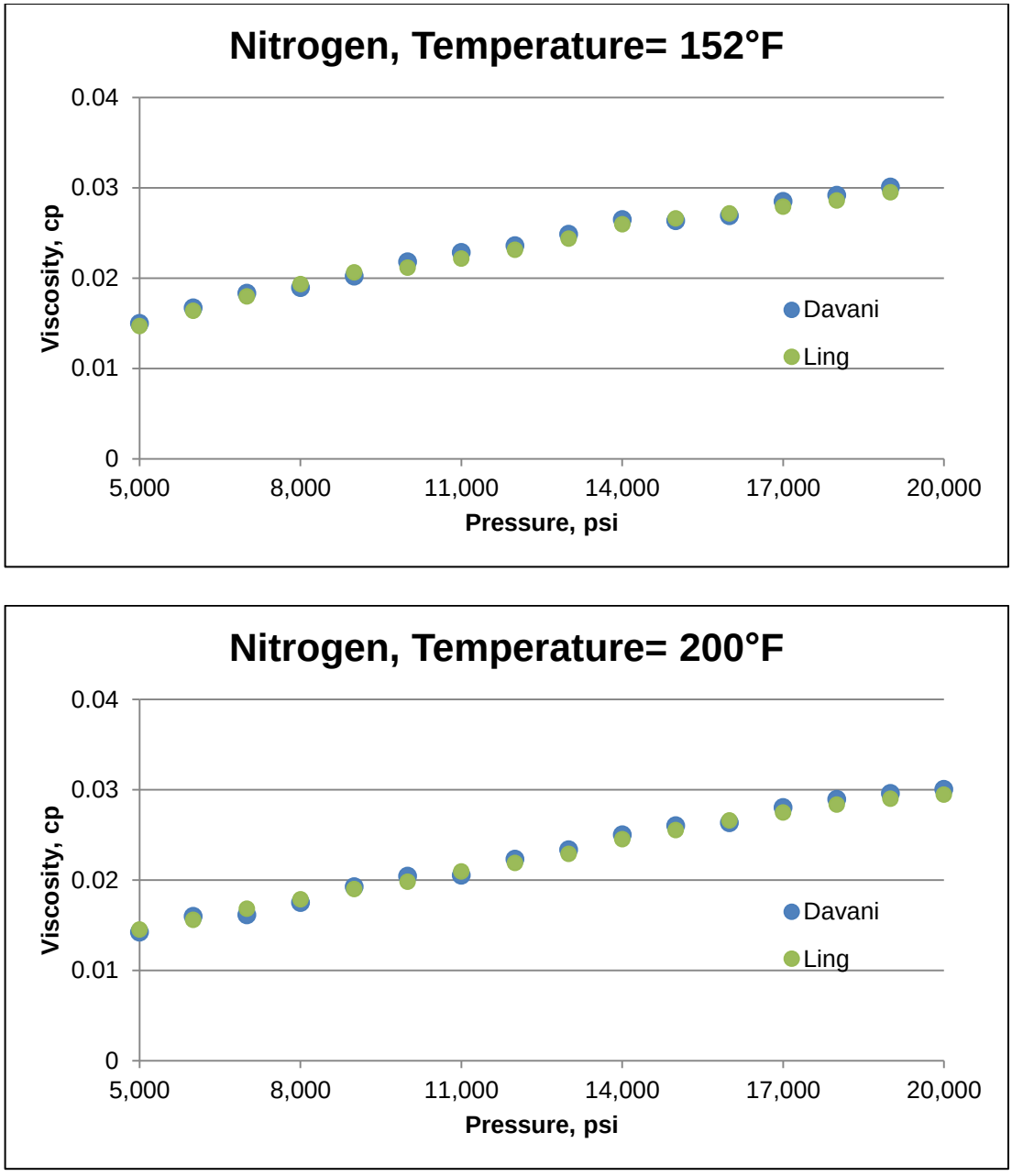

Fig. 3.1—Repeating the Ling (2010) nitrogen viscosity data verified that the viscometer system was working properly.

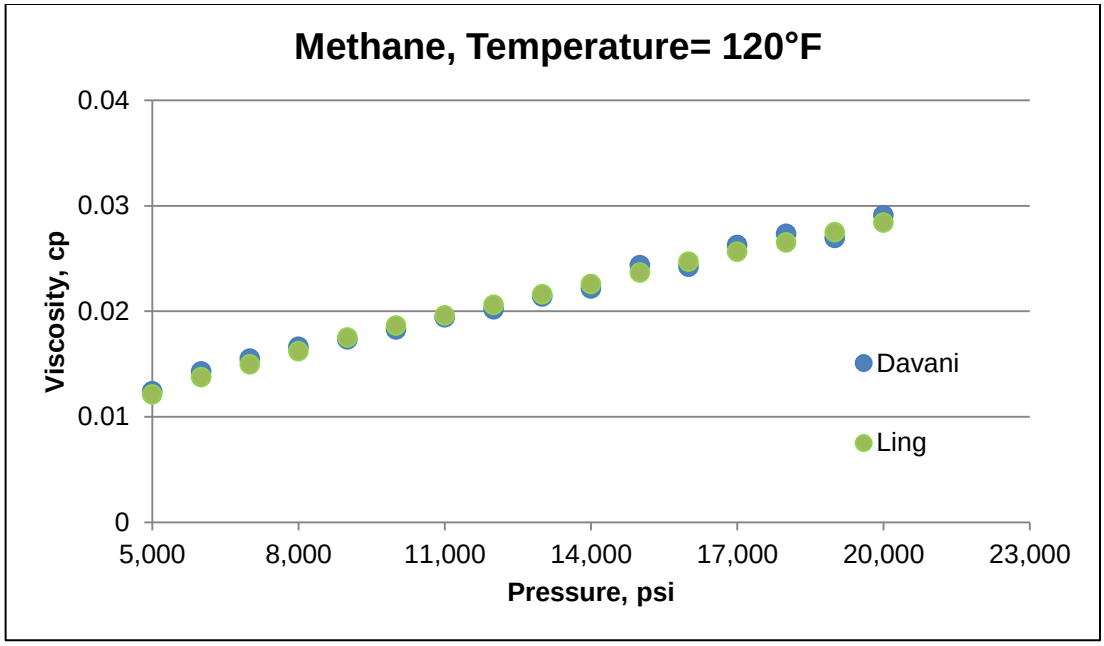

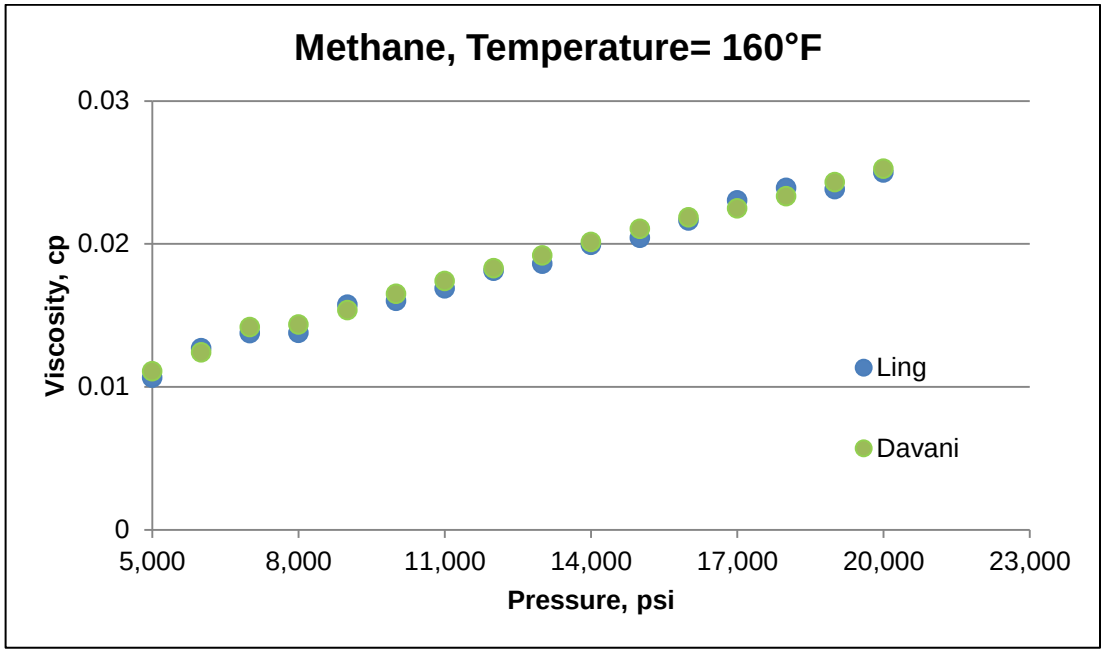

Fig. 3.2—Repeating the Ling (2010) methane viscosity data verified that the viscometer system was working properly.

3.2 Viscosity measurement of mixture of 90% methane and 10% nitrogen

A mixture of 90% methane and 10% Nitrogen was prepared by Matheson Tri-Gas Company with the primary standard purity. The initial pressure in the gas cylinder was 2,000 psig. 49 tests were performed to measure the viscosity at pressures between 5,000 and 20,000 psi, and temperatures of 120, 140, 160, 180, 200, 230, 250, 260, 280, 300, 320 and 340°F.

Table 3.1 lists the measured viscosity of a mixture of 90% methane and 10% nitrogen at different temperatures and pressures.

Table 3.1—Viscosity of a mixture of 90% methane and 10% nitrogen

Pressure, psi	Temperature, °F					
	120	140	160	180	200	230
5,000	0.02791	0.02698	0.0264	0.02533	0.02469	0.02396
6,000	0.03155	0.03032	0.02957	0.02848	0.02773	0.02692
7,000	0.03506	0.03369	0.03267	0.0315	0.03073	0.02966
8,000	0.03825	0.03695	0.03579	0.03439	0.03346	0.03234
9,000	0.04139	0.04006	0.03875	0.03726	0.03616	0.03504
10,000	0.04436	0.04311	0.04166	0.04012	0.03888	0.03767
11,000	0.04733	0.04598	0.04461	0.04289	0.04163	0.04033
12,000	0.05026	0.04892	0.04749	0.0456	0.04433	0.04297
13,000	0.05317	0.05179	0.0503	0.04824	0.04685	0.04544
14,000	0.05596	0.05461	0.05294	0.05078	0.04931	0.04792
15,000	0.05875	0.05734	0.05561	0.05341	0.05177	0.05031
16,000	0.06146	0.05992	0.05829	0.05597	0.0543	0.0528
17,000	0.06422	0.06264	0.06086	0.05847	0.05666	0.05511
18,000	0.06684	0.06521	0.06334	0.06096	0.05913	0.05749
19,000	0.06955	0.06783	0.06595	0.06344	0.06149	0.05972
20,000	0.07224	0.07036	0.06834	0.06586	0.06388	0.0621

Table 3.1—Cont.

Pressure, psi	Temperature, °F				
	260	280	300	320	340
5,000	0.02367	0.02350	0.02337	0.02322	0.02296
6,000	0.02640	0.02618	0.02599	0.02577	0.02543
7,000	0.02900	0.02873	0.02849	0.02824	0.02789
8,000	0.03165	0.03131	0.03095	0.03068	0.03024
9,000	0.03428	0.03390	0.03353	0.03306	0.03258
10,000	0.03686	0.03645	0.03602	0.03545	0.03499
11,000	0.03937	0.03891	0.03851	0.03781	0.03737
12,000	0.04181	0.04136	0.04086	0.04015	0.03972
13,000	0.04428	0.04374	0.04314	0.04243	0.04197
14,000	0.04673	0.04614	0.04540	0.04472	0.04422
15,000	0.04905	0.04843	0.04767	0.04690	0.04641
16,000	0.05136	0.05064	0.04994	0.04911	0.04850
17,000	0.05368	0.05287	0.05209	0.05121	0.05047
18,000	0.05590	0.05509	0.05426	0.05336	0.05251
19,000	0.05820	0.05736	0.05650	0.05553	0.05467
20,000	0.06045	0.05954	0.05874	0.05780	0.05686

3.2.1 Analysis of viscosity data of mixture of 90% methane and 10% nitrogen

The LGE and Sutton correlations were compared with the measured gas mixture viscosity. **Fig. 3.3** shows the results of this comparison for three different temperatures (120, 200 and 340°F). At low temperature, the two correlations overestimate the gas mixture viscosity, while at high temperature they underestimate. Similar results can be obtained for the other temperatures, as shown in Appendix A.

As it is shown in **Table 3.2,** the relative error of the LGE correlation compared to the lab data can be as high as 4.34% and it can be as high as 16.7% for the Sutton correlation which is significant. This large error proves the need for a gas viscosity correlation

validated against measured gas viscosity at HPHT conditions, so as to improve the accuracy of gas viscosity estimation at HPHT conditions.

Table 3.2—Error analysis for the viscosity of a gas mixture of 90% methane and 10% nitrogen, comparison between lab data and LGE and Sutton correlation

Temperature, °F	Lee		Sutton	
	Absolute Error (cp)	Relative Error (%)	Absolute Error (cp)	Relative Error (%)
120	0.001149107	2.122939662	0.008929392	16.70716311
140	0.000890762	1.71555064	0.008018311	15.60106279
160	0.000912739	1.732962405	0.007461656	15.00859088
180	0.00139406	2.830506513	0.007440397	15.68200783
200	0.001519572	3.233259908	0.007114481	15.55624201
230	0.001509708	3.273521206	0.00650793	14.7562358
260	0.000796734	1.757082601	0.005096255	11.55968554
280	0.001119589	2.46356497	0.00526094	12.37006269
300	0.001012571	2.286658803	0.004935697	11.89391008
320	0.001420786	3.411238362	0.005098148	12.6786571
340	0.001750814	4.386385476	0.005197476	13.285548

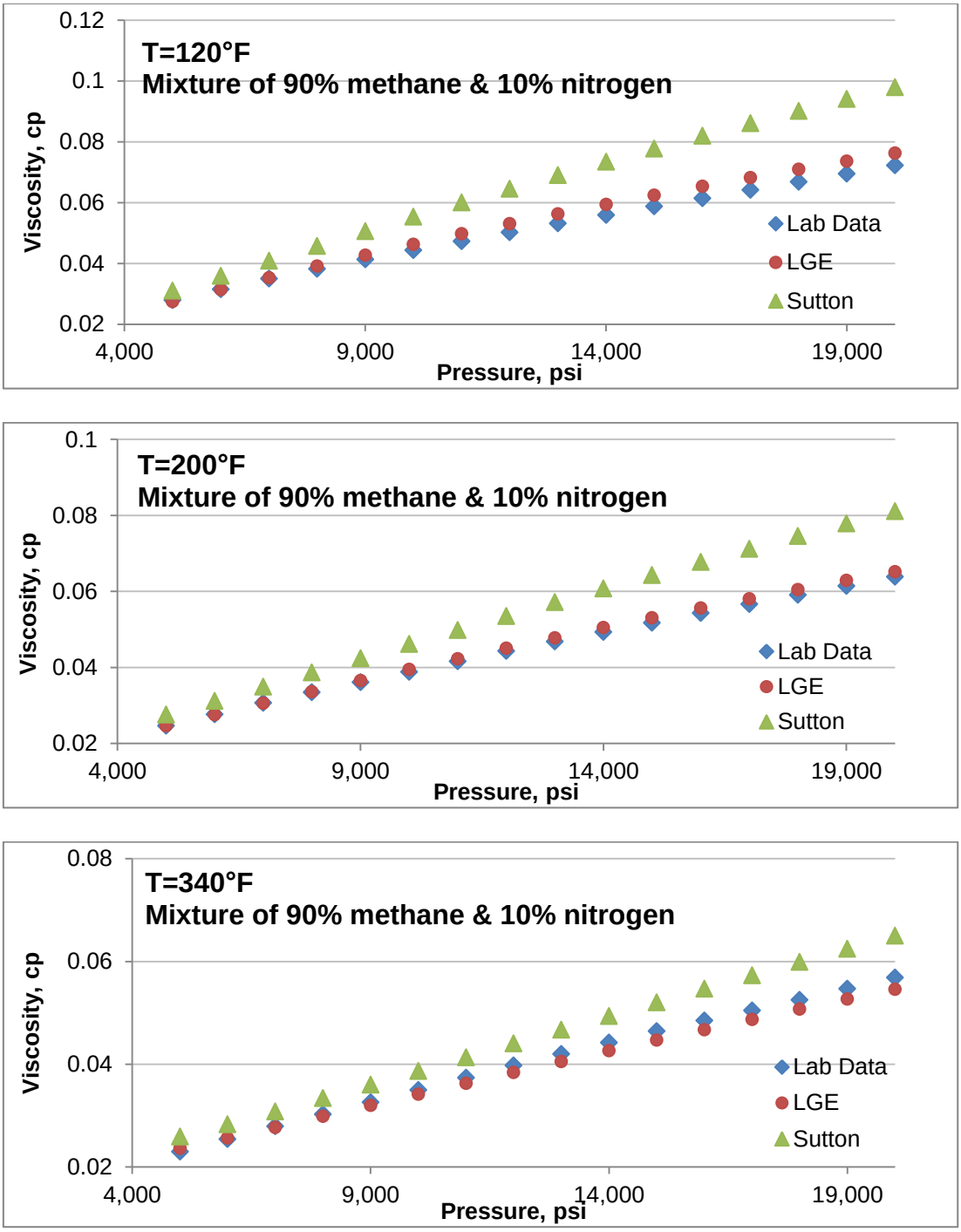

Fig. 3.3—LGE and Sutton correlation have been compared with measured gas viscosity of mixture of 90% methane and 10% nitrogen.

3.3 Viscosity measurement of mixture of 95% methane and 5% nitrogen

A mixture of 95% methane and 5% Nitrogen was prepared by Matheson Tri-Gas Company with the primary standard purity. The initial pressure in the gas cylinder was 2,000 psig. 53 tests were performed to measure the viscosity at pressures between 5,000 and 20,000 psi, and temperatures of 120, 140, 160, 180, 200, 230, 250, 260, 280, 300, 320 and 340°F.

Table 3.3 lists the measured viscosity of a mixture of 95% methane and 5% nitrogen at different temperatures and pressures.

Table 3.3—Viscosity data of mixture of 95% methane and 5% nitrogen

Pressure, psi	Temperature, °F					
	120	140	160	180	200	230
5,000	0.02689	0.02563	0.02519	0.02478	0.02409	0.02382
6,000	0.03036	0.02923	0.02849	0.02751	0.02683	0.02650
7,000	0.03388	0.03281	0.03177	0.03044	0.02958	0.02884
8,000	0.03744	0.03594	0.03471	0.03325	0.03216	0.03117
9,000	0.04056	0.03899	0.03767	0.03592	0.03477	0.03353
10,000	0.04372	0.04197	0.04039	0.03855	0.03731	0.03577
11,000	0.04639	0.04473	0.04300	0.04110	0.03969	0.03796
12,000	0.04912	0.04732	0.04553	0.04336	0.04197	0.04012
13,000	0.05178	0.04982	0.04780	0.04564	0.04408	0.04212
14,000	0.05422	0.05253	0.05016	0.04789	0.04623	0.04412
15,000	0.05679	0.05488	0.05244	0.05016	0.04834	0.04609
16,000	0.05954	0.05728	0.05483	0.05222	0.05043	0.04807
17,000	0.06200	0.05947	0.05708	0.05439	0.05257	0.04994
18,000	0.06426	0.06195	0.05937	0.05649	0.05439	0.05173
19,000	0.06682	0.06430	0.06151	0.05835	0.05615	0.05361
20,000	0.06935	0.06646	0.06376	0.06043	0.05781	0.05534

Table 3.3—Cont.

Pressure, psi	Temperature, °F				
	260	280	300	320	340
5,000	0.02377	0.02351	0.02317	0.02296	0.02278
6,000	0.02633	0.02584	0.02557	0.02511	0.02488
7,000	0.02866	0.02817	0.02765	0.02717	0.02689
8,000	0.03103	0.03035	0.02975	0.02926	0.02881
9,000	0.03327	0.03252	0.03188	0.03130	0.03070
10,000	0.03551	0.03453	0.03404	0.03317	0.03252
11,000	0.03779	0.03644	0.03588	0.03500	0.03428
12,000	0.03987	0.03831	0.03765	0.03670	0.03592
13,000	0.04167	0.04025	0.03950	0.03847	0.03743
14,000	0.04354	0.04221	0.04122	0.04011	0.03891
15,000	0.04525	0.04393	0.04312	0.04169	0.04048
16,000	0.04728	0.04551	0.04469	0.04330	0.04197
17,000	0.04909	0.04726	0.04652	0.04503	0.04353
18,000	0.05080	0.04890	0.04822	0.04660	0.04510
19,000	0.05252	0.05043	0.04968	0.04801	0.04681
20,000	0.05401	0.05195	0.05113	0.04932	0.04828

3.3.1 Analysis of viscosity data of mixture of 95% methane and 5% nitrogen

The LGE and Sutton correlations were compared with the measured gas mixture viscosity. **Fig. 3.4** shows the results of this comparison for three different temperatures (120, 200 and 340°F). Two correlations overestimate the gas mixture viscosity. Similar results can be obtained for the other temperatures, as shown in Appendix B.

As it is shown in **Table 3.4,** the relative error of the LGE correlation compared to the lab data can be as high as 4.4% and it can be as high as 26.9% for the Sutton correlation which is significant. This large error proves the need for a gas viscosity correlation validated against measured gas viscosity at HPHT conditions, so as to improve the accuracy of gas viscosity estimation at HPHT conditions.

Table 3.4— Error analysis for the viscosity of a gas mixture of 95% methane and 5% nitrogen, comparison between lab data and LGE and Sutton correlation

Temperature, °F	Lee		Sutton	
	Absolute Error (cp)	Relative Error (%)	Absolute Error (cp)	Relative Error (%)
120	0.002550933	4.509347736	0.014793628	26.94091354
140	0.001593173	2.896583143	0.012851169	24.10892636
160	0.001057802	2.040031542	0.011393551	22.00416307
180	0.001039351	2.012490834	0.010735758	21.68143568
200	0.000826986	1.627511604	0.009887706	20.62386825
230	0.000180514	0.40282131	0.008406852	18.23045531
260	0.000385689	0.857587118	0.007153866	15.97847568
280	0.000761834	1.69497112	0.006363929	14.4509206
300	0.001021446	2.287148026	0.005731753	13.24682678
320	0.00110868	2.504948739	0.005314984	12.54489131
340	0.001237415	2.834349653	0.00492702	11.9215913

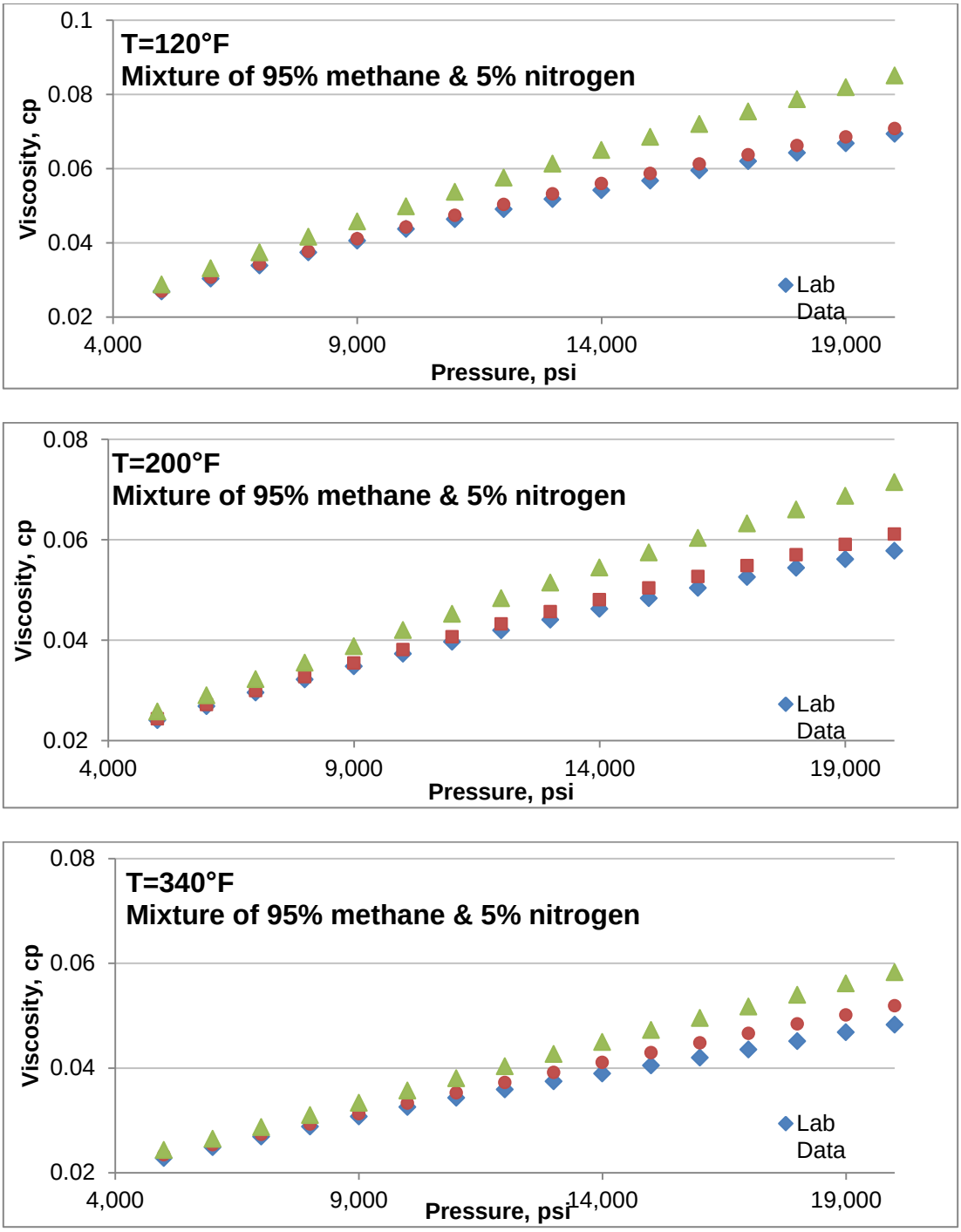

Fig. 3.4—LGE and Sutton correlation have been compared with measured gas viscosity of mixture of 95% methane and 5% nitrogen.

3.4 Viscosity measurement of mixture of 90% methane and 10% CO_2

A mixture of 90% methane and 10% CO_2 was prepared by Matheson Tri-Gas Company with the primary standard purity. The initial pressure in the gas cylinder was 2,000 psig. 49 tests were performed to measure the viscosity at pressures between 5,000 and 25,000 psi, and temperatures of 100, 140, 180, 220, 250, 280, 320 and 360 °F.

Table 3.5 lists the measured viscosity of a mixture of 90% methane and 10% CO_2 at different temperatures and pressures.

Table 3.5—Viscosity data of mixture of 90% methane and 10% CO_2

Pressure, psi	Temperature, °F							
	100	140	180	220	250	280	320	360
5,000	0.03307	0.03107	0.02952	0.02801	0.02635	0.02483	0.023949	0.023335
6,000	0.03762	0.03534	0.03364	0.03185	0.03007	0.02814	0.026746	0.025784
7,000	0.04251	0.03993	0.03780	0.03566	0.03354	0.03129	0.029726	0.02859
8,000	0.04732	0.04455	0.04211	0.03960	0.03725	0.03446	0.032506	0.031227
9,000	0.05217	0.04920	0.04614	0.04354	0.04108	0.03757	0.035461	0.034051
10,000	0.05739	0.05399	0.05054	0.04749	0.04465	0.04082	0.038445	0.036832
11,000	0.06246	0.05869	0.05477	0.05147	0.04810	0.04407	0.041534	0.039528
12,000	0.06764	0.06327	0.05923	0.05558	0.05158	0.04763	0.044686	0.042144
13,000	0.07255	0.06793	0.06335	0.05952	0.05499	0.05081	0.047756	0.044983
14,000	0.07734	0.07242	0.06739	0.06316	0.05834	0.05423	0.050683	0.047895
15,000	0.08217	0.07681	0.07174	0.06664	0.06181	0.05732	0.05381	0.050436
16,000	0.08681	0.08095	0.07588	0.07032	0.06489	0.06075	0.056977	0.0532
17,000	0.09151	0.08537	0.07974	0.07360	0.06835	0.06394	0.059908	0.055606
18,000	0.09627	0.08941	0.08364	0.07703	0.07156	0.06670	0.062341	0.058243
19,000	0.10055	0.09329	0.08707	0.08022	0.07449	0.06940	0.064936	0.060584
20,000	0.10497	0.09730	0.09075	0.08313	0.07707	0.07218	0.067225	0.063154
21,000	0.10897	0.10115	0.09380	0.08589	0.07966	0.07431	0.069518	0.065586
22,000	0.11262	0.10471	0.09654	0.08866	0.08241	0.07662	0.071516	0.067478
23,000	0.11612	0.10783	0.09944	0.09137	0.08443	0.07863	0.073482	0.069019
24,000	0.11901	0.11088	0.10196	0.09395	0.08665	0.08091	0.075468	0.070685
25,000	0.12135	0.11344	0.10437	0.09645	0.08871	0.08263	0.077085	0.072171

3.4.1 Analysis of viscosity data of mixture of 90% methane and 10% CO_2

The LGE and Sutton correlations were compared with the measured gas mixture viscosity. **Fig. 3.5** shows the results of this comparison for three different temperatures (100, 220 and 360°F). Two correlations overestimate the gas mixture viscosity. Similar results can be obtained for the other temperatures, as shown in Appendix C.

As it is shown in **Table 3.6,** the relative error of the LGE correlation compared to the lab data can be as high as 6.44% and it can be as high as 27.4% for the Sutton correlation which is significant. This large error proves the need for a gas viscosity correlation validated against measured gas viscosity at HPHT conditions, so as to improve the accuracy of gas viscosity estimation at HPHT conditions.

The analysis of the measured data provides a better insight to evaluate the applicability of the current gas viscosity correlations to estimate the gas viscosity at HPHT conditions.

Table 3.6— Error analysis for the viscosity of a gas mixture of 90% methane and 10% CO_2, comparison between lab data and LGE and Sutton correlation

Temperature, °F	Lee		Sutton	
	Absolute Error (cp)	Relative Error (%)	Absolute Error (cp)	Relative Error (%)
100	0.002396201	3.43575458	0.022767671	27.42993067
140	0.003004544	3.295850243	0.015363166	19.34699964
180	0.004308962	5.76285074	0.010899078	14.29942813
220	0.004267956	6.442579938	0.008581698	11.82878417
250	0.002677043	4.385452805	0.008761871	13.14053711
280	0.001065715	1.731674655	0.009263568	15.45070955
320	0.000798626	1.624607496	0.008681766	15.62600153
360	0.000649343	1.58960154	0.008405146	16.14025239

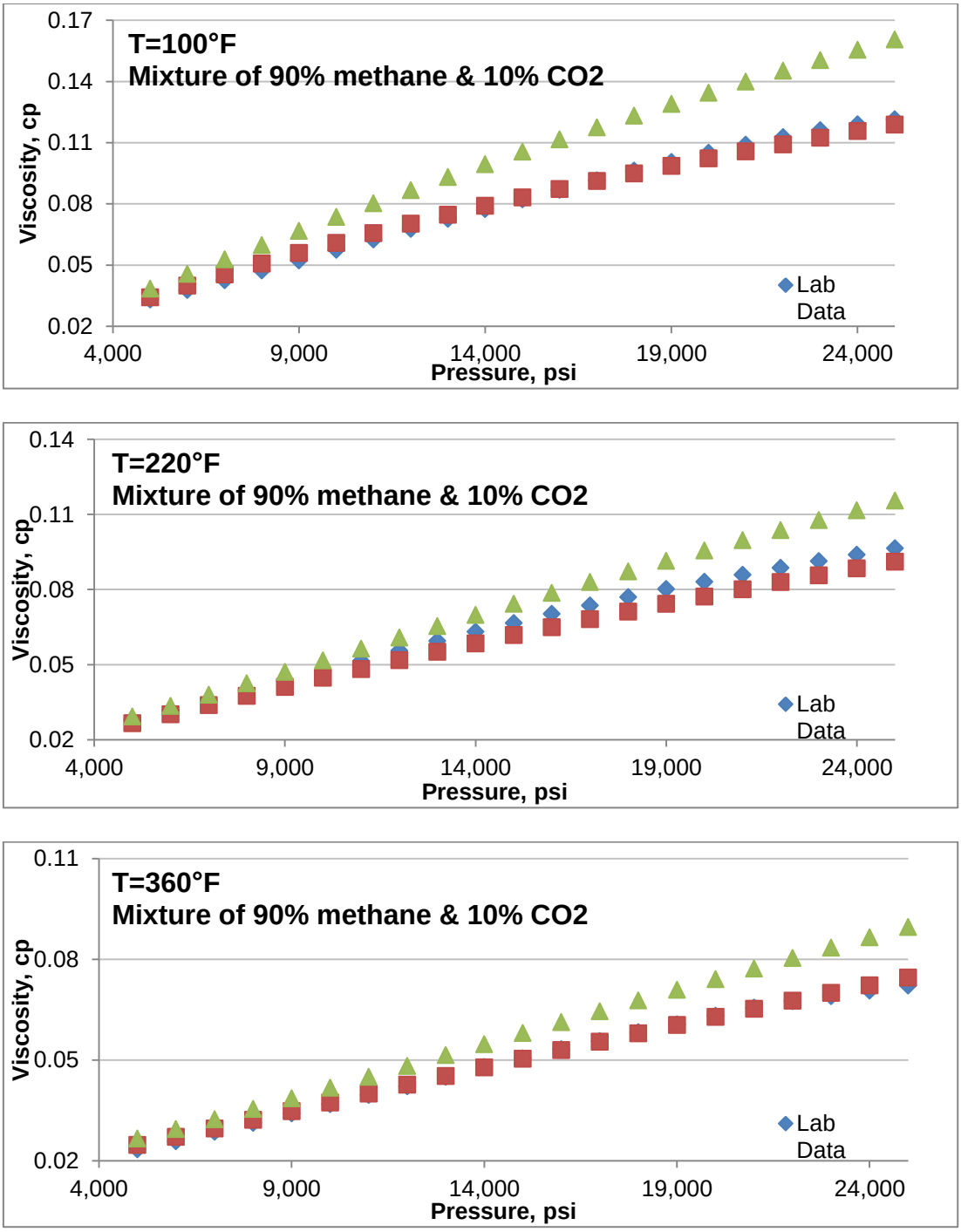

Fig. 3.5—LGE and Sutton correlation have been compared with measured gas viscosity of mixture of 90% methane and 10% CO_2.

CHAPTER IV

HPHT GAS VISCOSITY CORRELATIONS

4.1 Viscosity correlation development method

Starling and Ellington (1964) have proposed several semi-empirical expressions based to a certain extent on the theory of viscosity developed by Born and Green (1947). The final expression reported by Starling and Ellington is

$$\mu = \mu_0 \exp[X(T)\rho^{Y,T}] \quad \text{.....(4.1)}$$

Eq. 4.1 was later modified by Lee *et al*. (1964) to represent mixture and pure component data simultaneously. This equation has the following form:

$$\mu_g = K \exp(X \rho_g{}^{Y}) \quad \text{.....(4.2)}$$

$$K = \frac{(7.77 + 0.0063M)T^{1.5}}{122.4 + 12.9M + T} \quad \text{.....(4.3)}$$

where

$$X = 2.57 + \left[\frac{1914.5}{T}\right] + 0.0095M \quad \text{.....(4.4)}$$

$$Y = 1.11 - 0.04X \quad \text{.....(4.5)}$$

This formulation has been used or modified frequently by other investigator. Lee *et al*. (1966) optimized this formulation with a new set of data. Londono (2001) used a large database of gas viscosity of pure components and mixtures and adjusted Lee *et al*. formulation. Sutton (2005) modified this formulation with a wide range of viscosity data

and developed a new correlation. Viswanathan (2007) used methane viscosity of NIST vale for HPHT conditions and proposed a new correlation with the same formulation as Lee *et al* (1964). This formulation has been used in this research and its coefficients have been modified with a new set of data. Levenberg-Marquardt Algorithm (LMA) has been used to fit the new set of data with the corresponding model.

4.2 Levenberg-Marquardt Algorithm (LMA)

LMA is an iterative technique that locates the minimum of a multivariate function which is introduced as the sum of squares of non-linear real-valued functions (Levenberg, 1944; Marquardt, 1963). It has become a standard and robust method to solve non-linear least-squares problems (Mittelmann, 2004), and broadly adopted in a wide range of disciplines.

The LMA interpolates between the Gauss–Newton Algorithm (GNA) and the method of gradient descent. The LMA is more powerful than the GNA. The LMA can find a solution even if it starts very far off the ultimate minimum. However, for well-behaved functions and appropriate starting parameters, the LMA works slower than the GNA. LMA can be treated as a combination of steepest descent and the GNA (Lourakis, 2005), it means that when the solution is far off the target, the algorithm behaves like a steepest descent technique: slow, but guaranteed to converge and when the solution is close to the final solution, it becomes the GNA.

The main application of the LMA is in the least squares curve fitting problem: given a set of m empirical datum pairs of independent and dependent variables, (x_i, y_i), optimize

the parameters β of the model curve $f(x,\beta)$ in order to minimize the sum of the squares of the deviations.

$$S(\beta) = \sum_{i=1}^{m} \left[y_i - f(x_i, \beta) \right]^2 \quad \text{.....(4.6)}$$

An initial guess for the parameter vector, β should be provided. Mostly, an uninformed standard guess like $\beta^T = (1,1,...,1)$ can be an adequate initial guess but in more complicated problems initial guess should be close to the final solution in order to algorithm converges to final solution.

In each iteration step, the parameter vector, β, is replaced by a new estimate, $\beta + \delta$. To calculate δ, the functions $f(x_i, \beta + \delta)$ are estimated by their linearization

$$f(x_i, \beta + \delta) \approx f(x_i, \beta) + J_i \delta \quad \text{.....(4.7)}$$

where

$$J_i = \frac{\partial f(x_i, \beta)}{\partial \beta} \quad \text{.....(4.8)}$$

is the gradient of f with respect to β. At its minimum, the sum of squares, $S(\beta)$, the gradient of S with respect to δ will be zero. The above first-order approximation of

$$f(x_i, \beta + \delta) \quad \text{.....(4.9)}$$

gives

$$S(\beta + \delta) \approx \sum_{i=1}^{m} \left[y_i - f(x_i, \beta) - J_i \delta \right]^2 \quad \text{.....(4.10)}$$

Or in vector notation,

$$S(\beta + \delta) \approx \| y - f(\beta) - J\delta \|^2 \quad \text{.....(4.11)}$$

Taking the derivative with respect to δ and setting the result to zero gives:

$$(J^T J)\delta = J^T[y - f(\beta)] \quad (4.12)$$

where J is the Jacobian matrix whose i^{th} row equals J_i, and where f and y are vectors with i^{th} component $f(x_i, \beta)$ and y_i, respectively. This is a set of linear equations which can be solved for δ.

Levenberg's contribution is to replace this equation by a "damped version",

$$(J^T J + \lambda I)\delta = J^T[y - f(\beta)] \quad (4.13)$$

where I is the identity matrix, giving as the increment, δ, to the estimated parameter vector, β.

The (non-negative) damping factor, λ, is adjusted at each iteration step. If reduction of S is fast, a smaller value can be used, bringing the algorithm closer to GNA, whereas if an iteration step gives inadequate reduction in the residual, λ can be increased, giving a step closer to the gradient descent direction. It should be consider that the gradient of S with respect to β equals $2(J^T[y - f(\beta)])^T$. Consequently, for large values of λ, the step will be taken almost in the direction of the gradient. If either the length of the computed step, δ, or the reduction of sum of squares from the latest parameter vector, $\beta + \delta$, fall below predefined limits, iteration stops and the last parameter vector, β, is assumed to be the solution.

The main disadvantage of Levenberg's algorithm was that if the value of damping factor, λ, is large, inverting $J^TJ + \lambda I$ is not used at all. Marquardt (1963) described that each component of the gradient can be scaled according to the curvature so that there is

larger movement along the directions where the gradient is smaller. This technique avoids slow convergence in the direction of small gradient. Thus, Marquardt (1963) substituted the identity matrix, *I*, with the diagonal matrix including the diagonal elements of $J^T J$, introducing in the Levenberg–Marquardt algorithm:

$$(J^T J + \lambda diag(J^T J))\delta = J^T [y - f(\beta)] \quad (4.14)$$

More detail about the LMA is beyond the scope of this research, more comprehensive treatments can be found at the following references: Madsen, 2004; Nielsen, 1999; Nocedal and Wright, 1999; Kelley, 1999; Press, 1992.

4.3 Gas viscosity correlation for a mixture of methane and nitrogen

Measured gas viscosity data for a mixture of 90% methane and 10% nitrogen and for a mixture of 95% methane and 5% nitrogen were used to develop a correlation that could be used to estimate the viscosity of natural gas with high concentration of nitrogen.

$$\mu_g = 10^{-4} K \exp(X \rho_g{}^Y) \quad (4.15)$$

$$K = \frac{(7.7169 + 0.0173M)T^{1.5171}}{238.9481 + 15.67M + T} \quad (4.16)$$

where

$$X = 3.3231 + \left[\frac{816.9684}{T}\right] + 0.0122M \quad (4.17)$$

$$Y = 2.4268 - 0.2528X \quad (4.18)$$

Fig. 4.1 shows the relative error distribution of the model fitted to the measured viscosity data for the mixtures of methane and nitrogen. The Average Relative Error (ARE) of 1.64% confirmed the accuracy of the proposed model.

Fig. 4.2 shows the accuracy of the proposed model in comparison with the measured viscosity data for the mixtures of methane and nitrogen. The R^2 is close to unity, thus confirming the goodness of the model.

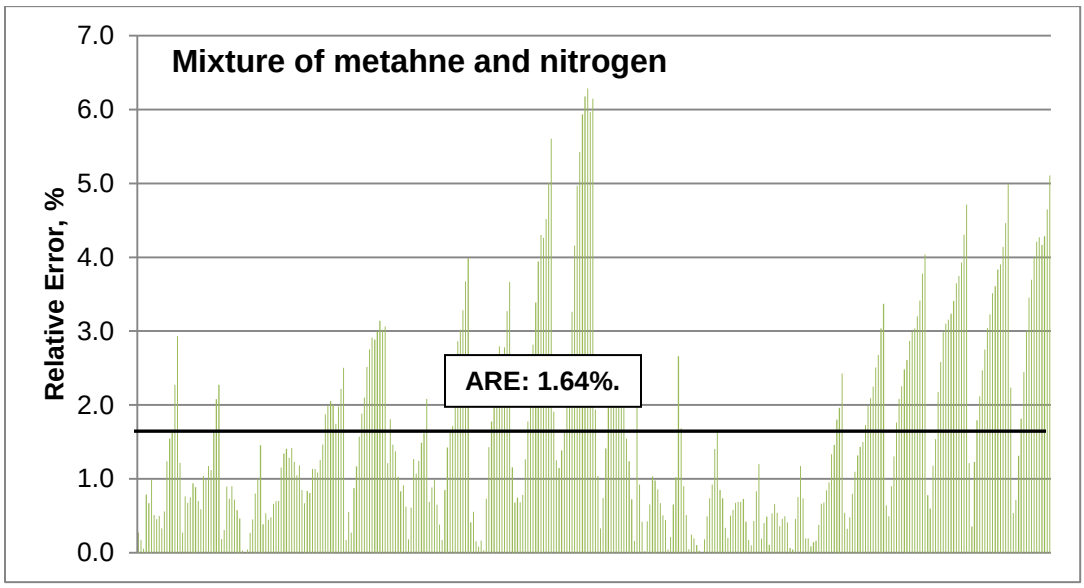

Fig. 4.1—Relative error distribution of fitting the proposed model to the measured viscosity data of mixture of methane and nitrogen shows ARE of 1.64%.

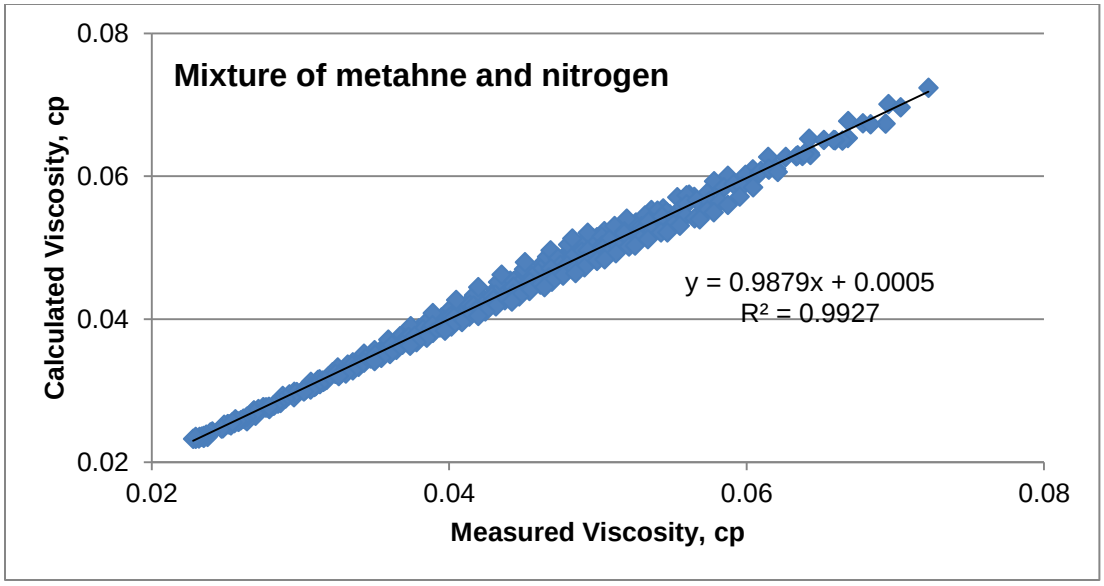

Fig. 4.2—The accuracy of fitted model to the measured viscosity data of mixture of methane and nitrogen is acceptable.

4.4 Gas viscosity correlation for a mixture of methane and CO_2

Measured gas viscosity data for a mixture of 90% methane and 10% CO_2 were used to develop a correlation that could be used to estimate the viscosity of natural gas with high concentration of CO_2.

$$\mu_g = 10^{-4} K \exp(X \rho_g{}^{Y}) \quad \text{.....(4.19)}$$

$$K = \frac{(11.2512 + 0.0189M)T^{1.4498}}{167.4363 + 15.4114M + T} \quad \text{.....(4.20)}$$

where

$$X = 3.7759 + \left[\frac{898.8384}{T}\right] + 0.0089M \quad \text{.....(4.21)}$$

$$Y = 2.2335 - 0.1779X \quad \text{.....(4.22)}$$

Fig. 4.3 shows the relative error distribution of the model fitted to the measured viscosity data for a mixture of methane and CO_2. The ARE of 2.55% confirmed the accuracy of the proposed model.

Fig. 4.4 shows the accuracy of the proposed model in comparison with the measured viscosity data of the mixture of methane and CO_2. The R^2 is close to unity, thus confirming the goodness of the model.

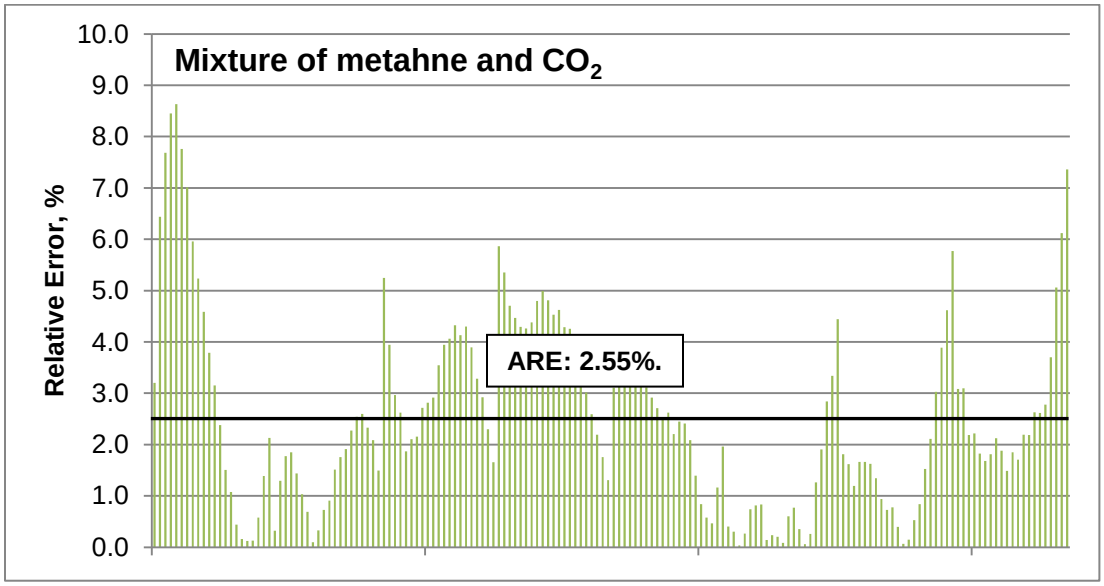

Fig. 4.3—Relative error distribution of fitting the proposed model to the measured viscosity data of mixture of methane and CO_2 shows ARE of 2.55%.

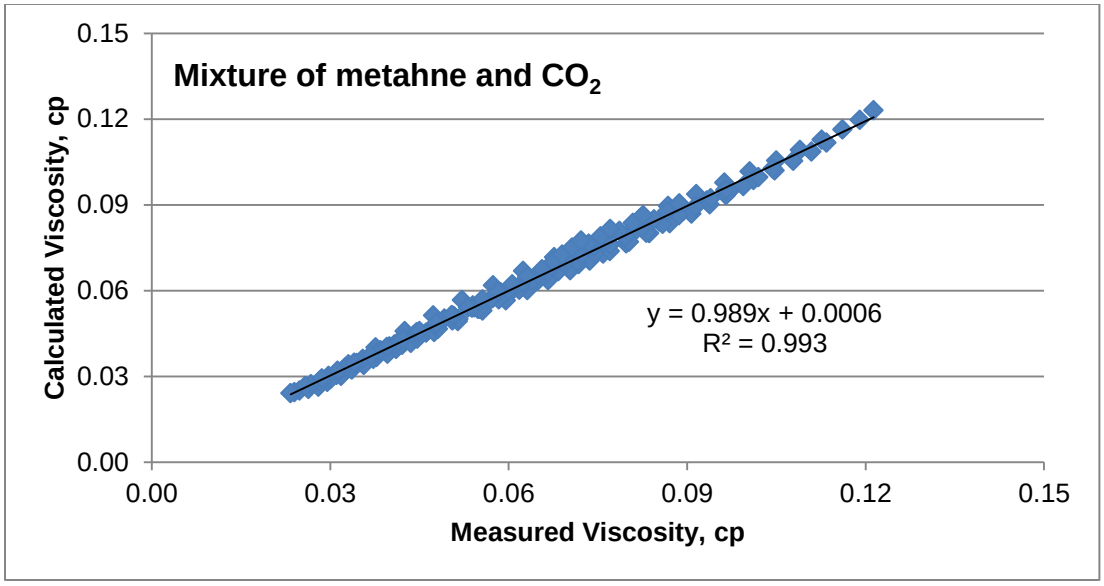

Fig. 4.4—The accuracy of fitted model to the measured viscosity data of mixture of methane and CO_2 is acceptable.

4.5 Gas viscosity correlation for a mixture of methane, nitrogen and CO_2

Ling *et al*. (2009) used a high-pressure viscosity sensor to measure methane viscosity at HPHT conditions (up to 25,000 psi and 415°F). A total of 51 experiments were run. **Table 4.1** shows the methane viscosity dataas measured by Ling (2010).

The methane viscosity data by Ling (2010), together with the measured gas viscosity data for the mixture of 90% methane and 10% nitrogen, for the mixture of 95% methane and 5% nitrogen, and for the mixture of 90% methane and 10% CO_2 were used to develop a correlation that could be used to estimate the viscosity of natural gas with high concentration of nitrogen and CO_2.

Table 4.1—Methane viscosity data (Ling 2010)

Pressure, psi	Temperature, °F						
	100	120	140	160	180	188	200
4,515	0.02454	0.02377	0.02309	0.02265	0.02226		0.021946
5,015	0.02630	0.02531	0.02447	0.02399	0.02376	0.02337	0.022922
5,515	0.02772	0.02675	0.02547	0.02517	0.02490	0.02460	0.024034
6,015	0.02977	0.02790	0.02678	0.02628	0.02599	0.02589	0.025375
6,515	0.03082	0.02886	0.02836	0.02746	0.02707	0.02684	0.0264
7,015	0.03156	0.02995	0.02959	0.02854	0.02806	0.02776	0.027481
7,515	0.03298	0.03108	0.03093	0.02968	0.02900	0.02877	0.028501
8,015	0.03413	0.03224	0.03200	0.03027	0.03018	0.02971	0.029476
8,515	0.03529	0.03344	0.03314	0.03124	0.03110	0.03064	0.0305
9,015	0.03656	0.03470	0.03421	0.03232	0.03195	0.03149	0.031464
9,515	0.03772	0.03585	0.03523	0.03349	0.03279	0.03242	0.032384
10,015	0.03879	0.03700	0.03620	0.03446	0.03376	0.03334	0.033318
10,515	0.03989	0.03807	0.03726	0.03548	0.03484	0.03410	0.034249
11,015	0.04101	0.03915	0.03813	0.03647	0.03552	0.03504	0.035141
11,515	0.04205	0.04020	0.03896	0.03739	0.03643	0.03594	0.035959
12,015	0.04305	0.04118	0.03986	0.03837	0.03732	0.03677	0.036797
12,515	0.04401	0.04218	0.04079	0.03931	0.03825	0.03759	0.037697
13,015	0.04505	0.04311	0.04182	0.04022	0.03916	0.03848	0.038397
13,515	0.04609	0.04412	0.04270	0.04113	0.04005	0.03932	0.03912
14,015	0.04714	0.04512	0.04369	0.04210	0.04088	0.04026	0.040028
14,515	0.04822	0.04614	0.04461	0.04304	0.04179	0.04117	0.040915
15,015	0.04915	0.04709	0.04558	0.04388	0.04272	0.04216	0.041717
15,515	0.05020	0.04812	0.04654	0.04467	0.04361	0.04307	0.042457
16,015	0.05126	0.04901	0.04743	0.04586	0.04443	0.04396	0.04323
16,515	0.05220	0.05004	0.04834	0.04690	0.04530	0.04486	0.043983
22,515	0.06461	0.06220	0.05931	0.05753	0.05566	0.05460	0.054183
23,015	0.06575	0.06277	0.06017	0.05837	0.05650	0.05550	0.055025
23,515	0.06683	0.06402	0.06116	0.05914	0.05719	0.05637	0.055835
24,015	0.06777	0.06505	0.06209	0.05975	0.05819	0.05726	0.056504
24,515	0.06893	0.06603	0.06301	0.06064	0.05915	0.05795	0.057314
25,015	0.07002	-	0.06389	0.06173	0.06007	-	-

Table 4.1—Cont.

Pressure, psi	Temperature, °F						
	220	225	230	250	260	280	300
4,515		0.02171	0.02162	0.02147	0.02140	0.02132	0.02126
5,015	0.022841	0.02283	0.02275	0.02239	0.02238	0.02221	0.02208
5,515	0.023846	0.02378	0.02366	0.02333	0.02334	0.02315	0.02294
6,015	0.024844	0.02480	0.02465	0.02426	0.02427	0.02405	0.02376
6,515	0.025958	0.02580	0.02564	0.02516	0.02520	0.02499	0.02466
7,015	0.026735	0.02670	0.02661	0.02611	0.02602	0.02586	0.02546
7,515	0.027936	0.02762	0.02747	0.02704	0.02692	0.02670	0.02624
8,015	0.028767	0.02874	0.02839	0.02794	0.02791	0.02758	0.02705
8,515	0.029538	0.02968	0.02934	0.02882	0.02873	0.02844	0.02776
9,015	0.030312	0.03051	0.03023	0.02959	0.02961	0.02928	0.02866
9,515	0.031153	0.03133	0.03108	0.03046	0.03041	0.03002	0.02943
10,015	0.032011	0.03216	0.03189	0.03126	0.03118	0.03083	0.03022
10,515	0.032913	0.03287	0.03263	0.03205	0.03194	0.03157	0.03094
11,015	0.033713	0.03372	0.03348	0.03287	0.03269	0.03237	0.03165
11,515	0.034526	0.03445	0.03419	0.03375	0.03338	0.03320	0.03241
12,015	0.035347	0.03526	0.03501	0.03455	0.03429	0.03399	0.03353
12,515	0.036202	0.03607	0.03589	0.03537	0.03504	0.03479	0.03438
13,015	0.03689	0.03690	0.03658	0.03614	0.03586	0.03556	0.03508
13,515	0.037756	0.03753	0.03733	0.03676	0.03666	0.03632	0.03584
14,015	0.038564	0.03862	0.03804	0.03752	0.03739	0.03714	0.03659
14,515	0.039468	0.03943	0.03892	0.03835	0.03827	0.03792	0.03725
15,015	0.040309	0.04041	0.03989	0.03932	0.03906	0.03885	0.03805
15,515	0.041134	0.04106	0.04068	0.03998	0.03988	0.03949	0.03882
16,015	0.041934	0.04184	0.04139	0.04084	0.04051	0.04035	0.03961
16,515	0.042697	0.04250	0.04211	0.04148	0.04127	0.04105	0.04048
17,015	0.043627	0.04331	0.04306	0.04222	0.04194	0.04193	0.04115
17,515	0.044316	0.04406	0.04382	0.04294	0.04281	0.04259	0.04196
18,015	0.045172	0.04471	0.04463	0.04365	0.04357	0.04336	0.04275
18,515	0.045864	0.04561	0.04537	0.04437	0.04445	0.04407	0.04336
19,015	0.046613	0.04642	0.04619	0.04514	0.04521	0.04480	0.04414
19,515	0.047246	0.04724	0.04691	0.04593	0.04609	0.04559	0.04491
20,015	0.047886	0.04804	0.04773	0.04665	0.04681	0.04622	0.04564
20,515	0.048719	0.04879	0.04858	0.04757	0.04759	0.04702	0.04646
21,015	0.049487	0.04951	0.04935	0.04842	0.04847	0.04786	0.04708
21,515	0.05039	0.05036	0.05010	0.04932	0.04915	0.04849	0.04791

Table 4.1—Cont.

Pressure, psi	Temperature, °F						
	220	225	230	250	260	280	300
22,015	0.05116	0.05115	0.05086	0.05008	0.04996	0.04915	0.04868
22,515	0.05199	0.05191	0.05166	0.05083	0.05080	0.04987	0.04928
23,015	0.052822	0.05280	0.05243	0.05141	0.05165	0.05060	0.05005
23,515	0.053689	0.05365	0.05321	0.05204	0.05226	0.05132	0.05071
24,015	0.05416	0.05442	0.05394	0.05294	0.05263	0.05195	0.05156
24,515	0.05494	0.05522	0.05454	0.05357	0.05335	0.05263	0.05200
25,015	0.055865	0.05608	-	-	0.05407	0.05337	-

Pressure, psi	Temperature, °F				
	320	340	360	380	415
4,515	0.021239	0.02096	0.02096	0.02128	0.02133
5,015	0.021905	0.021806	0.02181	0.02206	0.02205
5,515	0.022718	0.02283	0.02283	0.02284	0.02278
6,015	0.023559	0.02369	0.02369	0.02366	0.02361
6,515	0.024432	0.024428	0.02443	0.02435	0.02424
7,015	0.025242	0.025123	0.02512	0.02500	0.02494
7,515	0.02604	0.025847	0.02585	0.02578	0.02565
8,015	0.026787	0.02665	0.02665	0.02641	0.02637
8,515	0.027541	0.027475	0.02748	0.02740	0.02714
9,015	0.028338	0.028407	0.02841	0.02817	0.02786
9,515	0.029081	0.029079	0.02908	0.02886	0.02859
10,015	0.02982	0.029803	0.02980	0.02954	0.02922
10,515	0.030648	0.030575	0.03058	0.03032	0.02995
11,015	0.031407	0.03133	0.03133	0.03110	0.03054
11,515	0.032123	0.032021	0.03202	0.03178	0.03123
12,015	0.032827	0.032794	0.03279	0.03243	0.03194
12,515	0.033536	0.033562	0.03356	0.03306	0.03261
13,015	0.034248	0.034317	0.03432	0.03378	0.03333
13,515	0.035008	0.035008	0.03501	0.03437	0.03400
14,015	0.035747	0.035769	0.03577	0.03503	0.03467
14,515	0.036507	0.036495	0.03650	0.03568	0.03530
15,015	0.037274	0.037203	0.03720	0.03639	0.03599
15,515	0.038098	0.038035	0.03804	0.03708	0.03661
16,015	0.038847	0.03912	0.03912	0.03780	0.03730
16,515	0.03964	0.039713	0.03971	0.03849	0.03797

Table 4.1—Cont.

Pressure, psi	Temperature, °F				
	320	340	360	380	415
17,015	0.040475	0.040391	0.04039	0.03918	0.03866
17,515	0.041149	0.04099	0.04099	0.03986	0.03934
18,015	0.041889	0.042027	0.04203	0.04057	0.04000
18,515	0.042823	0.042721	0.04272	0.04138	0.04068
19,015	0.043501	0.04339	0.04339	0.04184	0.04132
19,515	0.044081	0.044037	0.04404	0.04255	0.04194
20,015	0.044759	0.044576	0.04458	0.04325	0.04254
20,515	0.045437	0.045262	0.04526	0.04391	0.04323
21,015	0.046056	0.045875	0.04588	0.04420	0.04380
21,515	0.046864	0.046576	0.04658	0.04486	0.04431
22,015	0.047585	0.047111	0.04711	0.04544	0.04502
22,515	0.04836	0.047883	0.04788	0.04599	0.04570
23,015	0.048937	0.048361	0.04836	0.04653	0.04628
23,515	0.049763	0.048909	0.04891	0.04717	0.04677
24,015	0.050833	0.049394	0.04939	0.04778	0.04740
24,515	0.051545	0.050105	0.05011	0.04895	0.04796
25,015	0.052277	0.050713	0.05071	-	0.04866

$$\mu_g = 10^{-4} K \exp(X \rho_g{}^{Y}) \quad \text{.....(4.23)}$$

$$K = \frac{(7.5031 + 0.01928M)T^{1.5373}}{250.7565 + 15.4096M + T} \quad \text{.....(4.24)}$$

where

$$X = 3.7425 + \left[\frac{1006.0274}{T}\right] + 0.01208M \quad \text{.....(4.25)}$$

$$Y = 2.9361 - 0.2662X \quad \text{.....(4.26)}$$

Fig. 4.5 shows the relative error (absolute value) distribution of the model fitted to the measured viscosity data of pure methane, mixture of methane and nitrogen and also mixture of methane and CO_2. The ARE of 5.05% confirmed the accuracy of the proposed model.

Fig. 4.6 shows the accuracy of the proposed model in comparison with the measured viscosity data of pure methane, mixture of methane and nitrogen and also mixture of methane and CO_2. The R^2 is close to unity, thus confirming the goodness of the model.

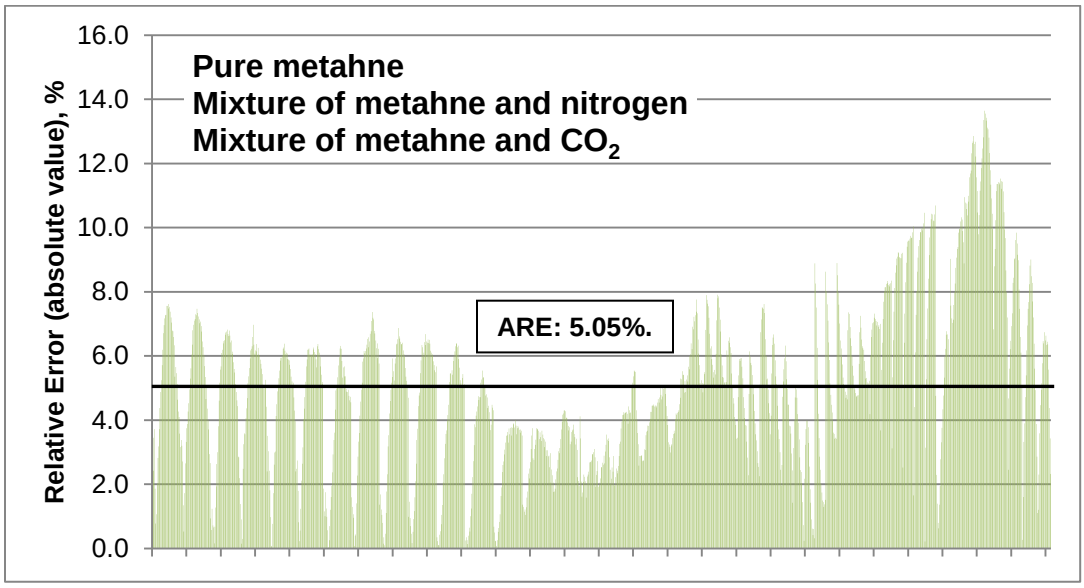

Fig. 4.5—Relative error (absolute value) distribution of fitting the proposed model to the measured viscosity data of pure methane, mixture of methane and nitrogen and also mixture of methane and CO_2 shows ARE of 5.05%.

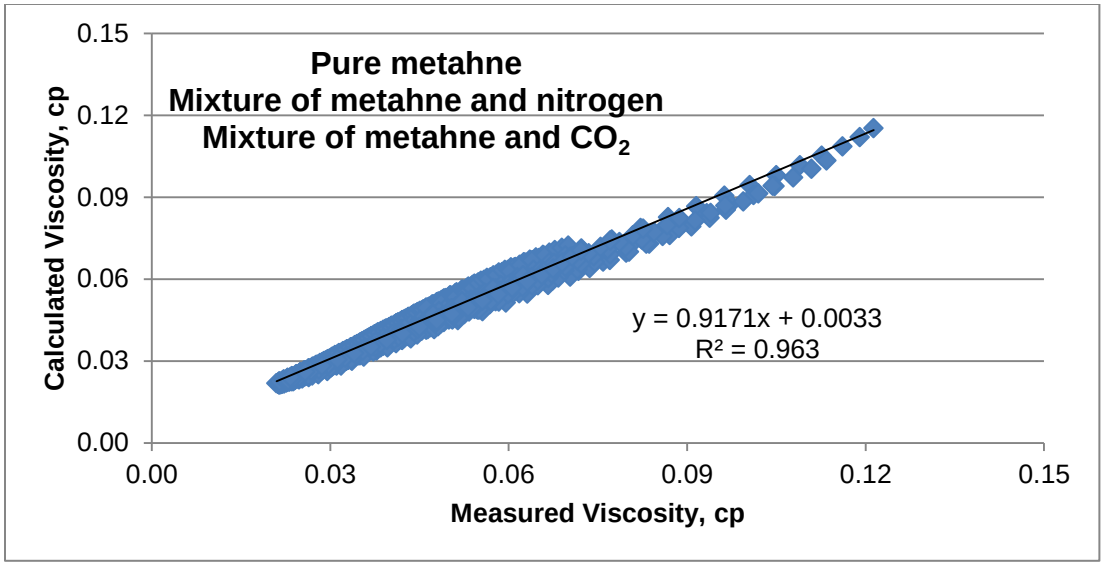

Fig. 4.6—The accuracy of fitted model to the measured viscosity data of pure methane, mixture of methane and nitrogen and also mixture of methane and CO_2.

CHAPTER V

SENSITIVITY OF CUMULATIVE PRODUCTION TO UNCERTAINTIES IN GAS VISCOSITY

5.1 Gas viscosity uncertainty effect on inflow performance relationship (IPR)

A Cartesian plot of bottomhole pressure versus surface flow rate is used to construct an IPR curve, which reflects the capacity of a gas reservoir to deliver fluid to the wellbore. The IPR curve is a diagnostic tool used in the industry to determine the performance of a flowing system.

The exact solution to the differential form of Darcy's law for compressible fluids under pseudo steady-state flow conditions is (Ahmed and McKinney, 2005):

$$q_g = \frac{kh\left(\overline{\psi}_r - \psi_{wf}\right)}{1422T\left[Ln\left(\frac{r_e}{r_w}\right) - 0.75 + s\right]} \quad \text{..... (5.1)}$$

where

$$\overline{\psi}_r = 2\int_0^{\overline{p}r} \frac{p}{\mu Z} dp \quad \text{..... (5.2)}$$

$$\overline{\psi}_{wf} = 2\int_0^{\overline{p}wf} \frac{p}{\mu Z} dp \quad \text{..... (5.3)}$$

This research used the trapezoidal method to solve the integrals in **Eqs 5.2** and **5.3** for a synthetic case. Because the case is representative of HPHT conditions, it is not

unrealistic to assume that the hydrocarbon reservoir fluid is pure methane. Since an accurate correlation to predict the viscosity of mixed gases at such conditions does not exist, we constrained the model to pure methane. Obviously, the problem becomes more significant when the reservoir gases are gas mixtures, such as methane with some quantities of ethane, propane, CO_2, nitrogen and/or hydrogen sulfide.

IPR curves were calculated using the viscosity and density of pure methane from the NIST tables for the selected pressure and temperature conditions. The original NIST gas viscosity values were then perturbated by ± 1% to ± 10%, and the IPR curves re-calculated.

The reservoir parameters used for the synthetic case are summarized in **Table 5.1**. It will be seen from **Fig. 5.1** that small changes in gas viscosity can have a dramatic impact on the IPR's.

Table 5.1—Reservoir descriptions

Temperature	400	^{o}F
Initial pressure	15,000	psi
Permeability	65	md
Reservoir radius	1,000	ft
Wellbore radius	0.25	ft
Thickness	15	ft
Skin	-0.4	

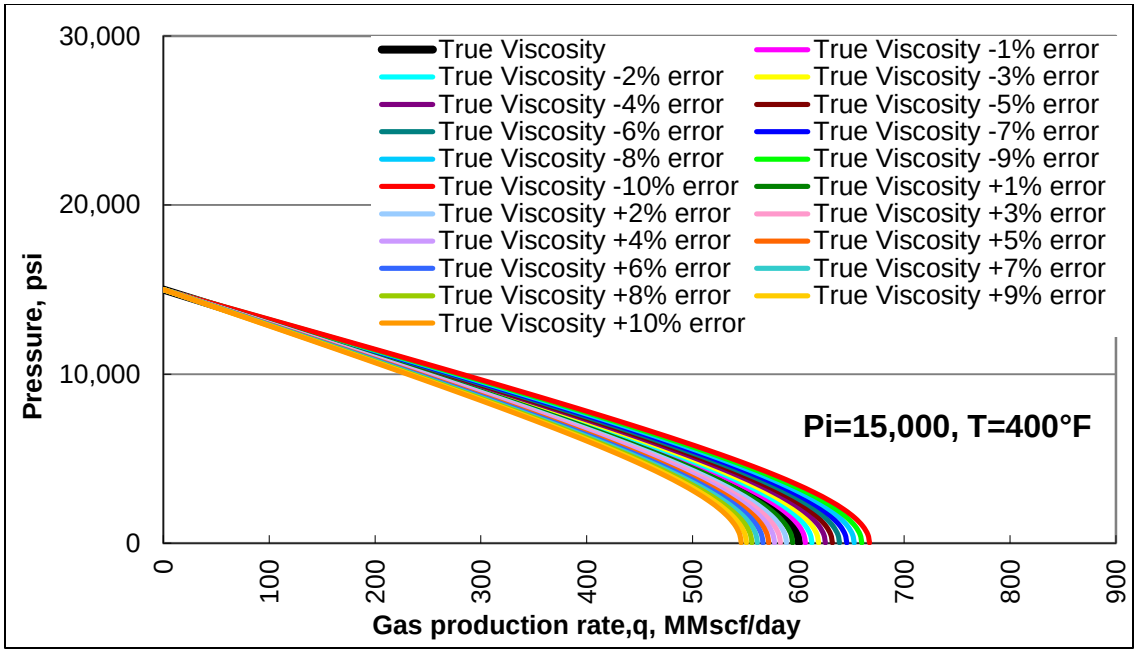

Fig. 5.1—Small errors in gas viscosity considerably shift the IPR curve to the left or right.

Fig. 5.2 shows the changes in calculated gas flow rates as the values of gas viscosities vary. A 10% error in the estimated gas viscosity causes a change of approximately 10% in the predicted value of gas flow rate. An interesting result is that underestimating the gas viscosity gives slightly worse results than overestimating the gas viscosity.

As the predicted gas flowrate would then be used in production forecasting, an error in viscosity estimation would be reflected in the accuracy of ultimate field recovery calculations, with a potential for under /over estimation of the reserves.

Hernandez *et al*. (2002) highlighted the impact of hydrocarbon viscosity prediction on the accuracy of reservoir engineering calculations. They focused on oil viscosity, not

gas viscosity, and concluded that, for light oils, a ±10% error in viscosity leads to a ±1-2% error in the prediction of cumulative production; for heavy oils, the same viscosity error results in a ±10% error in cumulative production.

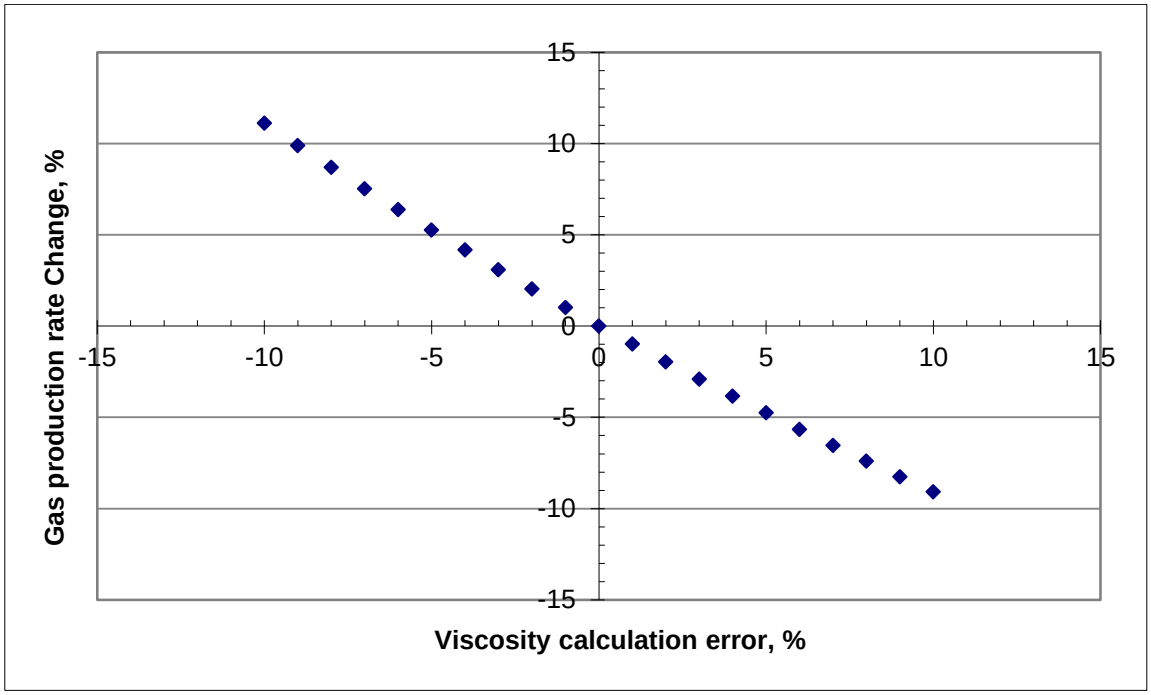

Fig. 5.2—Flowrate change relates directly to uncertainties in gas viscosity.

5.2 Comparing the measured gas viscosity data with the current gas viscosity models

Comparing the measured gas viscosity data with gas viscosity prediction values estimated by available gas viscosity correlations shows that a relative error up to 10% may be associated with the current gas viscosity prediction models at high pressures **(Fig. 5.3).**

The associated errors are not the same for all of the correlations in the entire pressure ranges, some of them work well at a certain pressure range and fail out of that range. **Fig. 5.4** illustrates how the current gas viscosity prediction models work at different pressure ranges. It also clearly points out, however, that the precision of the current gas viscosity models is acceptable at low and moderate pressure, but the models are not accurate enough for the higher pressures.

5.3 Gas viscosity uncertainty effect on cumulative production

The impact of uncertainty in gas viscosity on cumulative gas production was investigated by numerical reservoir simulations performed for a synthetic case including a single well in a pure methane gas reservoir of consistent rock and fluid properties throughout. Viscosity was defined as an input function of pressure and temperature. The goal was to study the differences between the LGE, Sutton, and NIST correlations, the three most common gas viscosity correlations in industry, and also the recently developed Ling correlation. All correlations were evaluated to determine how respect to an actual measurement of gas viscosity at HPHT conditions could affect the recovery factor of field cumulative production. Simulations were run for all five different case and results were evaluated.

The simulator performs an interpolation of the discretized input viscosity values to acquire a continuous viscosity function of pressure and temperature. An uncertainty associated with this interpolation procedure can be minimized by providing a sufficiently large number of input values, as was the case for this investigation.

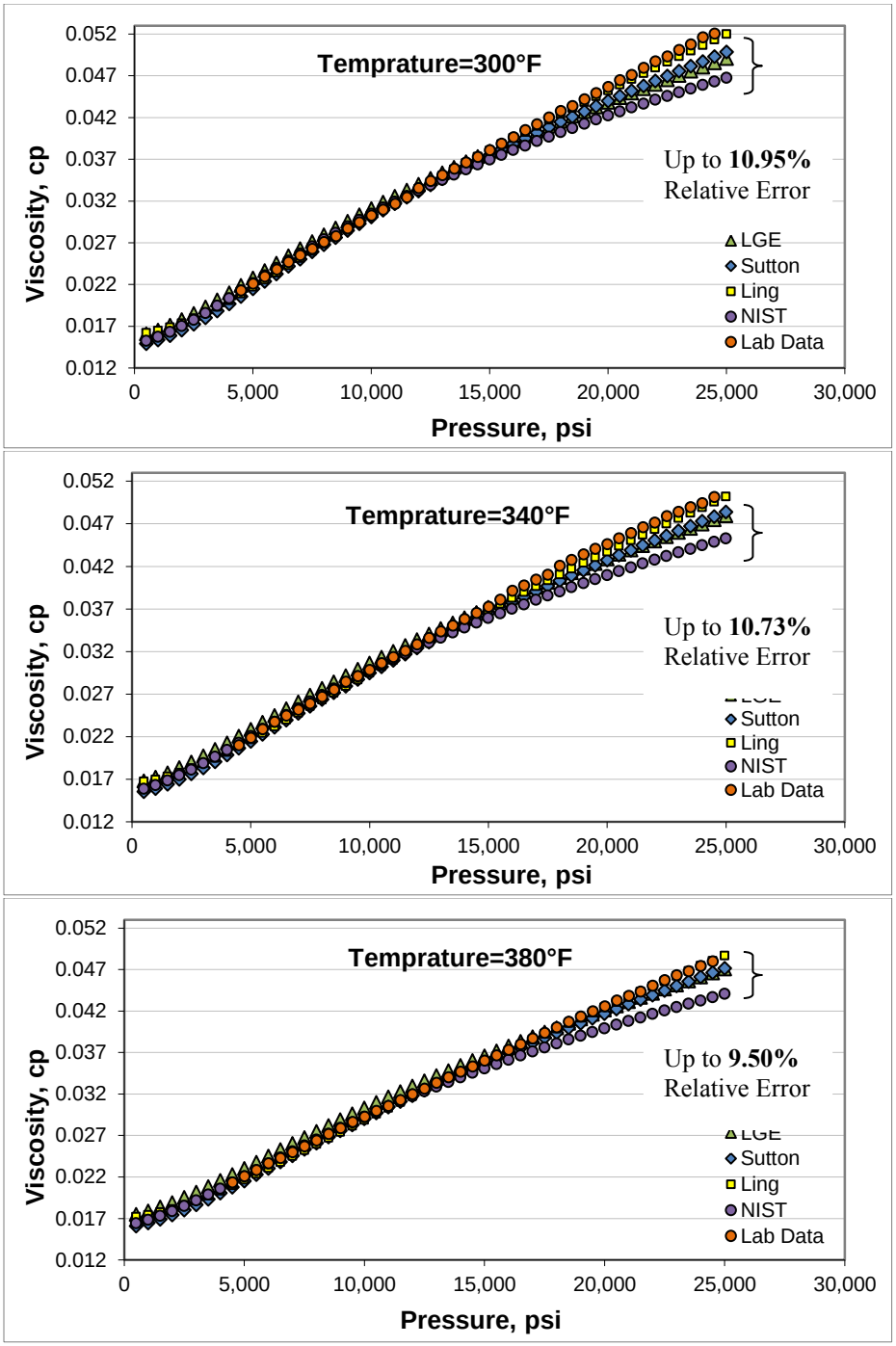

Fig. 5.3—Difference between the current gas viscosity prediction models and lab data can be as big as 10% relative error at high pressure.

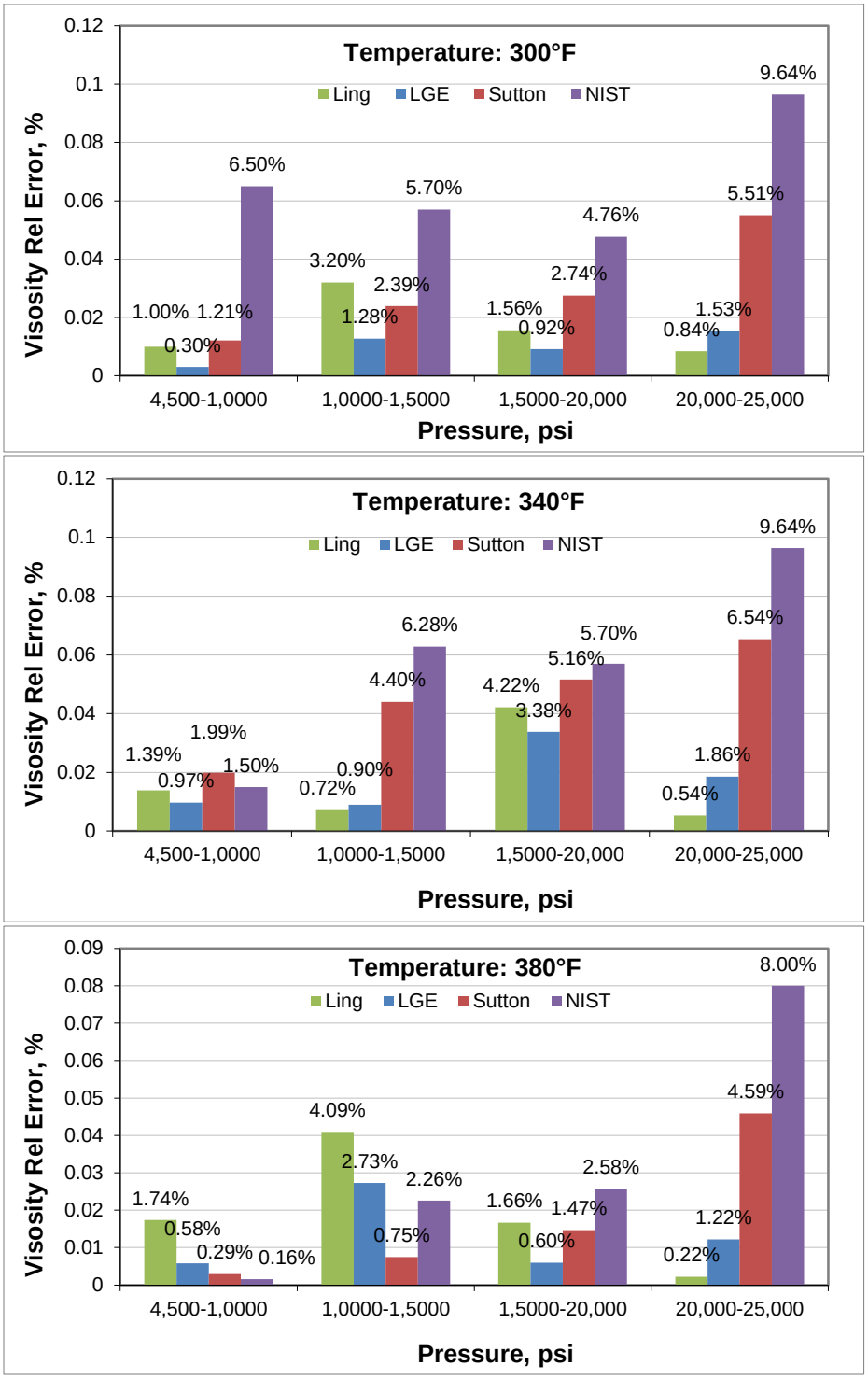

Fig. 5.4—The current gas viscosity prediction models are still reliable at low and moderate pressure, but they are not accurate enough for higher pressures.

The CMG software package (v. 2009.10) was used for this study, with an implicit calculation method and black oil modeling of the fluid properties. The reservoir characteristics used for the synthetic case are summarized in **Table 5.2**. No aquifer supported the pressure. Three different reservoir temperatures were investigated to indicate the relation between gas viscosity uncertainty and temperature. All the runs were performed assuming isothermal conditions.

Table 5.2—Reservoir parameters

Temperature, ^{o}F	300, 340, 380
Initial pressure, psia	25,000
Permeability, md	1
Thickness, ft	180
Porosity, %	10

5.3.1 Approach

Two different approaches have been used in this study to evaluate the effect of gas viscosity error on cumulative gas production forecasting:

5.3.2 Production time scenario

First, we estimate the recovery factor for a certain period of time: one and five years. Time is an important concern in any short-term project when the production time is

limited by contract or company policy and the recovery factor dictates the project budget and development.

5.3.3 Abandonment pressure scenario

Second, we let the reservoir pressure drop until it reaches to abandonment pressure of 2,000 psi, which is defined as the minimum surface pressure required delivering the gas to the sales point. This approach can yield the ultimate recovery. This scenario is the case when no time limitation restricts the production and surface pressure is the only parameter that dictates the life of the well.

5.3.4 Results analysis

Fig. 5.5 shows how a small error associated with gas viscosity estimation between different gas viscosity prediction models and actual measurements introduces a considerable change in gas recovery factor. In a worst scenario, the relative error can be as high as 9%, which is significant in the case of giant natural gas reservoirs.

Since ultimate production is just a function of pressure and gas compressibility factor and has nothing do to with the gas viscosity value, an accurate gas viscosity prediction may appear to be important only for short-term projects, but **Fig. 5.6** illustrates that the different gas viscosity prediction models introduced different abandonment times that could be as high as 8 years for our cases. Therefore, regardless of production time, an inaccurate gas viscosity estimation model may mislead the project budget and development.

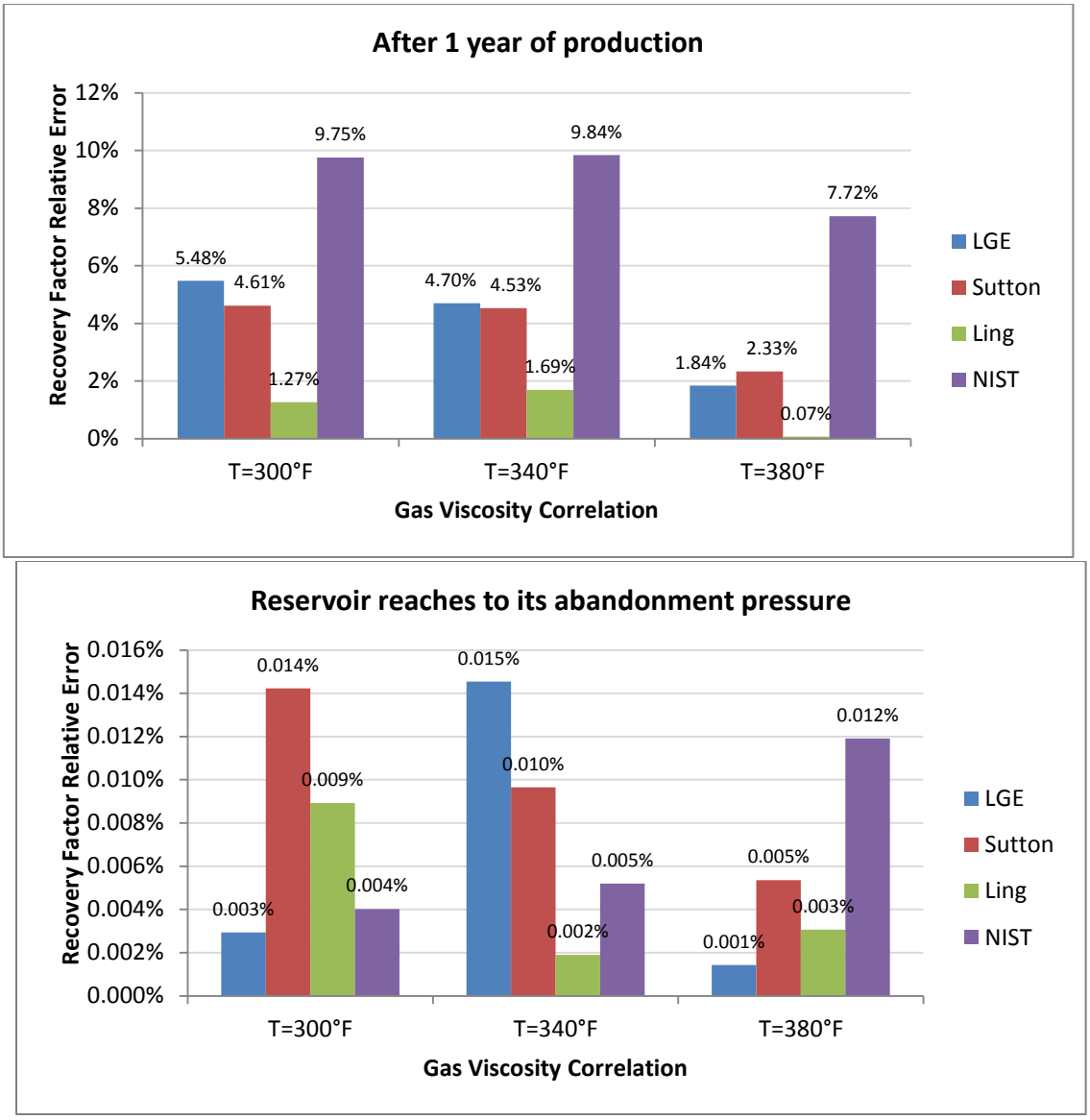

Fig. 5.5—Uncertainty associated with current gas viscosity correlation introduces up to 9.84% relative error in gas production recovery factor. Error is significant in the first year and will decrease as reservoir reaches to abandonment pressure.

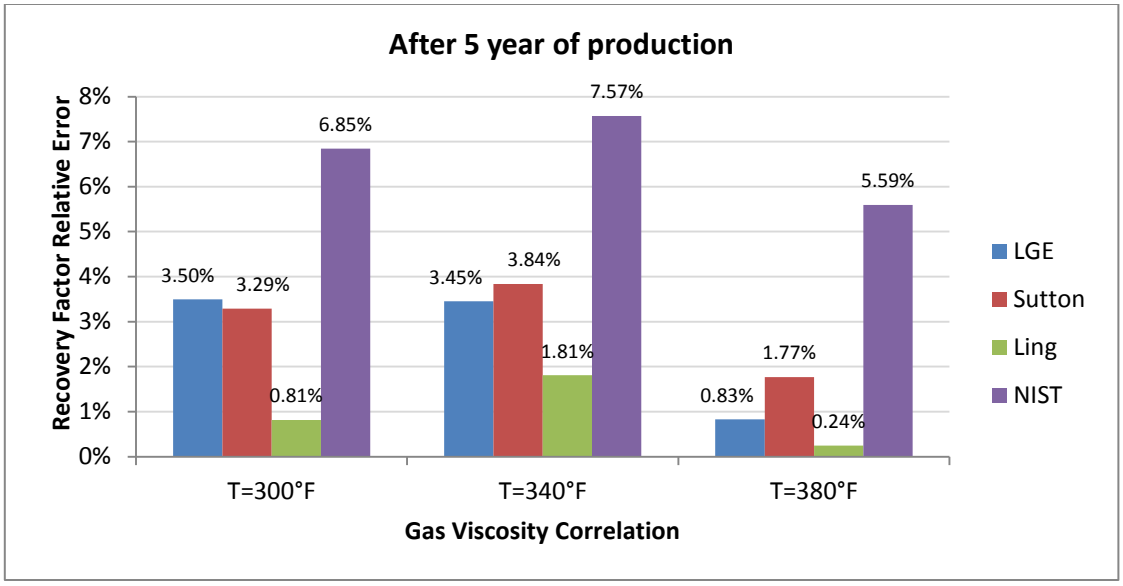
After 5 year of production
Recovery Factor Relative Error
8%
7%
6%
5%
4%
3%
2%
1%
0%
3.50%
3.29%
0.81%
6.85%
3.45%
3.84%
1.81%
7.57%
0.83%
1.77%
0.24%
5.59%
T=300°F
T=340°F
T=380°F
Gas Viscosity Correlation
LGE
Sutton
Ling
NIST

Fig. 5.5— Cont.

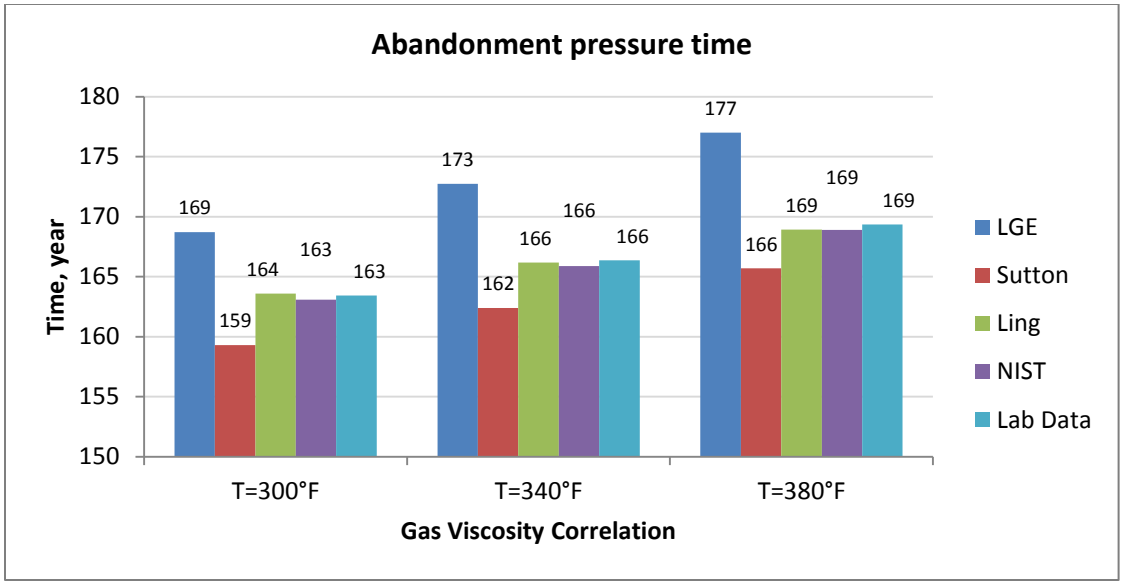

Fig. 5.6—Although the recovery factor relative errors are small as the reservoir approaches to its abandonment pressure, the time the reservoir reaches to abandonment pressure is a function of gas viscosity. The difference between lab data and current gas viscosity correlations can be over 8 years.

CHAPTER VI

CONCLUSIONS AND RECOMMENDATIONS

6.1 Conclusions

The accuracy of current gas viscosity correlations is satisfactory for low to moderate pressure (up to 10,000 psi), Comparing the measured gas viscosity with the values estimated by commonly used correlations shows a relative error up to +10% at high pressure.

Estimating gas viscosity at HPHT conditions with the current prediction models introduces a relative error in recovery factor estimation for a certain period of time of up to 9%. It also leads to improper forecast of well/reservoir life time up to 8 years difference based upon a certain abandonment pressure. These errors are significant with reference to the current giant natural gas reservoirs.

The effect of non-hydrocarbon impurities such as nitrogen and CO_2 should be taken into account to ensure better estimation of natural gas viscosity. The experimental data collected with this study show that, at low temperature, the LGE and Sutton correlations overestimate the viscosity of a mixture of 90% methane and 10% nitrogen, while at high temperature they underestimate it. The measured data also show that the LGE and Sutton correlations overestimate the viscosity of a mixture of 95% methane and 5% nitrogen and that of a mixture of 90% methane and 10% CO_2.

A HPHT gas viscosity correlation was developed to estimate the viscosity of a mixture of methane and nitrogen based upon measured data. This correlation is applicable for pressures up to 20,000 psi and temperatures up to 340°F.

A HPHT gas viscosity correlation was also developed to estimate the viscosity of a mixture of methane and CO_2 based upon measured data. This correlation is applicable for pressures up to 250,000 psi and temperatures up to 360°F.

Finally, a HPHT gas viscosity correlation was developed to estimate the viscosity of a mixture of methane, nitrogen and CO_2 based upon measured data. This correlation is applicable for pressures up to 250,000 psi and temperatures up to 415°F.

Using gas instead of liquid to calibrate a rolling ball viscometer over the entire pressure and temperature range of interest appears to be satisfactory for testing gases (as opposed to liquids). Optimizing tube inclination angle and ball/tube diameter ratio prevents turbulent flow effects around the ball, thus enhancing the accuracy of the measurement. Viscosity measurements of ultra-pure CO_2 confirmed this technique.

6.2 Recommendations

Measure the viscosity of different mixtures of methane and CO_2 to provide more data and so extend the validity of the newly developed correlation.

Measure the viscosity of ternary mixtures of methane, nitrogen and CO_2 from low to high pressure and at different temperatures to improve the accuracy of viscosity estimation for mixtures of methane, nitrogen and CO_2.

Design a rolling-ball viscometer that can withstand HPHT conditions and so measure gas viscosity at such conditions, in order to verify the accuracy of the measurements taken with the oscillating-piston viscometer and provide more confidence on the developed correlations.

Since all the current viscosity correlations require an accurate gas density estimation, it is strongly recommended to measure the gas density of methane, nitrogen, CO_2 and mixtures of them at HPHT condition to improve the accuracy of the calculated viscosity.

REFERENCES

Ahmed, T. and McKinney, P. 2005. *Advanced Reservoir Engineering.* Amsterdam, Netherlands: Gulf Professional Publishing.

Audonnet, F. and Padua, A.A.H. 2003. Viscosity and Density of Mixtures of Methane and n-Decane from 298 to 393 K and up to 75 MPa. *Fluid Phase Equil*. **216** (2): 235–244.

Baron J.D. Roof, J.G., and Well, F.W. 1959. Viscosity of Nitrogen, Methane, Ethane, and Propane at Elevated Temperature. *J. Chem. Eng. Data* **4**: 283-288.

Bessel, F. W. 1828. *Untersuchungen über die Länge des einfachen Secundenpendels.* Berlin: Dr. der Königl Akad der Wiss.

Block, R.B. 1940. On the Resistance to the Uniform Motion of a Solid through a Viscous Liquid. *J. Appl. Phys* **13** (1): 56-65.

Born, M. and H. Green. 1947. A general kinetic theory of liquids. III. Dynamical properties. *Proceedings of the Royal Society of London. Series A. Mathematical and Physical Sciences* **190** (1023): 455-474.

BP, 2008. *Statistical Review of World Energy*. June 2008. www.bp.com. Downloaded 15 February 2009.

BP, 2010. *Statistical Review of World Energy*. June 2010. www.bp.com. Downloaded 15 December 2010.

Bruschi, L. and Santini, M. 1975. Vibrating Wire Viscometer. *Rev. Sci. Instrum* **46**(11): 1560-1568.

Canet, X., Baylaucq, A., and Boned, C. 2002. High-Pressure (up to 140 MPa) Dynamic Viscosity of the Methane+Decane System. *Int. J. Therm* **22**: 1469–1486.

Carmichael, L. and Sage, B. 1963. Viscosity of Hydrocarbons. N-Butane. *J. Chem. Eng. Data* **8** (4): 612-616.

Carr, N.L., Kobayashi, R., and Burrows, D.B. 1954. Viscosity of Hydrocarbon Gases Under Pressure. *Trans., AIME* **201**: 264-272

Chan, R. and Jackson, D. 1985. An Automated Falling-Cylinder High Pressure Laser-Doppler Viscometer. *J. of Phys E: Sci. Instrum* **18**: 510-511.

Comings, E.W. and Egly, R.S. 1940. Viscosity of Gases and Vapors at High Pressures. *Ind. Eng. Chem.*. **32**: 714-718.

Comings, E.W., Mayland, B.J., and Egly, R.S. 1944. The Viscosity of Gases at High Pressures. *Bulletin of the University of Illinois Engineering Experiment Station* **354**: 11-70.

Davani, E., Ling, K., Teodoriu, C., McCain, WD Jr., and Falcone. G. 2009. More Accurate Gas Viscosity Correlation for Use at HPHT Conditions Ensures Better Reserves Estimation. Paper SPE 124734 presented at the SPE Annual Technical Conference and Exhibition, New Orleans, Louisiana, 4–7 October.

Davani, E., Ling, K., Teodoriu, C., McCain, WD Jr., and Falcone. G. 2009 Inaccurate Gas Viscosity at HPHT Conditions and Its Effect on Unconventional Gas Reserves Estimation. Paper SPE 122827 presented at the SPE Latin American and Caribbean Petroleum Engineering Conference, Cartagena, Colombia, 31 May–3 June.

Dealy J. M., *Rheometers for Molten Plastics.* New York: Van Nostrand Reinhold, 1982.

Dempsey, J.R.1965. Computer Routine Treats Gas Viscosity as a Variable. *Oil and Gas J* **63**: 141-143.

Dewitt, K.J. and Thodos, G. 1966. Viscosities of Binary Mixtures in the Dense Gaseous State: The Methane-CO_2 System. *The Can. J. Chem. Eng.* **44** (3): 148-151.

Diehl, J., Gondouin, M., Houpeurt, A., Neoschil, J., Thelliez, M., Verrien, J.P., and Zurawsky, R. 1970. *Viscosity and Density of Light Paraffins, Nitrogen and* CO_2. Paris: CREPS/Geopetrole.

Diller, D. 1982. Measurements of the Viscosity of Compressed Gaseous and Liquid Nitrogen + Methane Mixtures. *Int. J. Thermophys.* **3** (3): 237-249. DOI: 10.1007/bf00503319

Du Buat., P. L. G. 1786. *Principes d'hydraulique*. Paris: L'imprimerie de monsieur.

Flowers, A.E. 1914. Viscosity Measurement and a New Viscometer. *Proceedings of the Annual Meeting-American Society for Testing Materials* **14** (2): 665-616.

Jackson, W. 1956. Viscosities of the Binary Gas Mixtures, Methane-CO_2 and Ethylent-Argon. *J. Phys. Chem.* **60** (6): 789-791.

Jeje, O. and Mattar, L. 2004. Comparison of Correlations for Viscosity of Sour Natural Gas. Paper 2004-2004-214 presented at Petroleum Society's 5th Canadian International Petroleum Conference (55th Annual Technical Meeting), Calgary, Alberta, Canada, 8 – 10 June.

Jossi, J.A. Stiel, L.I., and Thodos G. 1962. The Viscosity of Pure Substances in the Dense Gaseous and Liquid Phases. *AIChE Journal* **8**(1): 59-62.

Golubev, I.F. 1959. *Viscosity of Gases and Gas Mixtures, a Handbook*. This book is a translation from Russian by the National Technical Information Service. Alexandria, Virginia.

Gonzalez, M.H. Richard, F.B. and Lee, A.L. 1966. The Viscosity of Methane. Paper SPE 1483 presented at the Annual Fall Meeting, Dallas, 2-5 Oct.

Halliburton, 2010. HPHT reservoirs definition. http://www.halliburton.com/ps/default.aspx?navid=1906&pageid=4139. Downloaded 15 November 2010.

Hernandez, J.C., Vesovic, V., Carter, J.N., and Lopez. E. 2002. Sensitivity of Reservoir Simulations to Uncertainties in Viscosities. Paper SPE 75227 presented at the SPE/DOE IOR Symposium, Tulsa, Oklahoma, 13–17. April.

Hersey, M.D. and Shore, H. 1928. Viscosity of Lubricants Under Pressure. *Mech. Eng.* **50**: 221-228.

Hersey, M.D. and Wash, J. 1916. Theory of Torsion and Rolling Ball Viscosimeters, and the Effect of Pressure on Viscosity. *J. Washington Academy Science* **6**: 525-530.

Hubbard, R. and Brown, G. 1943. Rolling Ball Viscometer. *Ind. Eng. Chem. Analytical Edition* **15** (3): 212-218. DOI: 10.1021/i560115a018

Kelley, C.T. 1999. *Iterative Methods for Optimization*. Philadelphia: SIAM Press.

Knapstad, B., Skjolsvik, P.A., and Oye, H.A. 1990. Viscosity of the n-Decane – Methane System in the Liquid Phase. *Ber. Bunsenges Phys. Chem* **94**: 1156–1165.

Kumagai, A., Kawase, Y., and Yokoyama, C. 1998. Falling Capillary Tube Viscometer Suitable for Liquids at High Pressure. Rev. *Rev. Sci. Instrum.* **69**: 1441-1445.

Kuss, E. 1952. High Pressure Research II: The Viscosity of Compressed Gases. Z. *Angew. Phys* **4**(6): 203-207.

Lee, A.L. 1965. Viscosity of Light Hydrocarbons. New York: *American Petroleum Institute*, Monograph on API Research Project 65.

Lee, A.L., Gonzalez, M.H., and Eakin, B.E. 1966. The Viscosity of Natural Gases. Paper SPE 1340 presented at the SPE Annual Technical Conference and Exhibition, Shreveport**,** Louisiana, 11–12. November. SPE-1340-MS.

Levenberg, K. 1944. A Method for the Solution of Certain Non-linear Problems in Least Squares. *Q. Appl. Math.* **2**(2):164–168.

Lewis, H.W. 1953. Calibration of Rolling Ball Viscometer. *Anal. Chem.* **25** (3): 507-508.

Ling, K. 2010. Gas Viscosity at High Pressure and High Temperature. PhD thesis, Texas A&M University, College Station, TX.

Ling, K., Teodoriu, C., Davani, E., and Falcone. G. 2009. Measurement of Gas Viscosity at High Pressures and High Temperatures. Paper IPTC 13528 presented at the International Petroleum Technology Conference, Doha, Qatar, 7–9 December.

Londono. F. 2001. New Correlations for Hydrocarbon Gas Viscosity and Gas Density. MS thesis, College Station, Texas: Texas A&M U.

Lourakis, M. I. A. 2005. *A Brief Description of the Levenberg-Marquardt Algorithm Implemented by Levmar*. Foundation for research and technology.

Heraklion Madsen, K., Nielsen, H.B., and Tingleff, O. 2004. Methods for Non-Linear Least Squares Problems. Technical University of Denmark, Lecture Notes. http://www.imm.dtu.dk/courses/02611/nllsq.pdf. Downloaded 15 June 2011.

Marquardt, D.W. 1963. An Algorithm for the Least-Squares Estimation of Nonlinear Parameters. *SIAM Journal of Applied Mathematics*, **11**(2):431–441.

Mittelmann, H.D. 2004. The Least Squares Problem.
http://plato.asu.edu/topics/problems/nlolsq.html. Downloaded 15 June 2011.

Nielsen, H.B. 1999. *Damping Parameter in Marquardt's Method*. Technical Report IMM-REP-1999-05. Aarhus, Denmark: Technical University of Denmark.

National Institute of Science and Technology (NIST). 2011. Web-Book of Thermodynamic Properties of Fluids. http://webbook.nist.gov,chemisty/fluid. Downloaded 11 November 2011.

Nocedal, J. and Wright, S.J. 1999. *Numerical Optimization*. New York: Springer.

Press, W.H., Teukolsky, S.A., Vetterling, A.W.T., and Flannery, B.P. 1992. *Numerical Recipes in C: The Art of Scientific Computing*. New York: Cambridge University Press.

Rankine, A.O. 1923. A Simple Viscometer for Gases. *J. Sci. Instr*. **1**: 105-111

Sage, B., Yale, W., and Lacey, W. 1939. Effect of Pressure on Viscosity of N-Butane and Iso-Butane. *Ind. Eng. Chem* **31**: 223-226.

Sage, B.H. and Lacey, W.N. 1938a. Effect of Pressure Upon Viscosity of Methane and Two Natural Gases. *Trans.AM.Inst.Mining Met.Engineers* **127**: 118-134.

Sage, B.H. and Lacey, W.N. 1938b. Viscosity of Hydrocarbon Solutions Viscosity of Liquid and Gaseous Propane. *Ind. Eng. Chem.* **30** (7): 829-834.

SPE E&P Glossary. 2010. HPHT Reservoirs Definition. http://www.spe.org/glossary/wiki/doku.php/terms:hpht. Downloaded 11 November 2010.

Starling, K. E., and Elington. R. T. 1964. Viscosity Correlations for Nonpolar Dense Fluids. *AIChE Journal* **10** (1):11–15.

Stephan, K., and Lucas, K. 1979. *Viscosity of Dense Fluids*. The Purdue Research Foundation. New York: Plenum Press.

Stokes, G.G. 1901. *Mathematical and Physical Papers III*. London, UK: Cambridge University Press.

Sutton, R. P. 2005. Fundamental PVT Calculations for Associated and Gas/Condensate Natural-Gas Systems. Paper SPE 97099 presented at the SPE Annual Technical Conference and Exhibition, Dallas, Texas, 9–12. October. SPE-97099 –MS-P.

Swift, G.W., Christy, J.A., and Kurata, F. 1959. Liquid Viscosities of Methane and Propane. *AIChE Journal* **5**: 98-102.

Tomida, D. Kumagai, A., and Yokoyama, C. 2005. Viscosity Measurements and Correlation of the Squalane + CO2 Mixture. *Int. J. Thermophys.* **28**(1): 133-145.

Tough, J.T., McCormick, W.D., and Dash, J.G. 1964. Vibrating Wire Viscometer. *Rev. Sci. Instrum.* **35 (**10): 1345-1348.

Trappeniers, N.J., van der Gulik, P.S., and van den Hooff, H. 1980. The Viscosity of Argon at Very High Pressure, up to the Melting Line. *Chem. Phys. Letters* **70 (**3): 438-443.

Van Wazer. J. R., Lyons, J. W., Kim, K. Y., and Colwell, R. E. 1963. *Viscosity and Flow measurement*: *A Labratory Handbook of Rheology.* Interscience Publishers, New York.

Wikipedia. 2011. Viscometer. http://en.wikipedia.org/wiki/Viscometer, Downloaded 11 May 2011.

Viswanathan, A. 2007. Viscosities of Natural Gases at High Pressures and High Temperatures. MS thesis, Texas A&M University, College Station, TX.

Walters, K. 1975. Rheometry; New York: John Wiley & Sons.

Wilhelm, J., Vogel, E., Lehmann, J. K., and. Wakeham W. A. 1998. A Vibrating Wire Viscometer for Dilute and Dense Gases. *Int. J. Thermophys.* **19 (**2): 391-401.

Xue, G. Data-Gupta, A, Valko, P., and Blasingame, T. A. 1997. Optimal Transformations for Multiple Regression: Application to Permeability Estimation from Well Logs. *SPE Formation Evaluation Journal* **12** (2): 85-93.

APPENDIX A

Comparison of viscosity of mixture of 90% methane and 10% nitrogen with LGE and Sutton correlations.

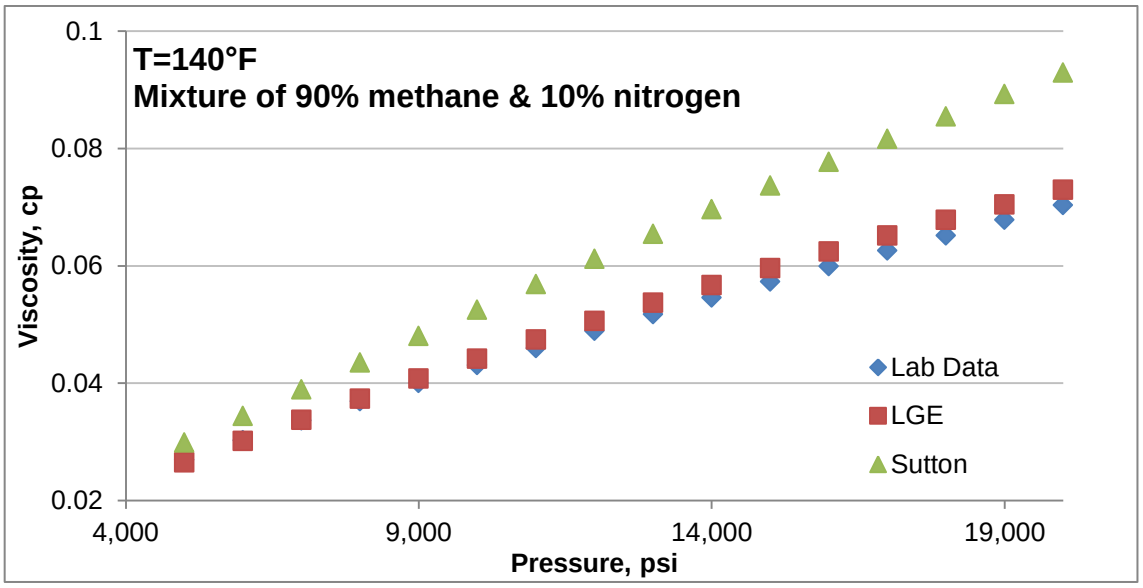

Fig. A.1—LGE and Sutton correlation have been compared with measured gas viscosity of mixture of 90% methane and 10% nitrogen at temperature of 140°F.

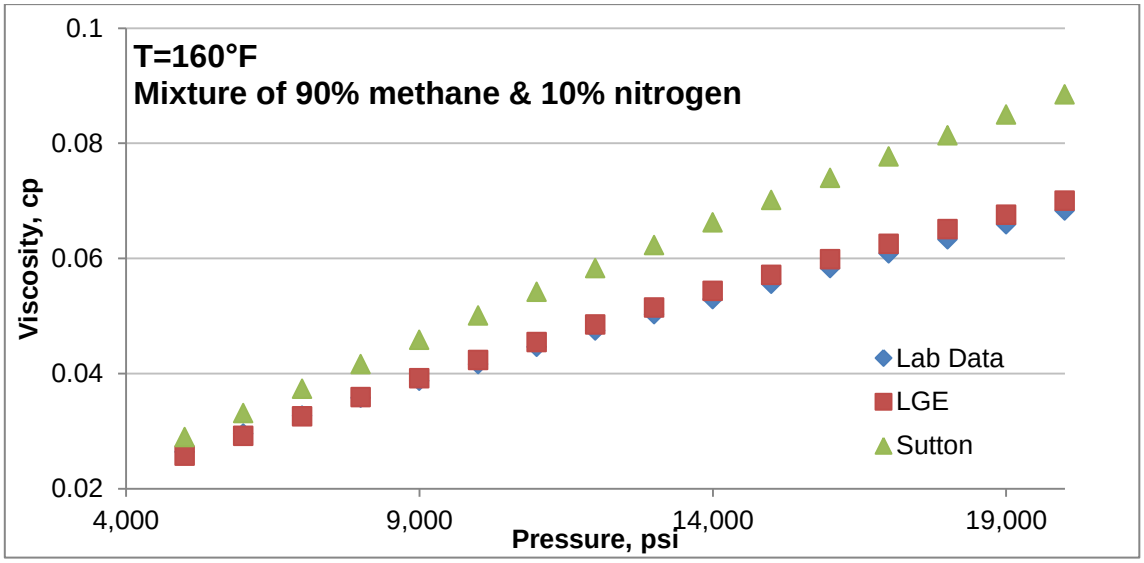

Fig. A.2—LGE and Sutton correlation have been compared with measured gas viscosity of mixture of 90% methane and 10% nitrogen at temperature of 160°F.

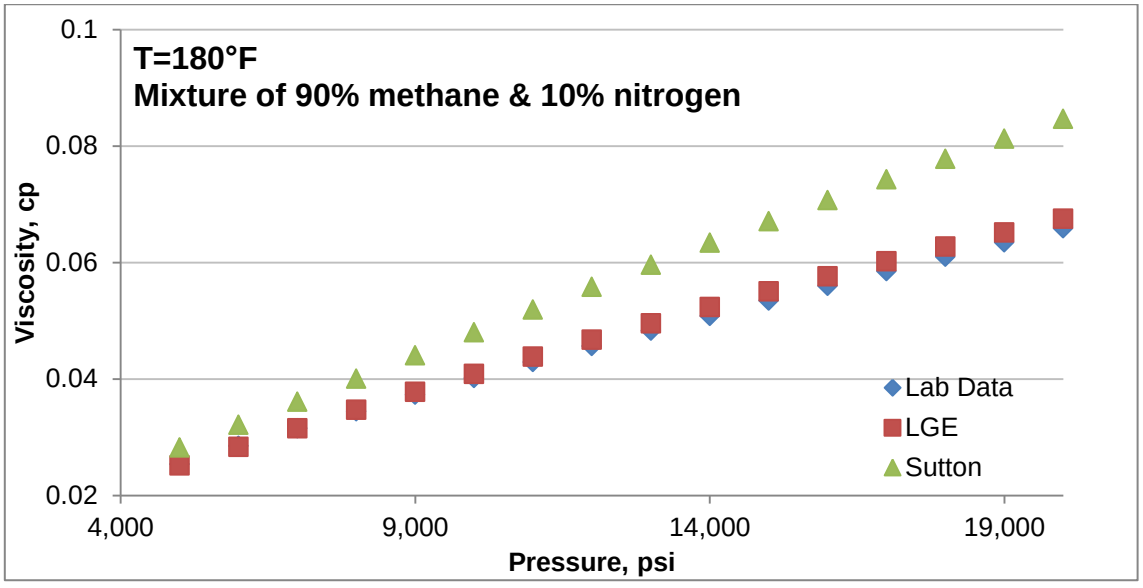

Fig. A.3—LGE and Sutton correlation have been compared with measured gas viscosity of mixture of 90% methane and 10% nitrogen at temperature of 180°F.

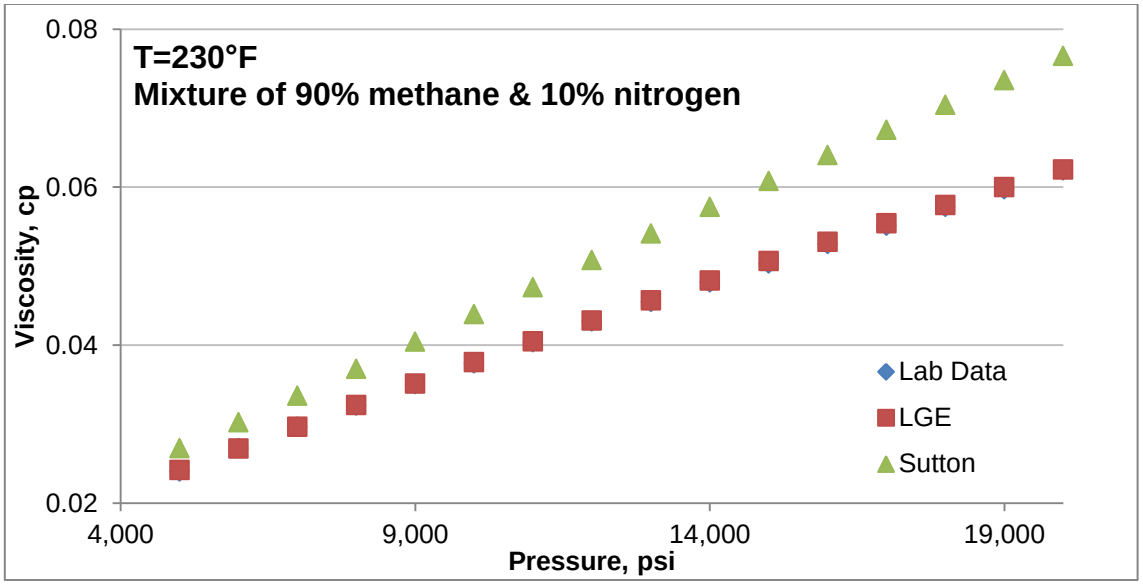

Fig. A.4—LGE and Sutton correlation have been compared with measured gas viscosity of mixture of 90% methane and 10% nitrogen at temperature of 230°F.

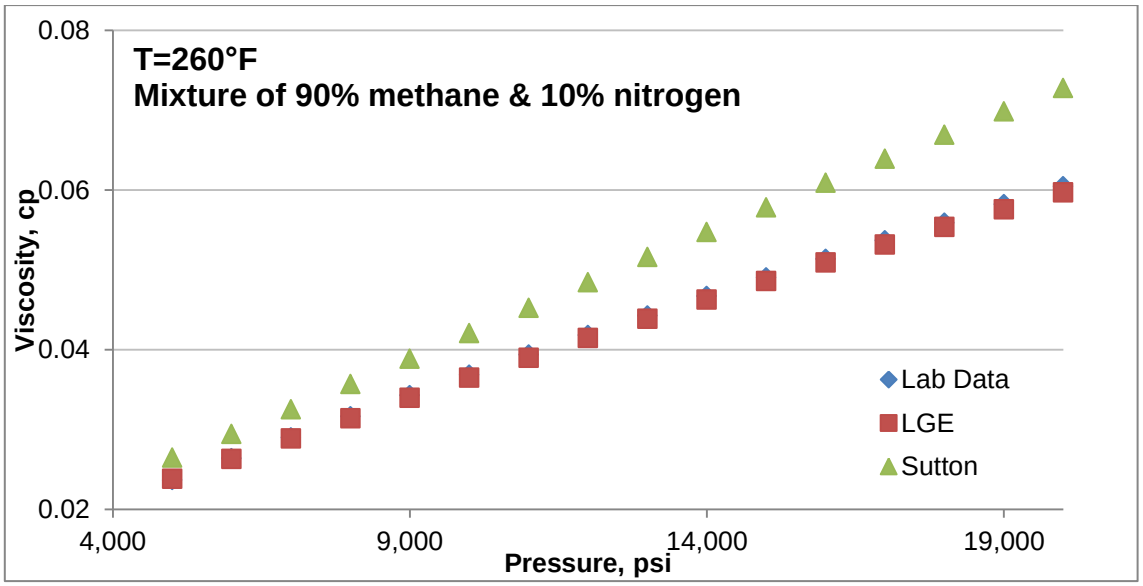

Fig. A.5—LGE and Sutton correlation have been compared with measured gas viscosity of mixture of 90% methane and 10% nitrogen at temperature of 260°F.

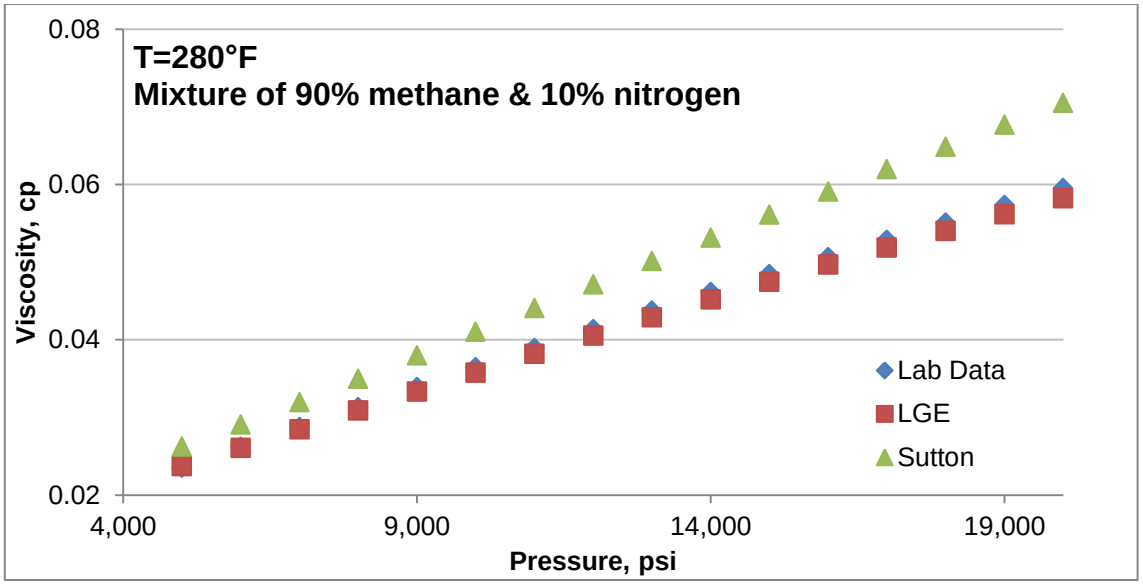

Fig. A.6—LGE and Sutton correlation have been compared with measured gas viscosity of mixture of 90% methane and 10% nitrogen at temperature of 280°F.

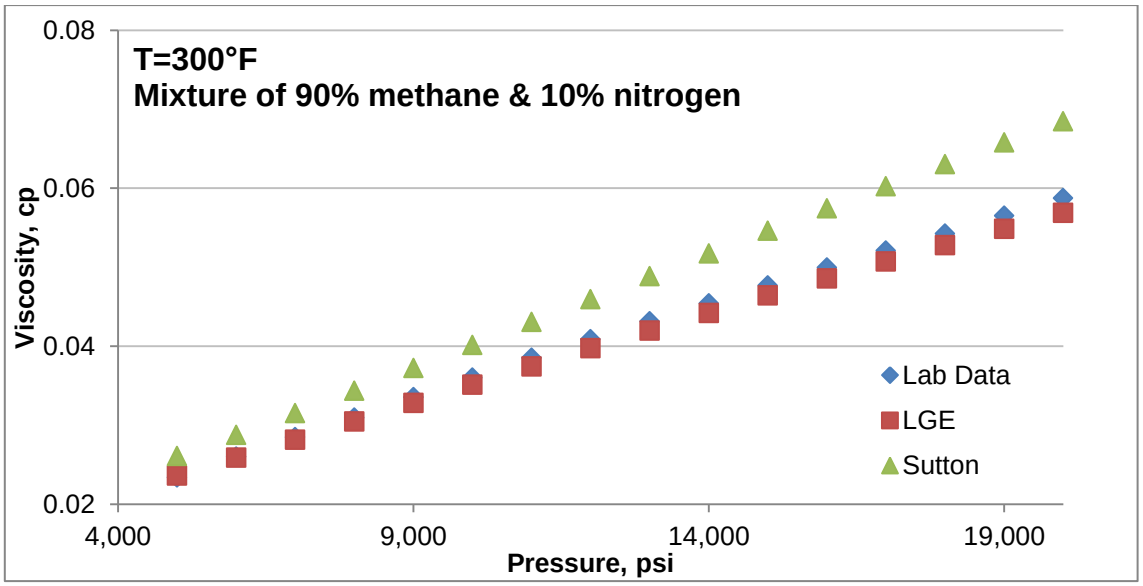

Fig. A.7—LGE and Sutton correlation have been compared with measured gas viscosity of mixture of 90% methane and 10% nitrogen at temperature of 300°F.

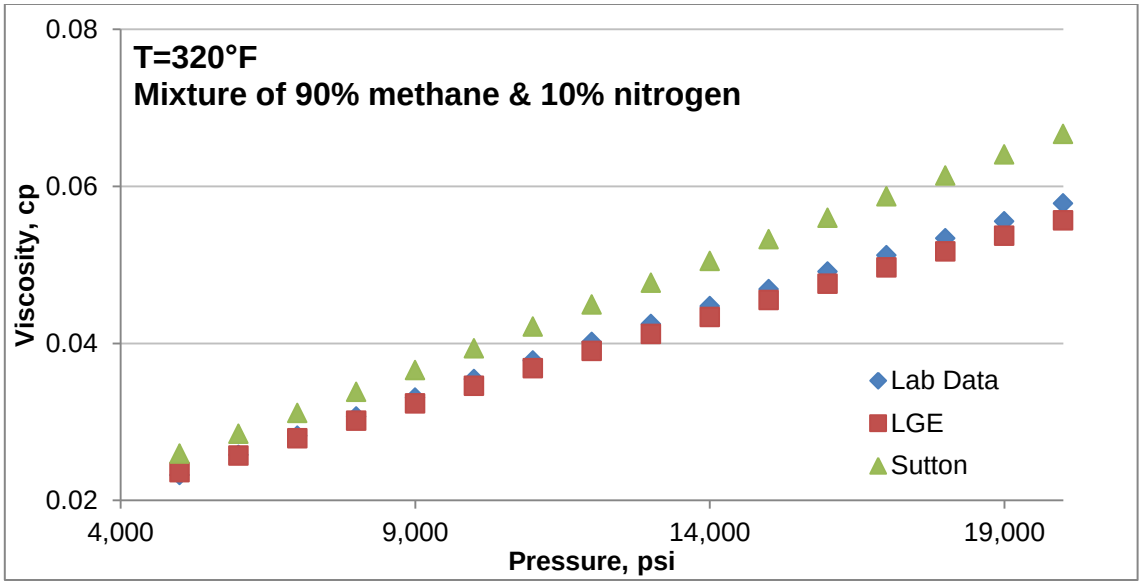

Fig. A.8—LGE and Sutton correlation have been compared with measured gas viscosity of mixture of 90% methane and 10% nitrogen at temperature of 320°F.

APPENDIX B

Comparison of viscosity of mixture of 95% methane and 5% nitrogen with LGE and Sutton correlations.

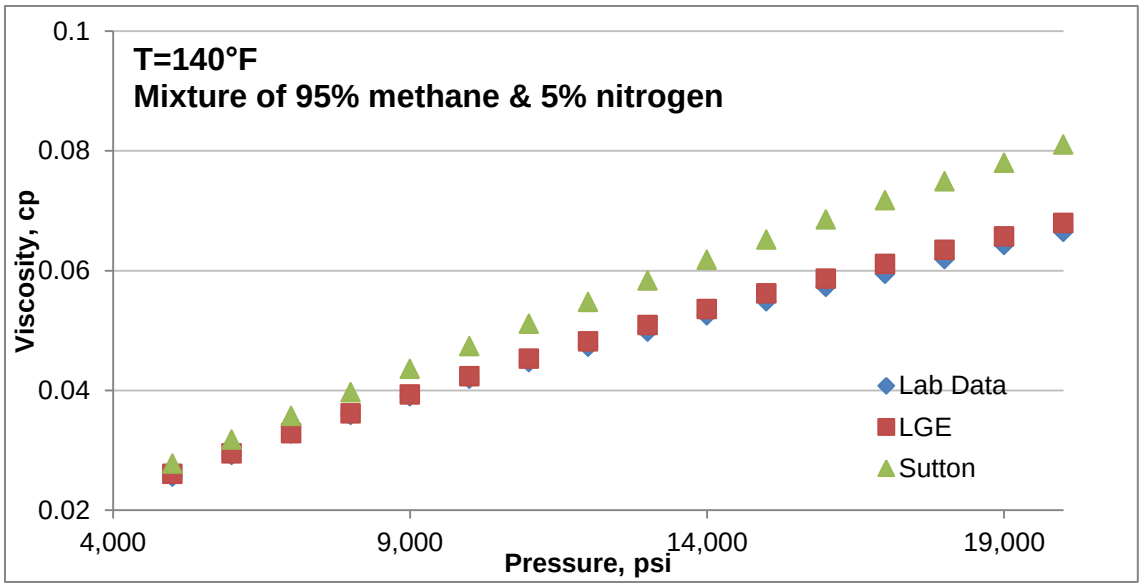

Fig. B.1—LGE and Sutton correlation have been compared with measured gas viscosity of mixture of 95% methane and 5% nitrogen at temperature of 140°F.

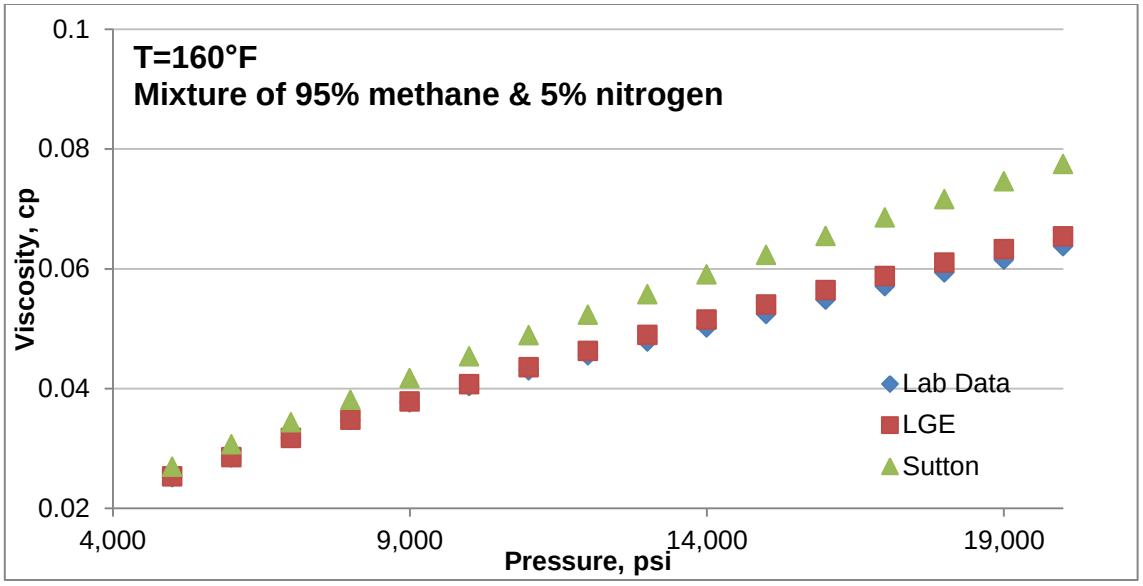

Fig. B.2—LGE and Sutton correlation have been compared with measured gas viscosity of mixture of 95% methane and 5% nitrogen at temperature of 160°F.

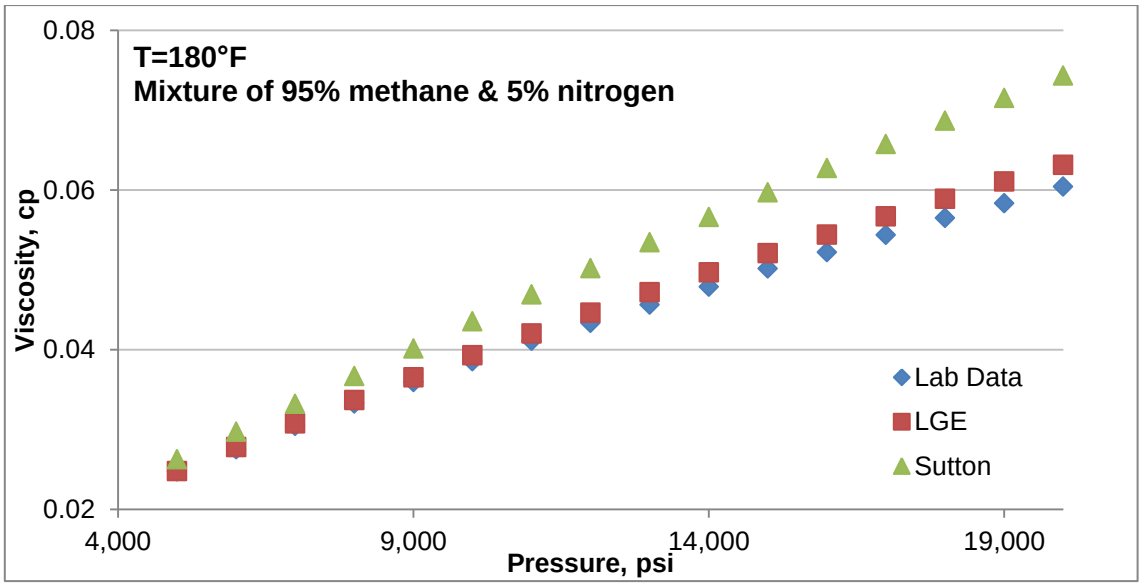

Fig. B.3—LGE and Sutton correlation have been compared with measured gas viscosity of mixture of 95% methane and 5% nitrogen at temperature of 180°F.

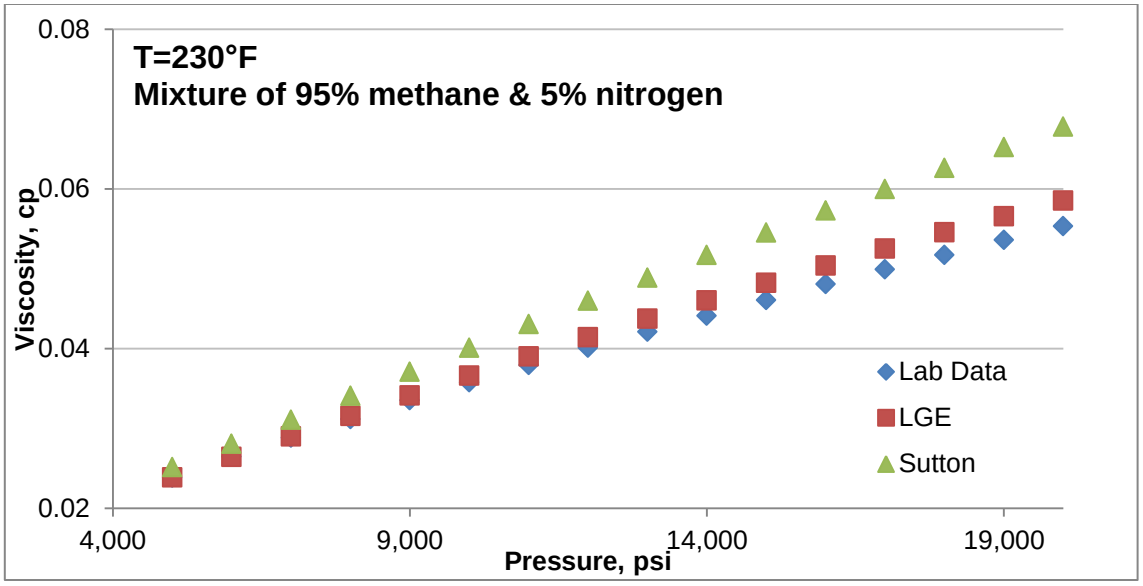

Fig. B.4—LGE and Sutton correlation have been compared with measured gas viscosity of mixture of 95% methane and 5% nitrogen at temperature of 230°F.

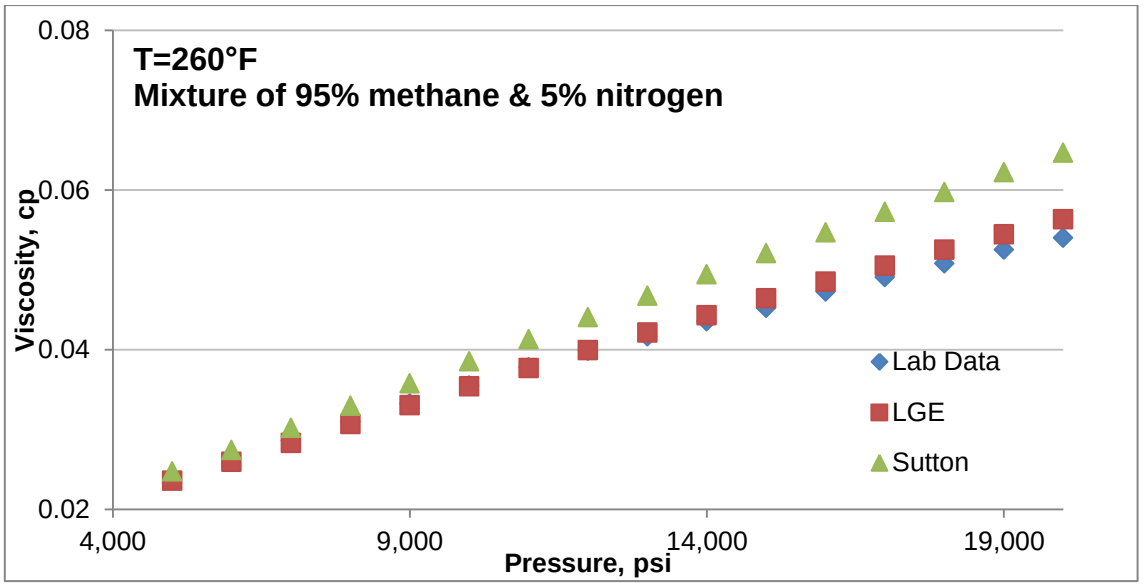

Fig. B.5—LGE and Sutton correlation have been compared with measured gas viscosity of mixture of 95% methane and 5% nitrogen at temperature of 260°F.

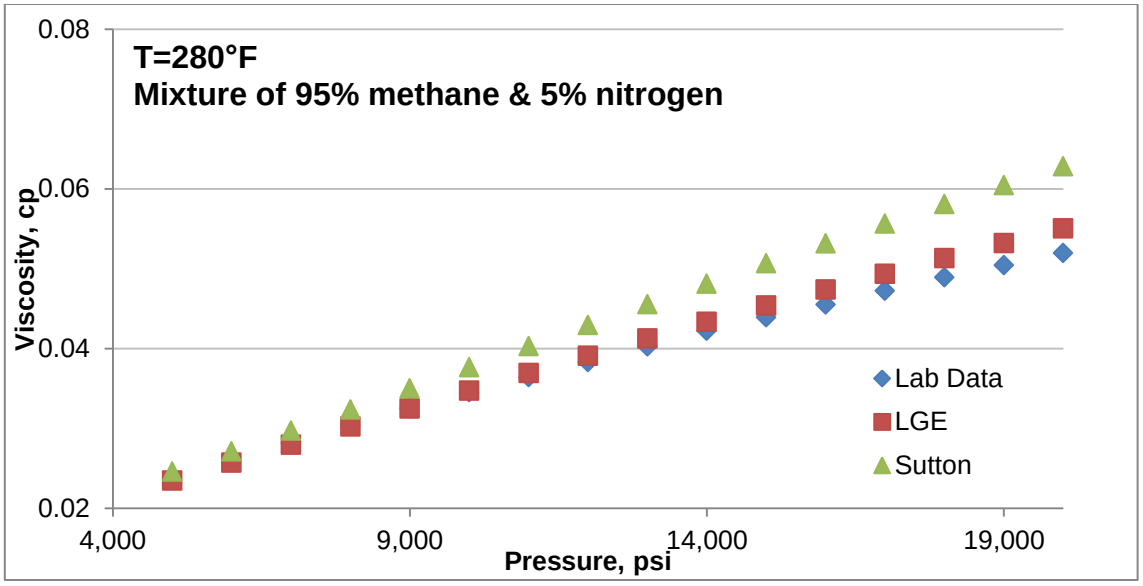

Fig. B.6—LGE and Sutton correlation have been compared with measured gas viscosity of mixture of 95% methane and 5% nitrogen at temperature of 280°F.

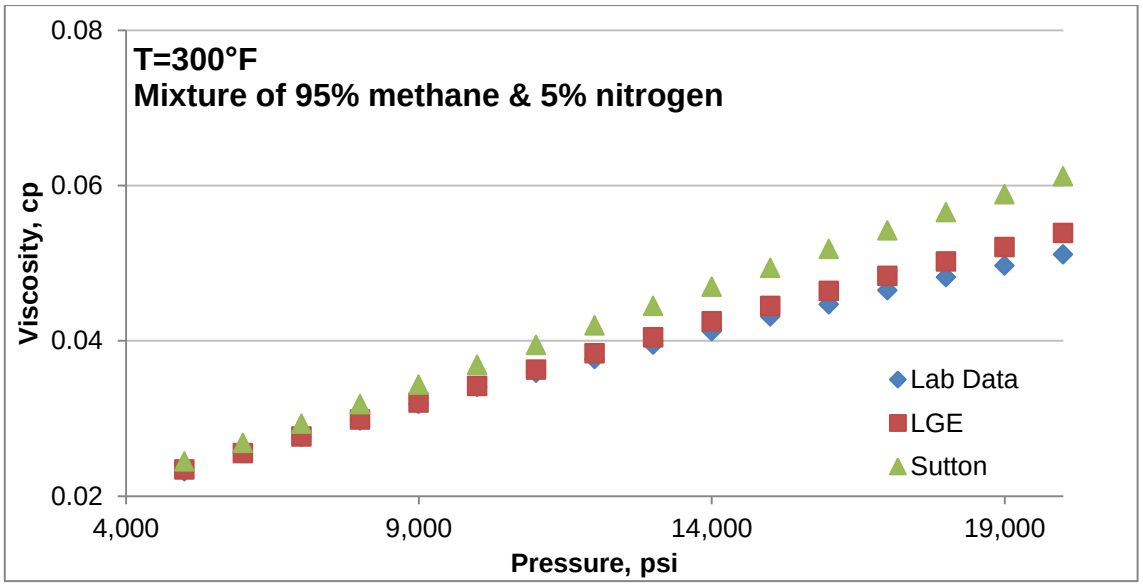

Fig. B.7—LGE and Sutton correlation have been compared with measured gas viscosity of mixture of 95% methane and 5% nitrogen at temperature of 300°F.

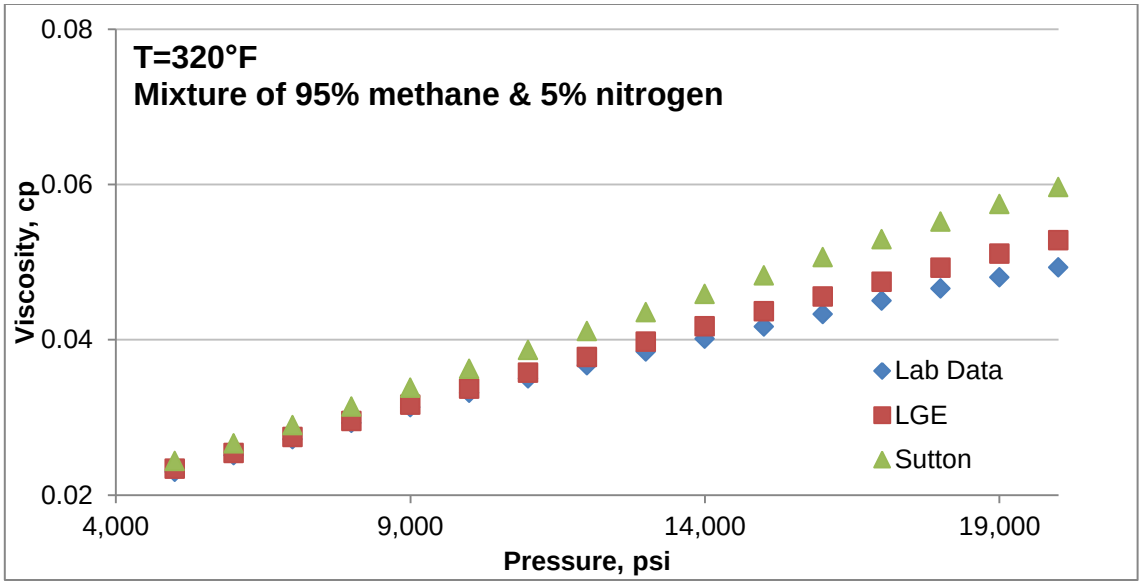

Fig. B.8—LGE and Sutton correlation have been compared with measured gas viscosity of mixture of 95% methane and 5% nitrogen at temperature of 320°F.

APPENDIX C

Comparison of viscosity of mixture of 90% methane and 10% CO_2 with LGE and Sutton correlation.

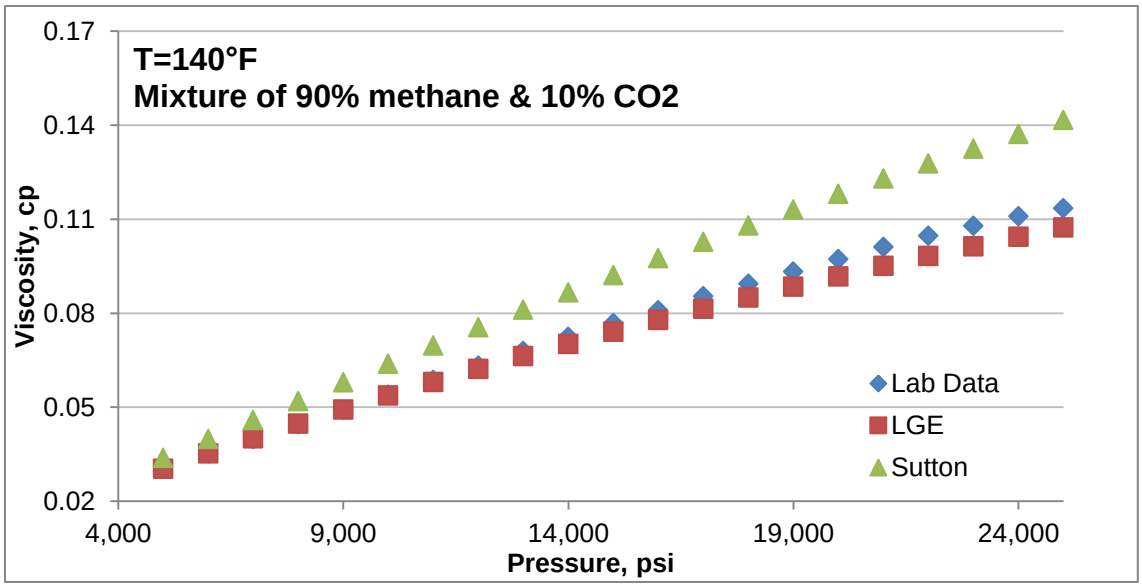

Fig. C.1—LGE and Sutton correlation have been compared with measured gas viscosity of mixture of 90% methane and 10% CO_2 at temperature of 140°F.

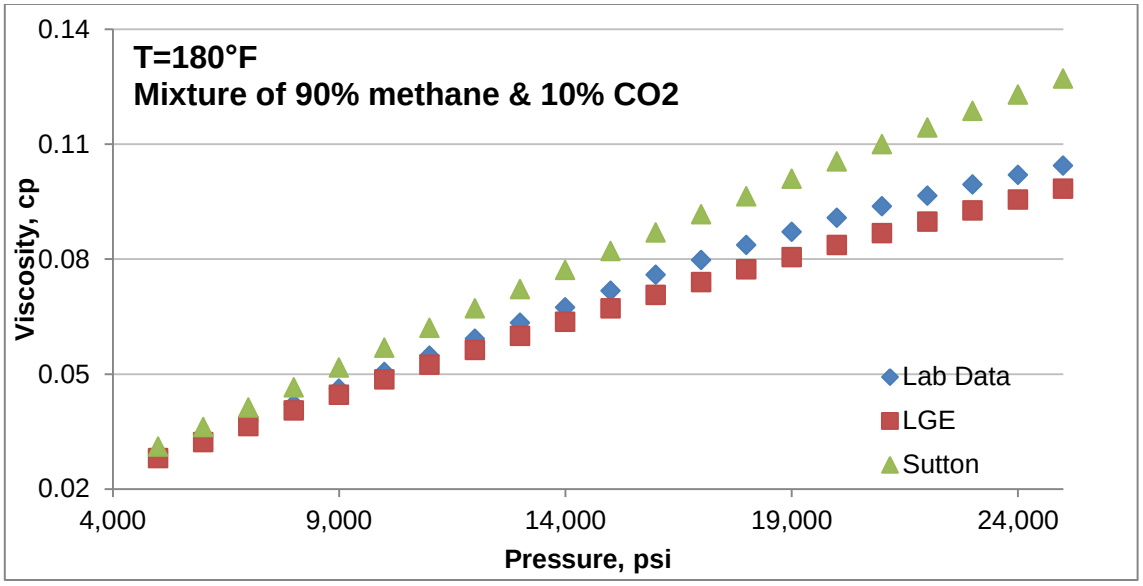

Fig. C.2—LGE and Sutton correlation have been compared with measured gas viscosity of mixture of 90% methane and 10% CO_2 at temperature of 180°F.

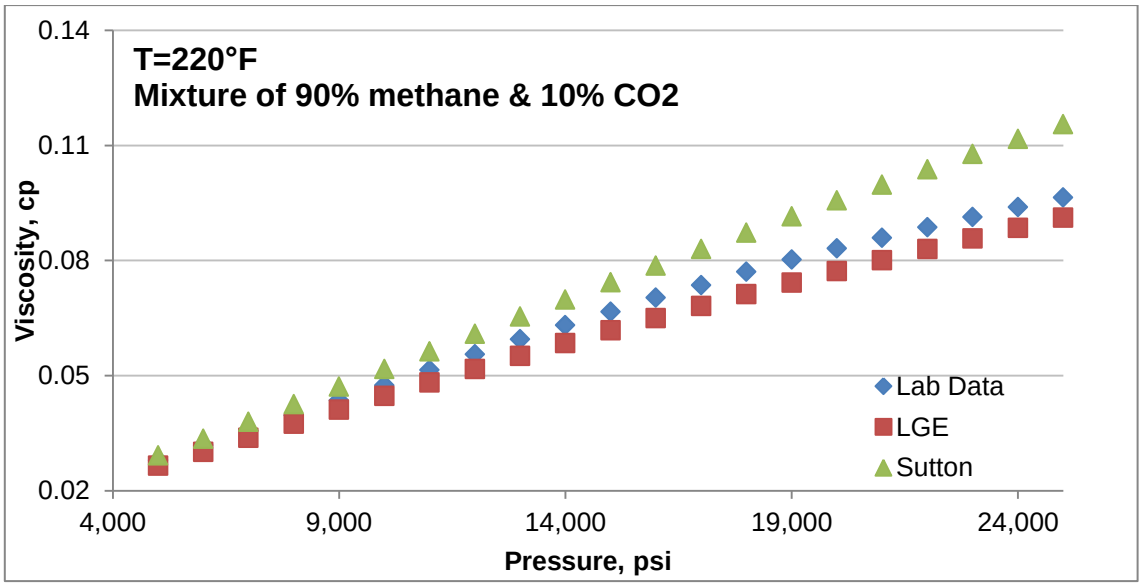

Fig. C.3—LGE and Sutton correlation have been compared with measured gas viscosity of mixture of 90% methane and 10% CO_2 at temperature of 220°F.

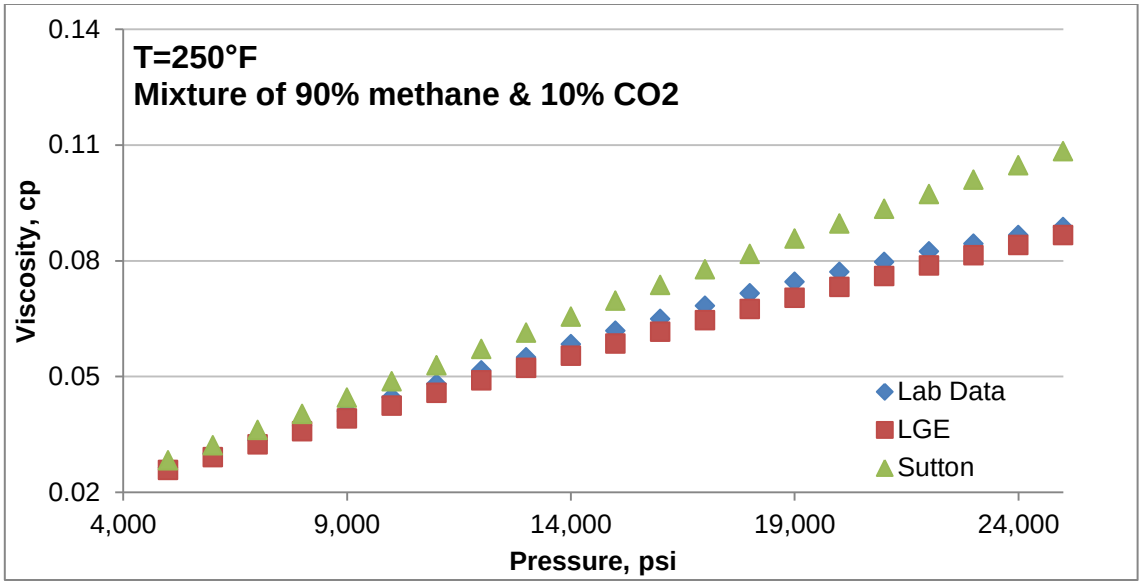

Fig. C.4—LGE and Sutton correlation have been compared with measured gas viscosity of mixture of 90% methane and 10% CO_2 at temperature of 250°F.

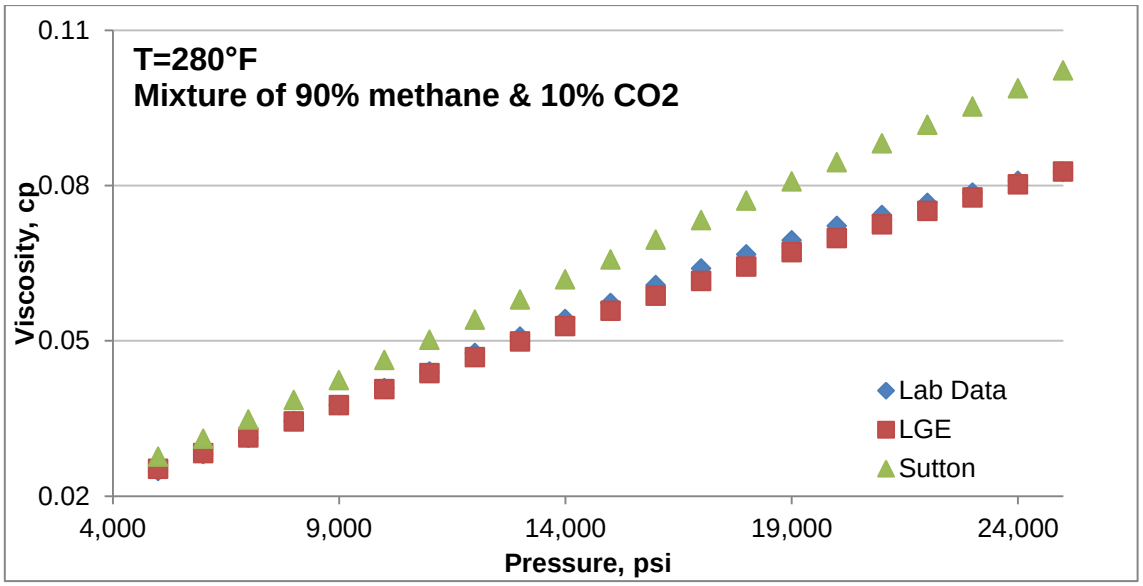

Fig. C.5—LGE and Sutton correlation have been compared with measured gas viscosity of mixture of 90% methane and 10% CO_2 at temperature of 280°F.

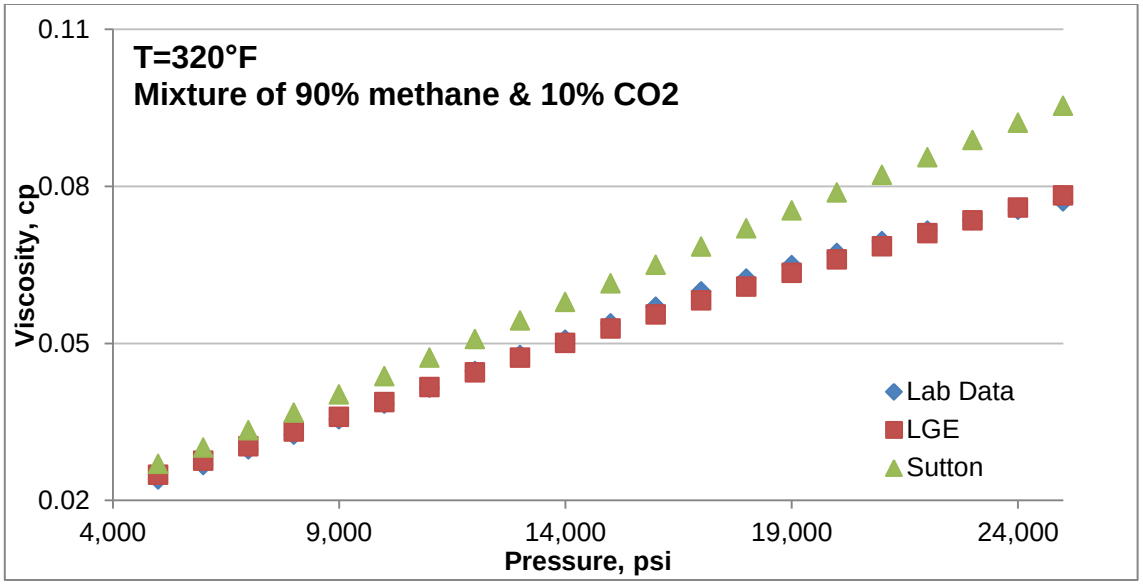

Fig. C.6—LGE and Sutton correlation have been compared with measured gas viscosity of mixture of 90% methane and 10% CO_2 at temperature of 320°F.

VITA

Name: Ehsan Davani

Contact Information: Department of Petroleum Engineering
Texas A&M University
3116 TAMU Richardson Building
College Station, TX 77843-3116

Email Address: e.davani@yahoo.com

Education: Ph.D., Petroleum Engineering, Texas A&M University
College Station, TX, 2011

M.S., Petroleum Engineering, Petroleum University of Technology, Iran, 2007

B.S., Petroleum Engineering, Sahand University of Technology, Iran, 2005

Professional Affiliation: Society of Petroleum Engineers, Member